

AD-A064 296

UNITED TECHNOLOGIES CORP STRATFORD CT SIKORSKY AIRCR--ETC F/G 1/3
ADVANCED COUPLING DEVELOPMENT PROGRAM.(U)

OCT 78 R A STONE

DAAJ02-74-C-0054

UNCLASSIFIED

SER-510004

USARTL-TR-78-40

NL

1 OF 2

AD
A064 296



USARTL-TR-78-40

LEVEL

12



ADVANCED COUPLING DEVELOPMENT PROGRAM

Robert A. Stone
Sikorsky Aircraft
Division of United Technologies Corporation
Stratford, Connecticut 06602

DDC
RECEIVED
FEB 2 1979
C

AD A 0 6 4 2 9 6

October 1978

Final Report for Period 15 June 1974 - 30 October 1977

DDC FILE COPY

Approved for public release;
distribution unlimited.

Prepared for
APPLIED TECHNOLOGY LABORATORY
U. S. ARMY RESEARCH AND TECHNOLOGY LABORATORIES (AVRADCOM)
Fort Eustis, Va. 23604

69 02 02 077

APPLIED TECHNOLOGY LABORATORY POSITION STATEMENT

This report provides the details of a program initiated to design, manufacture, and test an advanced technology coupling for future U. S. Army helicopter application.

Current drive system environments are already taxing the limitations of existing couplings. The continuing evolution of small, high-speed helicopter engines and the increasing interest in rotor isolation systems will require that future couplings be capable of operating at speeds around 20,000 rpm, transmitting 1500 HP at angular misalignments of up to 3° steady state and 5° transient.

The results of this effort have been the documentation of current coupling operating limitations, an estimate of future requirements, and the testing of three coupling concepts. Two modifications to one of the coupling concepts were also tested (one stainless steel version and one composite version) in an attempt to meet the projected requirements. None of the five couplings tested were able to meet the projected requirements; however, the program did demonstrate that a composite coupling could be developed to operate at 4727 in.-lb torque at 15,000 rpm and 1.5° angular misalignment.

Mr. Michael Dobrolet, Propulsion Technical Area, Aeronautical Technology Division, served as Project Engineer for this project.

DISCLAIMERS

The findings in this report are not to be construed as an official Department of the Army position unless so designated by other authorized documents.

When Government drawings, specifications, or other data are used for any purpose other than in connection with a definitely related Government procurement operation, the United States Government thereby incurs no responsibility nor any obligation whatsoever; and the fact that the Government may have formulated, furnished, or in any way supplied the said drawings, specifications, or other data is not to be regarded by implication or otherwise as in any manner licensing the holder or any other person or corporation, or conveying any rights or permission, to manufacture, use, or sell any patented invention that may in any way be related thereto.

Trade names cited in this report do not constitute an official endorsement or approval of the use of such commercial hardware or software.

DISPOSITION INSTRUCTIONS

Destroy this report when no longer needed. Do not return it to the originator.

UNCLASSIFIED

SECURITY CLASSIFICATION OF THIS PAGE (When Data Entered)

REPORT DOCUMENTATION PAGE		READ INSTRUCTIONS BEFORE COMPLETING FORM
1. REPORT NUMBER USARTL TR-78-48	2. GOVT ACCESSION NO.	3. RECIPIENT'S CATALOG NUMBER
4. TITLE (and Subtitle) ADVANCED COUPLING DEVELOPMENT PROGRAM	5. TYPE OF REPORT & PERIOD COVERED Final 6/15/74 to 10/30/77	
7. AUTHOR(s) Robert A. Stone	6. PERFORMING ORG. REPORT NUMBER SER-510004	
9. PERFORMING ORGANIZATION NAME AND ADDRESS Sikorsky Aircraft Division of United Technologies Corporation Stratford, Connecticut 06602	8. CONTRACT OR GRANT NUMBER(s) DAAJ02-74-C-0054	
11. CONTROLLING OFFICE NAME AND ADDRESS Applied Technology Laboratory, U.S. Army Research and Technology Laboratories (AVRADCOM) Fort Eustis, Virginia 23604	10. PROGRAM ELEMENT, PROJECT, TASK AREA & WORK UNIT NUMBERS 62207A 1G262207AH89 02 006 EK	
14. MONITORING AGENCY NAME & ADDRESS (if different from Controlling Office) 138 p.	12. REPORT DATE Oct 1978	
16. DISTRIBUTION STATEMENT (of this Report) Approved for public release; distribution unlimited.	13. NUMBER OF PAGES 138	
17. DISTRIBUTION STATEMENT (of the abstract entered in Block 20, if different from Report) Final rept. 15 Jun 74-30 Oct 77,	15. SECURITY CLASS. (of this report) Unclassified	
18. SUPPLEMENTARY NOTES	15a. DECLASSIFICATION/DOWNGRADING SCHEDULE	
19. KEY WORDS (Continue on reverse side if necessary and identify by block number) Couplings Transmissions Helicopters	16. 1G262207AH89	17. 82
20. ABSTRACT (Continue on reverse side if necessary and identify by block number) This report documents a four-phase effort in the development of an advanced technology coupling. A coupling survey (design and operational requirements definition; conceptual and detail design; fabrication; static testing and dynamic testing) was conducted. Two concepts out of seven developed in the program were chosen for fabrication and testing. One coupling, a composite flexure element design, successfully completed a basic dynamic performance test and demonstrated superior operational capability to a stainless steel counterpart.		

DD FORM 1 JAN 73 1473

EDITION OF 1 NOV 65 IS OBSOLETE
SYN 0102-014-6601

Unclassified

SECURITY CLASSIFICATION OF THIS PAGE (When Data Entered)

323 800

elt

PREFACE

This program was conducted by Sikorsky Aircraft, Division of United Technologies Corporation, Stratford, Connecticut, for the Applied Technology Laboratory, U. S. Army Research and Technology Laboratories under Contract DAAJ02-74-C-0054. The period of performance was June 15, 1974 to October 30, 1977.

U. S. Army technical direction was provided by Mr. M. Dobrolet of the Applied Technology Laboratory.

Acknowledgment is made to the engineering staff of Sikorsky Aircraft in general and to Mr. P. FitzGerald, Mr. Jules Kish, and Mr. George Karas for their technical counseling and support in this program effort.

ACCESSION for	
NTIS	W. Section <input checked="" type="checkbox"/>
DGC	Buff Section <input type="checkbox"/>
UNANNOUNCED	<input type="checkbox"/>
JUSTIFICATION	
BY	
DISTRIBUTION/AVAILABILITY CODES	
Dis	SP. CHIL
A	

TABLE OF CONTENTS

	<u>Page</u>
PREFACE	3
LIST OF ILLUSTRATIONS	8
LIST OF TABLES	13
INTRODUCTION	14
SURVEY	16
Survey Scope and Aim	16
Operational Characteristics and Requirements	16
Design Torque	16
Operating Speed	17
Misalignment	18
Weight and Size	18
Spring Rates	19
Critical Speed Effects	19
Centrifugal Effects	20
Balance Effects	20
Current Usage Baseline	22
Gear Coupling	22
Flexible Disk Coupling	24
Elastomeric Coupling	27
Diaphragm Coupling	27
Maintenance, Service, and Replacement Criteria	30
Typical Failure Modes	32
Current Applications Baseline	37
Low-Speed Couplings	37
High-Speed Couplings	37
Coupling Stiffness Ranges	39
Future Requirements Baseline	39
Torque and Speed Requirements	39
Angular Misalignment Requirement	44
Requirements Definition	47

5 02 02 077

TABLE OF CONTENTS (Cont'd)

	<u>Page</u>
COUPLING DESIGN	51
Conceptual Design	51
Diaphragm Coupling	52
Loop-Belt Coupling	52
Circumferential Belt Coupling	55
Elastomeric Coupling	55
Filament-Wound Coupling	55
Tension Strap Coupling	59
Helical Strap Coupling	59
Preliminary Design	62
Basic Load Relationships	62
Composite Joint Analysis	62
Material Selection	65
Typical Coupling Sizing	65
Coupling Selection Parameters	73
Weight	76
Cost	76
Reliability	76
Operational Limits	84
Coupling Selection	85
TEST FACILITY	92
Dynamic Test Facility	92
Static Test Facility	92
TESTS	99
Dynamic Test Procedure	99
Dynamic Test Results	99
Static Test Procedure	99
Static Test Results - Tension Strap Coupling	99
Static Test Results - Helical Strap Coupling	104
Assessment Test Procedure	116
Assessment Test Results	116

TABLE OF CONTENTS (Cont'd)

	<u>Page</u>
INTERIM COUPLING PROGRAM	117
Stainless Steel Tension Strap Coupling Design . . .	117
Composite Tension Strap Coupling Design	117
Fabrication	119
Static Tests	119
Dynamic Test - Stainless Steel Coupling	126
Dynamic Test - Composite Coupling	132
CONCLUSIONS AND RECOMMENDATIONS	137
Conclusions	137
Recommendations	138

LIST OF ILLUSTRATIONS

<u>Figure</u>		<u>Page</u>
1	Speed versus Centrifugal Force	21
2	Gear Coupling	23
3	Flexible Disk Coupling	25
4	Multi-Pack Flexible Disk Coupling	26
5	Elastomeric Coupling	28
6	Diaphragm Coupling	29
7	Typical Fracture, Flexible Disk Coupling . .	33
8	Typical Fracture, Gear Coupling	34
9	Typical Fracture, Diaphragm Coupling	35
10	Typical Fracture, Elastomeric Coupling . . .	36
11	Torque versus Speed Trending, High-Speed Engine Couplings	43
12	Engine/Gearbox Preferred Configuration, A.I.S. Motion Study	45
13	Engine/Gearbox Alternate Configuration, A.I.S. Motion Study	46
14	Angular Misalignment versus Speed, High-Speed Engine Couplings	48
15	Diaphragm Coupling Concept	53
16	Loop-Belt Coupling Concept	54
17	Circumferential Belt Coupling Concept	56
18	Elastomeric Coupling Concept	57
19	Filament-Wound Coupling Concept	58

LIST OF ILLUSTRATIONS (Cont'd)

<u>Figure</u>		<u>Page</u>
20	Tension Strap Coupling Concept	60
21	Helical Strap Coupling Concept	61
22	Basic Load Model	63
23	Composite Joint Model and Ply Mix Matrix . .	64
24	Stress versus Cycles - Unidirectional Composites Tension - Tension Fatigue	67
25	Alternating Stress versus Steady Stress, Unidirectional Kevlar 49/Epoxy Configuration.	68
26	Maximum Stress versus Coupling Radius, Circumferential Strap Design	69
27	Loop-Belt Analytical Model	70
28	Loop-Belt Analytical Model Isolated Elements.	71
29	Maximum Stress versus Section Thickness, Loop-Belt Coupling Diameter	74
30	Diaphragm Coupling Design	75
31	Loop-Belt Coupling Design	77
32	Circumferential Belt Coupling Design	78
33	Elastomeric Coupling Design	79
34	Filament-Wound Coupling Design	80
35	Tension Strap Coupling Design	81
36	Helical Strap Coupling Design	82
37	Helical Strap Coupling Assembly Drawing . . .	87
38	Tension Strap Coupling Assembly Drawing . . .	88

LIST OF ILLUSTRATIONS (Cont'd)

<u>Figure</u>		<u>Page</u>
39	Helical Strap Coupling Specimen	90
40	Tension Strap Coupling Specimen	91
41	High-Speed Test Facility, Motor/Clutch and Gearbox Arrangement	93
42	High-Speed Test Facility, Back-to-Back Input Gearboxes	94
43	High-Speed Test Facility, Dummy Box Input, Test Shaft Side	95
44	High-Speed Test Facility, Angular Misalign- ment Adjusting Jack	96
45	High-Speed Test Facility, Test Shaft Containment System	97
46	Static Overtorque Test Fixture	98
47	Test Shaft and Adapter Flanges	100
48	Test Shaft and Coupling Parts	101
49	Test Coupling Specimen Flange Fracture	102
50	Torque versus Torsional Deflection, Tension Strap Coupling	103
51	NASTRAN Model, Composite Helical Strap Coupling	105
52	NASTRAN Model, Composite Helical Strap Coupling	106
53	Strain Gage Locations, Helical Strap Coupling	107
54	Torque versus Torsional Deflection, Composite Helical Strap Coupling	108

LIST OF ILLUSTRATIONS (Cont'd)

<u>Figure</u>		<u>Page</u>
55	Helical Strap Coupling Fracture	109
56	Analysis and Test Correlation, Gage No. 1, Helical Strap Coupling	110
57	Analysis and Test Correlation, Gage No. 2, Helical Strap Coupling	110
58	Analysis and Test Correlation, Gage No. 3, Helical Strap Coupling	111
59	Analysis and Test Correlation, Gage No. 4, Helical Strap Coupling	111
60	Analysis and Test Correlation, Gage No. 5, Helical Strap Coupling	112
61	Analysis and Test Correlation, Gage No. 6, Helical Strap Coupling	112
62	Analysis and Test Correlation, Gage No. 7, Helical Strap Coupling	113
63	Analysis and Test Correlation, Gage No. 8, Helical Strap Coupling	113
64	Analysis and Test Correlation, Gage No. 9, Helical Strap Coupling	114
65	Analysis and Test Correlation, Gage No. 10, Helical Strap Coupling	114
66	Analysis and Test Correlation, Gage No. 11, Helical Strap Coupling	115
67	Analysis and Test Correlation, Gage No. 12, Helical Strap Coupling	115
68	Steel Strap Coupling Redesign	118
69	Composite Strap Coupling Redesign	120

LIST OF ILLUSTRATIONS (Cont'd)

<u>Figure</u>		<u>Page</u>
70	Steel Strap Coupling Test Specimen	121
71	Composite Strap Coupling Test Specimen	122
72	Deflection versus Torque, Steel Strap Coupling	123
73	Deflection versus Torque, Composite Strap Coupling	123
74	Static Torque Test, Steel Strap Coupling	124
75	Static Torque Test, Composite Strap Coupling	125
76	Axial Deflection versus Load, Composite Strap Coupling	127
77	Dynamic Test Fracture, Steel Strap Coupling	128
78	Dynamic Test Fracture, Test Shaft Containment	129
79	Dynamic Test Fracture, Test Box Flange	130
80	Dynamic Test Fracture, Slave Box Flange	131
81	Working Endurance Limit, Steel Tension Strap Coupling	133
82	Dynamic Test Specimen Inspection, Composite Strap Coupling	135
83	Dynamic Test Specimen Inspection, Coupling Parts, Composite Strap Coupling	136

LIST OF TABLES

<u>Table</u>		<u>Page</u>
1	Low-Speed Couplings, Tail Rotor Drive and Interconnecting Rotor Shafts	38
2	High-Speed Couplings, Engine Drive Shafts . .	40
3	Coupling Stiffness Ranges	41
4	Advanced Turbine Technology	42
5	Unidirectional Composite Allowables	66
6	Reliability Rating	84
7	Operational Limits Rating	85
8	Coupling Design Selection Matrix	86

INTRODUCTION

The shaft coupling is an indispensable element in the drive system of every helicopter, and its performance limitations must be considered a prime constraint in the design of drive shaft systems. The primary functions of the coupling are to connect shafting between the components of a drive system and to transmit power while accommodating angular misalignments resulting from relative motion or location of the coupled components. Errors in relative location are created by accumulated manufacturing tolerances, while errors in relative motion are created by differential thermal expansions, deflection of the drive system components, and deflection of the airframe structure to which the drive shafts are mounted.

Power transmitted through a coupling is the product of torque and speed. The primary functional parameters of the coupling thus become torque, speed, and misalignment. These basic functional requirements are further compounded by the effects of mass imbalance, shaft whip, critical speeds, and a wide range of environmental conditions. In addition, some aircraft couplings have moving parts that require lubrication and maintenance. Wear, loss of lubricant, and seal failure combine to limit coupling life and impose environmental constraints on this type coupling. In spite of these drawbacks, many successful applications of couplings with moving contact have found wide acceptance by the industry, i.e., gear couplings.

Couplings which accommodate misalignment through a flexure element eliminate the need for lubrication and seals, are simple and lightweight, but are restricted in angular misalignment capacity. Misalignment induces component flexure which produces alternating stresses that can limit coupling life. The coupling designer's problem in this case is to proportion the strength and stiffness required to transmit the torque or steady loads with the misalignment which imposes alternating loads, such that the resulting coupling satisfies both strength and misalignment requirements.

Component demands for light weight, maintenance- and service-free operation, fail-safe operation and long life, combine to form a rigorous set of requirements.

Increased engineering development effort can improve coupling operational capability to meet the demands of current as well as future helicopter drive systems in several areas. First, increased angular misalignment capacity can accommodate projected requirements for envisioned vibration/acoustical isolation systems. Second, use of composite materials can reduce weight and increase coupling performance capability. Third, simplification and reduction in the number of components of the coupling assembly can increase compatibility with balance considerations, increase reliability, and increase MTBR.

In the program reported herein, the prime objective was to design, fabricate, and test an advanced technology coupling. This coupling was to embody misalignment, torque, and speed capabilities to meet projected operational requirements of future Army helicopters. Under this program effort, current helicopter drive system coupling applications were surveyed. The data acquired was used to establish a baseline requirement profile to be subsequently trended for future-generation helicopters. A set of realistic design criteria was then selected for the development of two advanced technology couplings.

A search was conducted to examine previous coupling designs and a study made of new and novel concepts. From this effort seven concepts emerged, of which two designs were chosen for detail design, fabrication, and testing. The two concepts chosen were similar in that each comprised a flexure element to accommodate angular misalignment. These flexure element designs eliminated the need for lubrication, servicing, and sealing elements required by designs which allow relative motion between parts.

Two designs were chosen for fabrication and test: the stainless steel tension strap coupling and the composite helical strap coupling. Both these original coupling designs failed to meet the initial test condition and were subject to redesign. The composite version of the redesigned coupling successfully completed the assessment test of 9×10^6 cycles operating at 4700 inch-pounds torque at 15,400 rpm and 1.5 degrees angular misalignment. The use of a composite flexure element reduced coupling weight by 20% and eliminated fretting which had precipitated the failure in the steel strap designs. This coupling, which weighed less than 1 pound, demonstrated that development effort can improve coupling performance capability while at the same time reduce weight and improve reliability.

SURVEY

SURVEY SCOPE AND AIM

Sikorsky Aircraft has investigated past as well as current coupling designs to build a comprehensive base for upgrading coupling technology. This effort consisted of a two-phase survey. The initial effort was a documentation of couplings currently in use by the helicopter industry and the identification of operational characteristics with regard to speed, torque, misalignment, lubrication, inspection and maintenance, as well as performance limitations.

The second phase of the survey was more general in scope with the purpose of developing new and innovative coupling concepts. A search of coupling patents and a survey of industrial coupling and power transmission equipment were conducted to stimulate the formulations of advanced coupling design concepts.

On the basis of both aspects of this survey, a design and operational requirements definition was established for the couplings developed in this program. The advanced technology coupling was to be designed, built, and tested to satisfy a realistic set of parameters that would best meet the overall requirements of the most demanding range of practical operations. One aim of the survey was to determine the specific coupling operational need that would yield the greatest advantage by application of advanced technology.

OPERATIONAL CHARACTERISTICS AND REQUIREMENTS

Design Torque

The basic function of the transmission coupling is to transmit torque at a given speed while maintaining a constant velocity during the relative displacement between the coupled transmission components.

Torque and speed are a function of the power being transmitted and can be expressed as

$$T = \frac{63,025 \text{ (hp)}}{\text{rpm}} \quad (1)$$

where

T = torque in in.-lbs
hp = horsepower
rpm = rotation speed in revolutions per minute

In a helicopter drive system, consideration must be given to momentary peak torques that occur for short intervals of time. Limit power is defined as the maximum power experienced in service and can sometimes be as high as twice the normal rated power to compensate for momentary peak torques. Ultimate torque is defined as 1.5 times the limit torque.

Operating Speed

In the design of any drive system, two basic parameters may be varied which affect the choice of operating speed: the shaft length between supports and the shaft diameter. The same power can be transmitted at lower torque by operating at higher speeds minimizing weight. However, to assure drive shaft control of dynamic stresses, shaft natural frequencies become a paramount consideration. A shaft's natural frequency is a function of its mass distribution, length, and stiffness. Drive shaft lengths are dictated by helicopter configuration requirements, handling, or installation constraints. Having chosen the shaft material, the designer has only the shaft diameters to vary in controlling the shaft natural frequency. Normally, the shaft outside diameter (OD) is varied to avoid shaft natural frequencies within 40% of the chosen operating speed.

Long drive shaft systems comprising two or more shaft segments employ couplings to join these segments together. The couplings' weight and stiffness characteristics become part of the shaft system and influence its critical speed. Flexible couplings provide an end condition whose stiffness can be modeled between that of a simple support and a fixed end. Thus the coupling's stiffness and weight contribution must be considered in determining the system mode shape and natural frequency.

A coupling that exhibits low axial and bending stiffness under conditions of misalignment can reduce vibratory stresses which are induced into the adjacent shafts and supporting hardware.

In addition, the coupling should be a constant speed device and should also be a precise connection that does not introduce vibration excitation or nonlinearities into the system.

Misalignment

The primary function of the coupling is to transmit power from one component in the drive system to another while at the same time accommodating misalignments.

Helicopters use couplings to accommodate the inevitable misalignments between rotating shafts in a drive train which are caused by accumulated dimensional variations, deflection of the supporting structure under load, and differential thermal expansion.

These misalignments subject the coupling to both steady and alternating stresses which must be considered in the coupling design if the system is to operate satisfactorily.

The ability of the coupling to accommodate any combination of these misalignments without developing large restoring moments or forces is mandatory. Such moments and forces would not only have an adverse effect on the coupling itself, but would impose these damaging loads on the bearings and shafts of the adjacent equipment.

Angular misalignment is the most influential factor determining the operational life of any coupling, since this is the source of an alternating stress which occurs once every shaft revolution. When a given coupling is subjected to a high steady load compared to its ultimate capacity, it will have little reserve for coping with misalignments. Conversely, if the same coupling is lightly loaded, it will have a greater capacity for misalignment. This may be readily seen by considering the likeness of a Goodman diagram which has alternating stress as an ordinate, and steady stress as an abscissa. Substitute coupling angular misalignment for alternating stress and torque for the steady stress. The coupling capacity is a combination of both the torque and angular misalignment.

Weight and Size

In the design of helicopter hardware, every effort must be exercised to reduce weight and size. The weight of each aircraft part has a direct influence on aircraft weight empty, while the size of each aircraft part has an impact on the aircraft volume efficiency with its ensuing adverse effect on drag. Helicopter couplings must usually be tailored to meet specific operational requirements which preclude the use of an off-the-shelf coupling. The designer then, in conjunction with the coupling fabricator, must consider the use of lightweight alloys such as aluminum and titanium. Advances in composite structures are also very attractive because of their high specific strength.

Spring Rates

Helicopter drive shaft couplings can be imagined as having four degrees of freedom: torsion, radial, axial and bending. The measure of these degrees of freedom is the coupling spring rate. In most applications, it is desirable that the coupling exhibit high torsional and radial stiffness in combination with relatively soft axial and bending stiffness.

High radial and torsional stiffness is desirable from an end support condition and its resulting effect on critical speed. Low axial and bending stiffness under conditions of misalignment can reduce the alternating stresses induced in adjacent shafts and attending hardware.

Critical Speed Effects

In any rotating shaft system there exists a series of discrete speeds at which the centrifugal forces induced by shaft unbalance cause progressively greater shaft deflections. At these speeds, called critical speeds, the restoring forces developed by the shaft are equal to the centrifugal forces developed by the shaft and there is no stable amplitude of deflection. If allowed to rotate at a critical speed, the deflection amplitudes of the shaft will build up until the yield point of the shaft material is exceeded and failure occurs.

In a typical helicopter drive shaft system, the shafts are designed to operate at approximately 20% to 40% below their first bending critical speed when operating at the highest speed expected in service. The highest expected operating speed can often be 120% of normal operating speed; thus, the shaft first bending critical speed is designed to be 144% to 168% of operating speed. Vibration modes below the first bending critical speed are often induced in the helicopter drive shaft system because of the typically low spring rates of the supports. Dampers are employed to control vibration amplitudes resulting from the "rigid body" modes.

The shape which a shaft assumes depends on its speed and the type of end connection. The ends may be simply supported, an end condition closely approximated in practice by using a universal joint, or the ends may be fixed, an end condition approximated in practice by rigid flange connections. Couplings are normally considered flexible ends whose rigidity

lies somewhere between that of the simply supported and fixed end condition. The axial and bending stiffness of a coupling influences the critical speed of the shaft system in which it operates and should be considered in the critical speed analysis.

Centrifugal Effects

With the advent of turbine engines, helicopter drive systems have had to accommodate ever-increasing operational speeds. Inherent unbalance due to manufacturing tolerances with respect to the mass distribution, as well as the location of coupling elements relative to the axis of rotation, has brought about the need for greater balancing accuracy. The basic relationship for centrifugal force is expressed as

$$F_C = m \times r \left(\frac{\text{rpm} \times \pi}{30} \right)^2 \quad (2)$$

From equation (2) it is readily seen that the centrifugal force is a function of the speed squared. When speeds of 10,000 to 30,000 rpm are squared, the resultant force becomes significant even when the product of the mass and its radius is minimal.

Balance Effects

Shaft systems are balanced to minimize eccentricity between the shaft system center of gravity and the axis of rotation. These eccentricities are formed as a result of manufacturing tolerances.

In low-speed shaft assemblies it is possible to individually balance the component parts. Replacement of worn or defective hardware is permissible because the overall balance accuracy can still be achieved. However, as the shaft speeds increase, the allowable balance tolerance becomes very small and balancing as an assembled unit is required.

Figure 1 shows a curve of speed versus centrifugal force for a shaft with a constant 1.0 ounce/inch unbalance. To determine the force generated by the unknown balance, multiply the force in pounds at the ordinate by the ounce/inch unbalance determined for the rotating shaft.

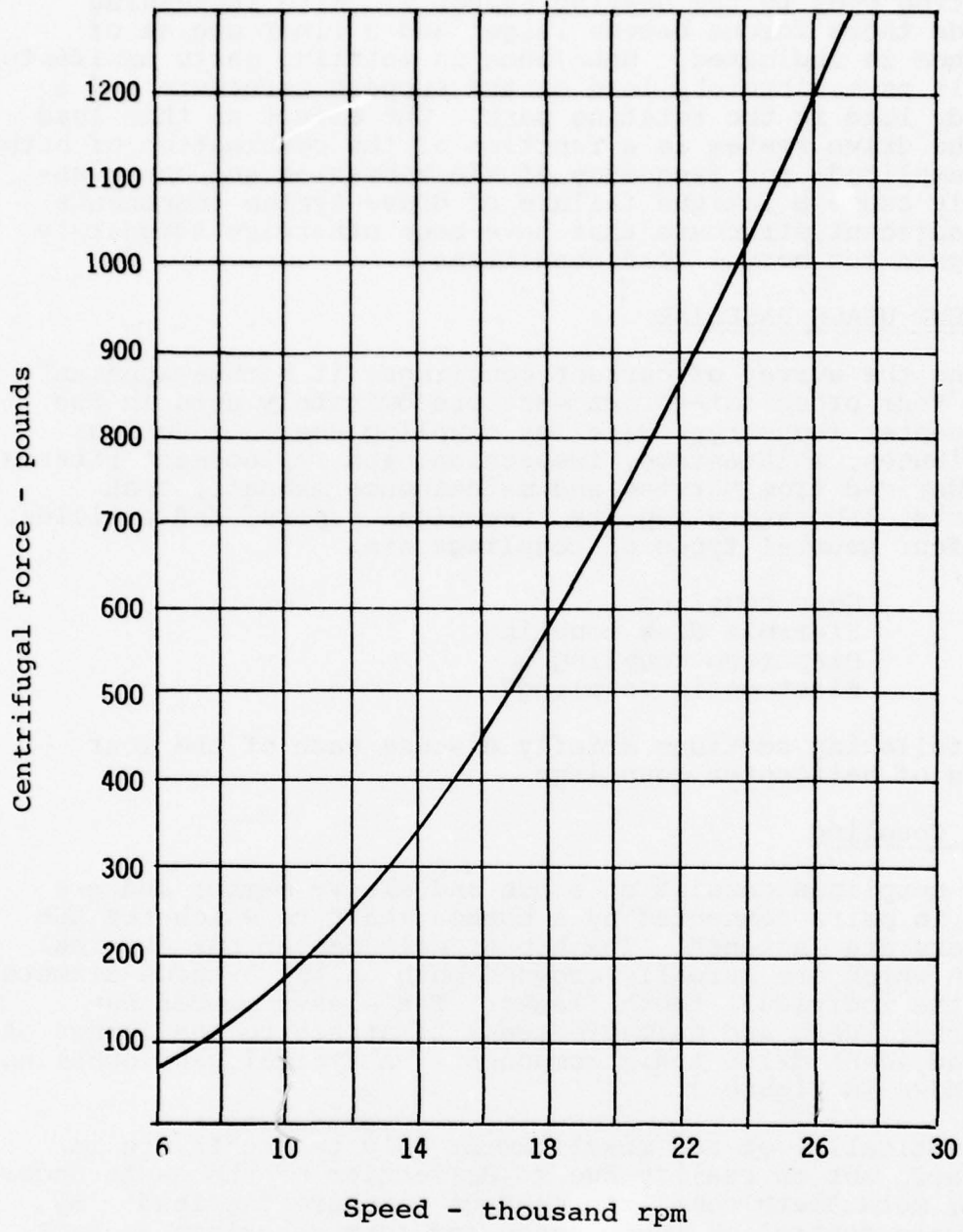


Figure 1. Speed versus Centrifugal Force.

Forces created by unbalance will be transferred from the rotating body to the bearing supports. With increasing speeds these forces become larger and a finer degree of balance is indicated. Unbalance in rotating parts manifests itself as a vibratory load on the support structure and a steady load in the rotating part. The effect of this load on the drive system is a function of the combination of both the amplitude and frequency of the vibration and can eventually cause a fatigue failure of drive system components and adjacent structure that have been otherwise adequately designed for normal load conditions.

CURRENT USAGE BASELINE

During the survey of current couplings, it became apparent that four broad categories were predominately used in the helicopter industry. Data for coupling usage, coupling attributes, maintenance, inspection, and replacement criteria was derived from service and maintenance manuals, test reports, laboratory reports, technical papers, and articles. The four general types of couplings are:

- . Gear coupling
- . Flexible disk coupling
- . Diaphragm coupling
- . Elastomeric coupling

The following sections briefly discuss each of the four types of helicopter couplings.

Gear Coupling

Gear couplings consist of a hub and sleeve member and are used in pairs connected by a common shaft to which the hub members are fastened. The hub or male member has external teeth which are normally crowned both on the outside diameter and the individual tooth flanks. The sleeve member has internal teeth and suitable means to attach to the flange of the adjacent drive train component. A typical gear coupling is shown in Figure 2.

Theoretically, at any misalignment only two teeth are in contact, but in reality due to deflection of the teeth under load, more teeth come into contact to share the load. By accurate control of tooth space and form, backlash is kept to a minimum.



Figure 2. Gear Coupling.

The gear coupling can be made to accommodate relatively large axial displacements under zero or low torque conditions, which is a feature unique to this design.

The relative motion, sliding and rolling, between mating teeth requires that prime consideration be given to lubrication, seals, and service intervals. Loss of lubricant is the major single cause of failure of the gear coupling.

Flexible Disk Coupling

The flexible disk coupling shown in Figure 3 is the most widely used coupling in the helicopter industry. The flexible disk coupling is lightweight, simple, maintenance free, fail safe, readily inspectable, and is adaptable to a wide range of torques and speeds where the angular misalignment requirement is small (i.e., less than 1/2 degree). To provide higher angular misalignment capability, designs using combinations of disk packs in series have been formulated. Figure 4 illustrates a coupling of this type which can accommodate 2-1/2 degrees at speeds up to 3000 rpm.

The flexure in a series disk pack design occurs at the centroid of each disk pack. Bending is displaced over a significant axial length since the disk packs are separated by an amount sufficient to provide clearance for the attachment hardware. The series disk pack coupling is speed limited because each disk pack behaves as a pinned joint having low radial constraint. At high speeds, this lack of restraint can create instability in the coupling.

The basic, single pack, flexible disk coupling has excellent reliability and inspectability. "On condition" determination can be specified for replacement in most cases. Failures are readily detected at periodic inspection intervals because cracks appear in the outside laminates of the disk pack first, normally in the area of the bolt attachment. Crack propagation is slow and the ability of the coupling to carry full load for extended periods of operation after initial failure is a desirable fail-safe feature.

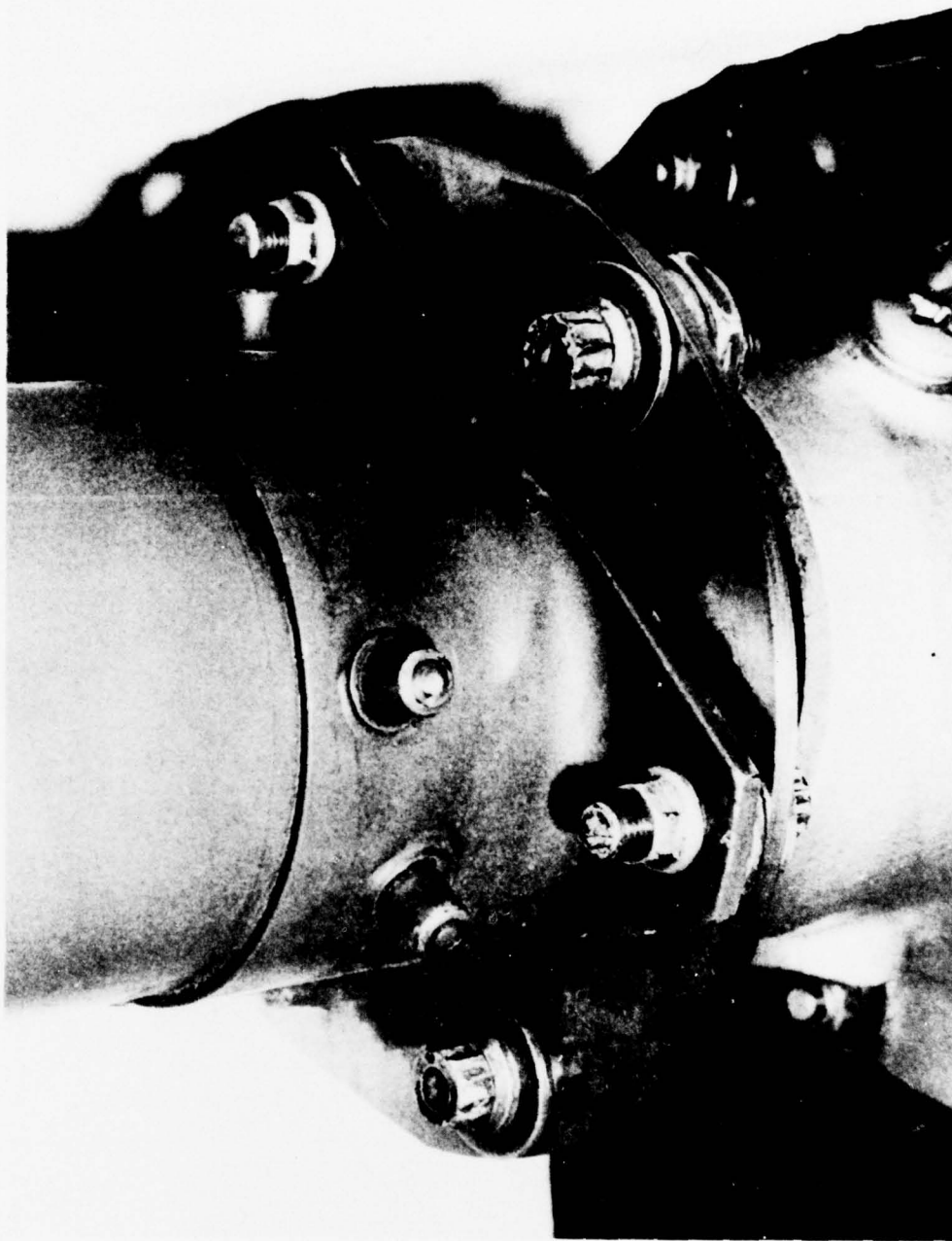


Figure 3. Flexible Disk Coupling.

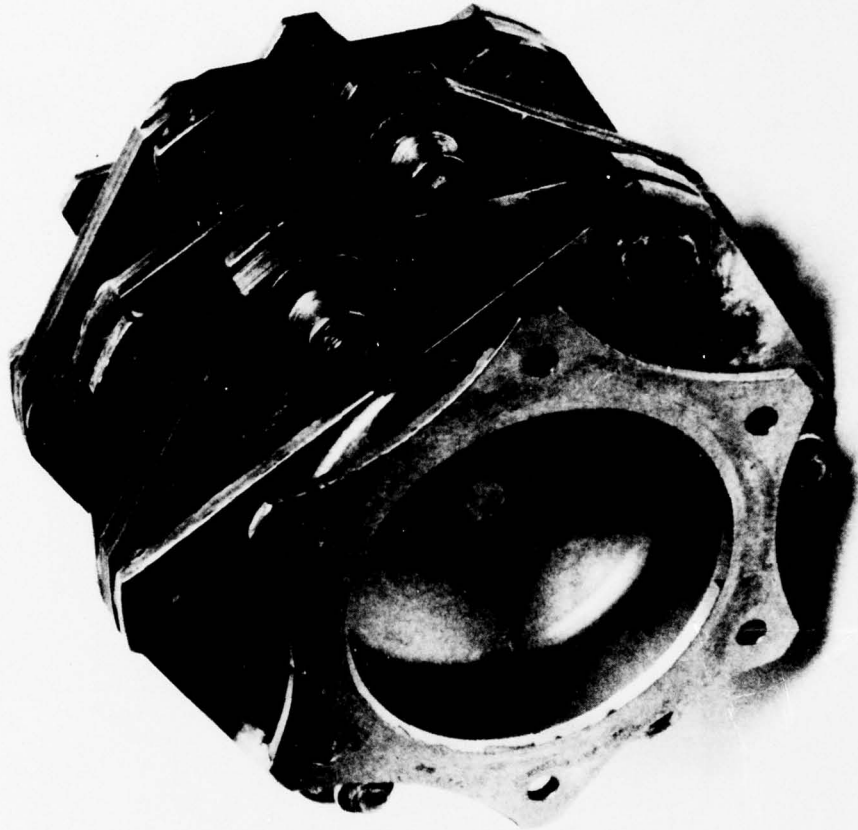


Figure 4. Multi-Pack Flexible Disk Coupling.

Elastomeric Coupling

A third common type of helicopter drive shaft coupling is the elastomeric coupling. The successful application of this type of coupling found favor in the early helicopter transmission systems where torsional compliance was an important parameter due to the use of reciprocating engines.

The rubber or elastomeric coupling has many configurations, but basically the designer takes advantage of the elastic properties in shear to accommodate angular misalignment and relatively high stiffness in compression to transmit torque. These couplings consist of flanged hubs or rims of metal with rubber in any number of shapes interposed between. An example of the elastomeric coupling is shown in Figure 5. Here the elastomer is captured and alternately bonded to the paddle-like elements of the driver and driven forged flange members.

Elastomeric couplings can operate at moderate speeds and at moderate torques where torsional shock is a concern. If operated at angular misalignment or with axial motion, all relative deflections are absorbed through the flexure of the elastomer.

Basic advantages of the elastomeric coupling include low maintenance and service requirements, good inspectability, and load path redundancy.

Ambient temperatures limit usage, and service life is subject to deterioration due to aging of the elastomer.

Diaphragm Coupling

A fourth common type of helicopter coupling is the diaphragm coupling. The diaphragm coupling consists of one or more parallel-sided disk elements connected alternately at the inner and outer diameters and is one of the most recent coupling types to find broad acceptance in helicopter applications.

A typical diaphragm coupling is shown in Figure 6. Contoured disks, or diaphragms, are connected by alternately welding or riveting at the inner and outer rims. The diaphragm is sometimes contoured with exponentially varying thickness to provide uniform stress distribution in both torsion and bending. Flexure takes place in the profiled area of the diaphragm which is free of holes, sharp corners, or load transfer joints. Since the diaphragms are arranged in series, the maximum



Figure 5. Elastomeric Coupling.

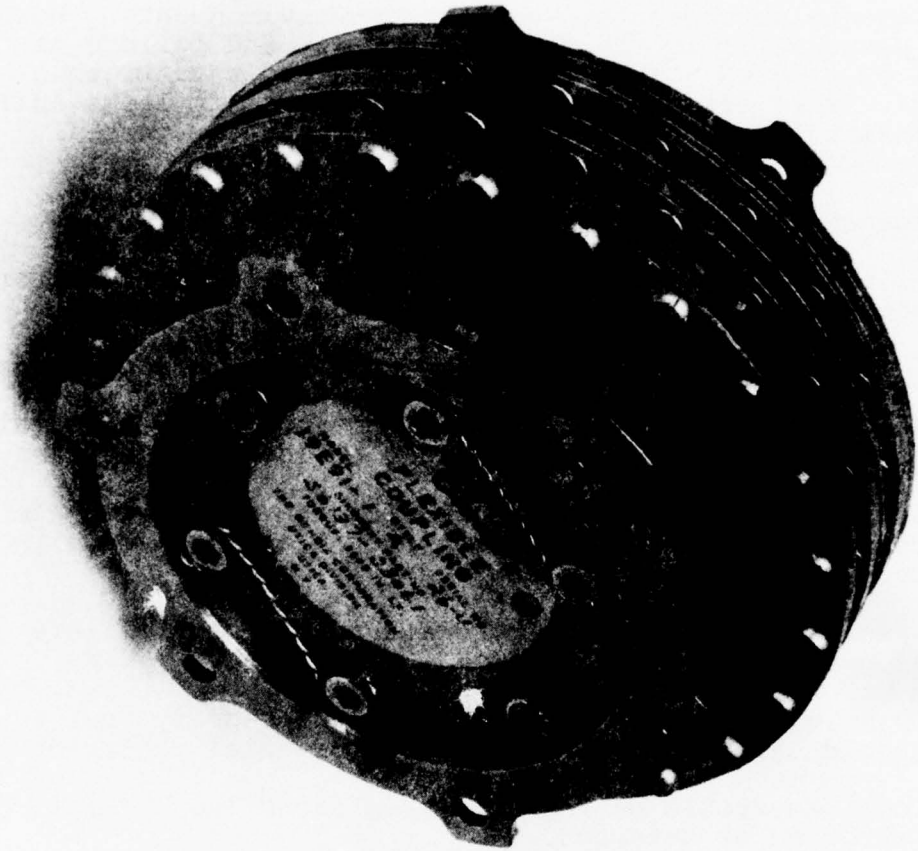


Figure 6. Diaphragm Coupling.

angular misalignment is controlled by the number of diaphragms employed. Like the multiple pack flexible disk couplings, above a given number of diaphragms the coupling lacks stability and a ball and socket restraint is used to prevent shaft whipping. This added complexity defeats the simplicity and the otherwise lubrication-free attributes of the basic coupling.

The diaphragm coupling is stiff torsionally and soft axially and in bending. It complies readily with high-speed balance requirements and operates well in most environments. However, crack propagation in the disks is not low and failure of welded or riveted joints leads to rapid and catastrophic failure. This design is not fail-safe since it lacks ability to transmit torque for any length of time after initial failure occurs.

Maintenance, Service, and Replacement Criteria

The following maintenance, service, and replacement criteria are recommended for the four basic coupling types.

For a gear coupling, the following criteria are recommended:

- . Requires periodic lubrication and inspection intervals to observe signs of overheating or loss of lubricant.
- . Access for inspection and lubrication must take into consideration necessity for removal and disassembly of coupling for this procedure.
- . Specific MTBR's should be observed although failure is progressive.
- . Shimming for axial location is not necessary, but shaft should have some means provided for axial restraint.
- . Coupling should be replaced when excessive backlash or vibration is detected.

For a disk coupling, the following criteria are recommended:

- . No maintenance or lubrication requirement.
- . Access for inspection is mandatory to determine if laminates are cracked.
- . Provisions for rotating the coupling and observation of all fastener interfaces are necessary.
- . With few exceptions, "on condition" replacement is used. Coupling can still operate after initial distress. Installation procedure normally requires shimming shaft flange for accurate axial positioning to avoid building in an initial bending stress.

For a diaphragm coupling, the following criteria are recommended:

- . No maintenance or lubrication required.
- . Access for inspection mandatory to inspect all diaphragm surfaces for scratches, dents, cracks, and rust by rotating coupling.
- . Coupling should be replaced where excessive backlash or vibration is detected. Shimming for axial location is not normally required, but shaft must have some means provided for axial restraint.
- . Coupling removal based on rated MTBR.

For an elastomeric coupling, the following criteria are recommended:

- . No maintenance or lubrication required.
- . Access for visual inspection to determine condition of elastomer and bond required.
- . Coupling to be replaced "on condition." Failure is progressive and coupling can function at moderate speeds and torques after initial failure has occurred.
- . Coupling should be replaced when cracking, flaking, bulging, or other signs of elastomer deterioration or separation of bond are observed.

Installation normally requires shimming for length. Coupling can provide its own axial restraint.

Typical Failure Modes

The following paragraphs discuss and give examples of typical failure modes of the four basic types of couplings.

The flexible disk coupling exhibits cracks in the outer laminations in close proximity of the spherical washer. Fatigue cracks originate at localized fretting areas of contact where the disk packs are secured by fasteners to the respective flanges. A slight gap or bulging of the laminate in the edge view indicates a laminate failure. Because the outer laminations can be easily observed, this type failure is readily detectable during normal inspection intervals. Figure 7 shows an example of a fatigue crack approximately halfway through the top laminate. This disk pack would ordinarily have many more hours of life if operated in this condition.

Failure of a gear coupling is accompanied by vibration and overheating and is progressive, taking place over a substantial period of time. Loss of lubricant due to seal leakage or "boiling off" due to overheating results in gear tooth pitting and spalling. Ultimately, the gear tooth fails as shown in Figure 8.

The failure of the diaphragm coupling is relatively rapid and catastrophic. Failure of a diaphragm is precipitated by fatigue cracks originating at stress concentrations such as spline root radii, rim-wells, clamp rings, or rivet joints, depending on the coupling construction. Figure 9 shows the propagation route of a typical failure of this type coupling. Signs of distress are vibration, or at very low speeds, an audible clicking sound.

The failure of the elastomeric coupling is progressive, and the coupling can continue to operate for an appreciable period of time subsequent to the initial failure. Vibration is a reliable distress signal, and visual inspection will reveal rubber shedding or cracking, or bond separation at the flange fingers. The failure shown in Figure 10 has progressed to an extreme degree where fatigue failure of the flange member has taken place.

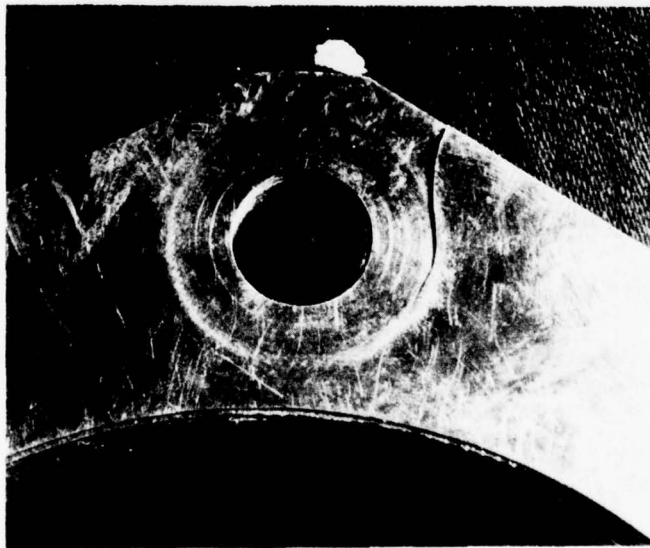
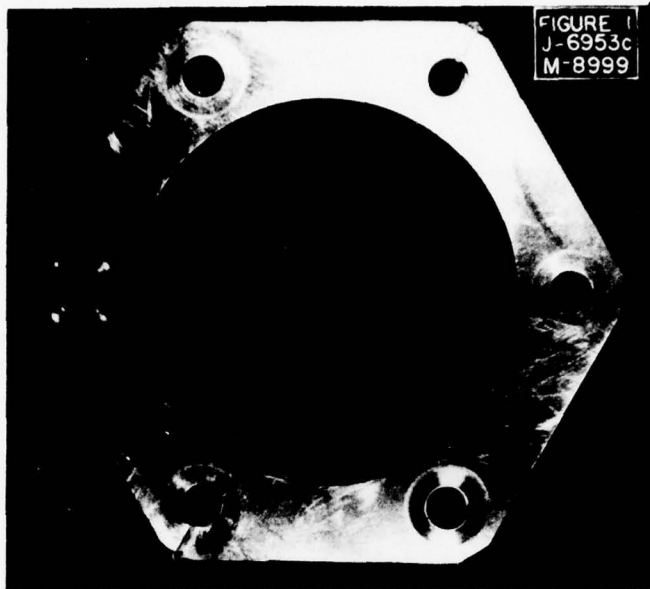


Figure 7. Typical Fracture, Flexible Disk Coupling.

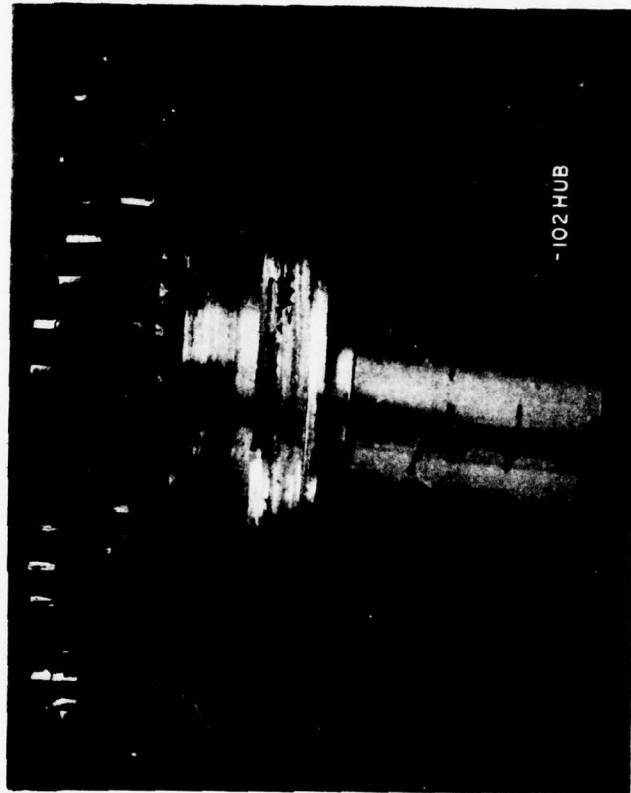


Figure 8. Typical Fracture, Gear Coupling.

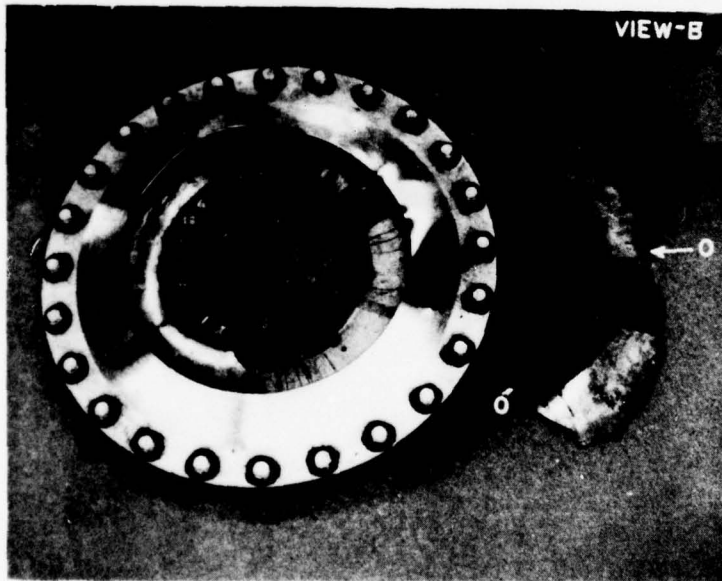
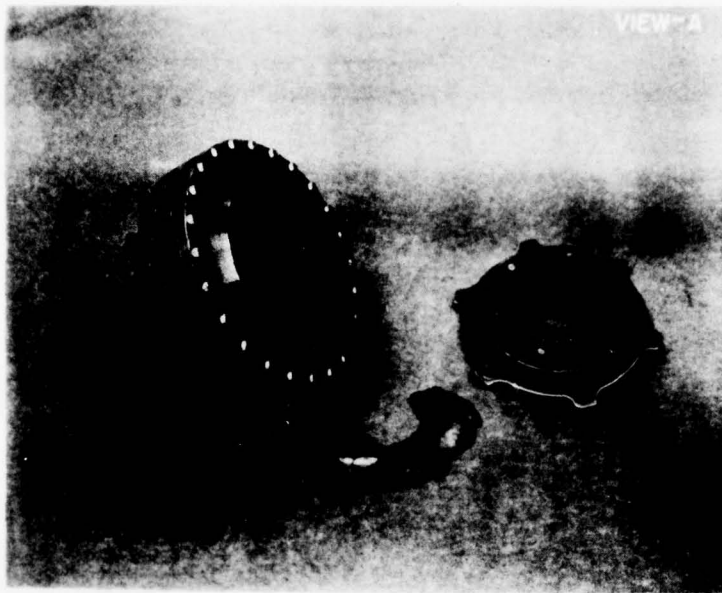


Figure 9. Typical Fracture, Diaphragm Coupling.

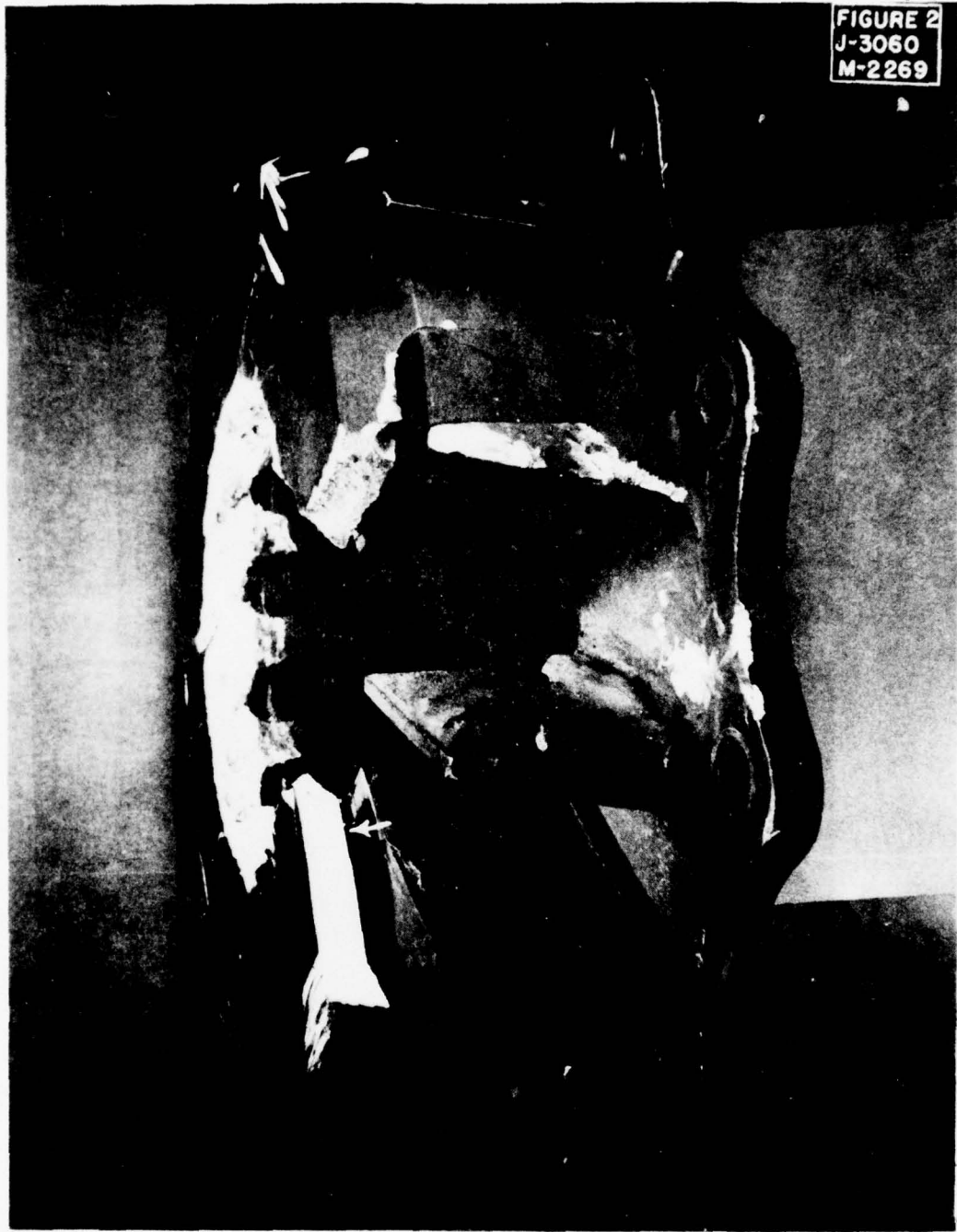


Figure 10. Typical Fracture, Elastomeric Coupling.

CURRENT APPLICATIONS BASELINE

The survey of current helicopter coupling applications was divided into two categories. Low-speed couplings ranging in operating speeds from 2000 to 5000 rpm were placed in one category, while high-speed couplings ranging in operating speeds from 6000 to 25,000 rpm were placed in the second category.

Low-Speed Couplings

Low-speed couplings are used in tail rotor drive shaft and interconnecting rotor shaft drive systems. In this application, the angular misalignment capacity required is small, the torque capacity high, and the speed low.

The angular misalignment capacity required is small as a result of the long drive shaft segments used to reduce weight by limiting bearing supports. For instance, a shaft segment of 6 feet in length would require a combined installation and deflection displacement of .625 inch to produce a continuous 1/2 degree angular misalignment at the coupling.

Of the four types of couplings, the flexible disk coupling is the most widely used in the low-speed group.

The tail rotor drive shaft and interconnecting rotor shaft coupling applications were further divided into three groupings of light, medium, and heavy helicopter categories with respective gross weights of zero to 10,000 lbs, 10,000 to 20,000 lbs, and 20,000 to 120,000 lbs, respectively.

The basic coupling parameters of speed, torque, and angular misalignment for this category of low-speed couplings are shown in Table 1.

High-Speed Couplings

High-speed couplings are primarily used in engine drive shaft systems. Since multiengine helicopter propulsion systems are common, the high-speed coupling group cannot be categorized by helicopter gross weight.

The high-speed engine drive shaft coupling is basically a high torque, low angular misalignment coupling. The most demanding operational constraint in high-speed couplings is that of misalignment because of the induced vibratory stress. The effects of mass imbalance were also amplified, being a function of the speed squared.

TABLE 1. LOW-SPEED COUPLINGS, TAIL ROTOR DRIVE AND INTERCONNECTING ROTOR SHAFTS

Gross Weight (lb)	Shaft Type	No. of Segments	Avg Length (ft)	Speed (rpm)	Torque (in.-lb)	Angular Misalignment (deg)	Coupling Type
			<u>LIGHT HELICOPTERS</u>				
9000	T.D.S.	5	5	3900	2260	1/2	Gear
3000	T.D.S.	3	N/A	6000	330	1/2	Flexible Disk
4483	T.D.S.	6	5	4550	880	1/2	Flexible Disk
2400	T.D.S.	1	15	2046	985	1/2	Diaphragm
			<u>MEDIUM HELICOPTERS</u>				
20,800	I.R.S.	5	6	2574	34,000	1/2	Flexible Disk
15,500	T.D.S.	5	5	4200	5000	1/2	Flexible Disk
12,500	T.D.S.	4	6	3300	5345	1/2	Flexible Disk
13,000	T.D.S.	2	12	3150	5600	1/2	Elastomeric
18,626	T.D.S.	2	15	3030	7270	1/2	Flexible Disk
			<u>HEAVY HELICOPTERS</u>				
33,000	I.R.S.	7	5	7040	35,000	1/2	Flexible Disk
35,000	T.D.S.	6	7	3011	15,700	1/2	Flexible Disk
35,000	P.D.S.	1	9.5	2298	20,600	1/2	Flexible Disk
38,000	T.D.S.	6	6.6	3016	14,000	1/2	Flexible Disk
38,000	P.D.S.	1	5.7	2468	17,000	1/2	Flexible Disk
57,000	T.D.S.	6	7.0	4271	25,400	1/2	Flexible Disk
57,000	T.D.S.	1	9.5	2628	41,000	1/2	Flexible Disk

The survey of data for high-speed applications is shown in Table 2.

Coupling Stiffness Ranges

Torsional, axial, and bending stiffnesses of couplings influence the characteristics of the drive system. Axial and bending stiffness influences the load transmitted to the supporting structure and bearings positioning the shaft. Torsional stiffness affects the shaft system response to variations in the power being transmitted.

Each coupling must be evaluated on the basis of its individual stiffness characteristics for the particular drive system application, since stiffness attributes vary greatly. Table 3 consists of general stiffness ranges exhibited by the four coupling types.

FUTURE REQUIREMENTS BASELINE

After developing the data for present coupling operational capabilities, the next task was to define the requirements that would encompass future helicopter drive system needs. Preliminary analysis indicates that helicopter propulsion systems of the future will use lightweight, high-speed turbines now in the development or planning stage. Plans also call for the implementation of vibration isolation systems to provide improved comfort levels for crew and passengers.

Current couplings that can meet the high-speed, high-angular-misalignment requirement are relatively heavy, require lubrication and servicing, and involve tenuous maintenance, balance, and inspection procedures.

Torque and Speed Requirement

To identify the future speed requirement of helicopter couplings, a chart of advanced turbine technology data (Table 4), was compiled. From this data Figure 11 was derived showing speed versus torque trends along with current baseline speed/ torque relationships. As can be seen from Figure 11 and Table 4, the highest future requirement for speed is approximately 20,000 rpm.

TABLE 2. HIGH-SPEED COUPLINGS, ENGINE DRIVE SHAFTS

Horsepower	Speed (rpm)	Torque (in.-lb)	Misalignment (deg)	Weight (lb)	Coupling Type
700	2300	19,150	.5	5.32	Elastomeric
1520	2520	38,000	.33	10.77	Elastomeric
2100	2600	51,000	.33	9.96	Elastomeric
1250	18966	4,040	.5	2.98	Flexible Disk
670	19500	2,160	.5	2.3	Gear
4000	9000	28,000	.33	3.78	Flexible Disk
3200	6000	33,000	.5	2.95	Flexible Disk
3600	6000	42,000	1.0	3.00	Flexible Disk
1500	20000	4,720	.5	2.40	Flexible Disk
4000	16000	33,600	.5	3.00	Flexible Disk
1400	6300	14,100	1.0	7.5	Gear

TABLE 3. COUPLING STIFFNESS RANGES

	Flexible Disk	Diaphragm	Gear	Elastomeric
Torsional in.-lb/radian	200,000/ 800,000	4,000,000/ 400,000,000	5,000,000/ 500,000,000	200/ 600,000
Axial lb-in.	200/ 1500	small	small	100/ 300,000
Bending in.-lb/radian	400/ 10,000	10/ 1000	small	100/ 500,000
Radial lb-in.	200,000/ 4,000,000	50,000/ 2,000,000	1,000,000/ 400,000,000	100/ 100,000

TABLE 4. ADVANCED TURBINE TECHNOLOGY

Manufacturer	Designation	Max Cont Horsepower	Output (rpm)	Status
<u>U.S. Engines</u>				
Allison	250-C28	478	6016	Development
Allison	250-C30	598	6016	Proposed
Allison	XT70-AD-700	8000	11500	Development
Garrett	TSE-231-1	403	6000	Development
Garrett	TSE-731-P2	3600	9600	Proposed
General Electric	T64/S5C1	4625	15600	Proposed
General Electric	T700-GE-700	1250	20000	Development
Lycoming	T5319A	1500	6450	Development
Lycoming	LTS-101-650	550	5966	Development
Lycoming	LTC-4B-12	3600	16000	Proposed
Lycoming	LTC-4V-1	4200	17000	Proposed
Lycoming	PLT-27A	1832	20000	Proposed
UACL	PTGB-34	750	6230	Development
<u>European Engines</u>				
Rolls Royce	H1400-1	1250	19500	Production
Turbo Meca	TURMO IIIC	1260	22340	Production

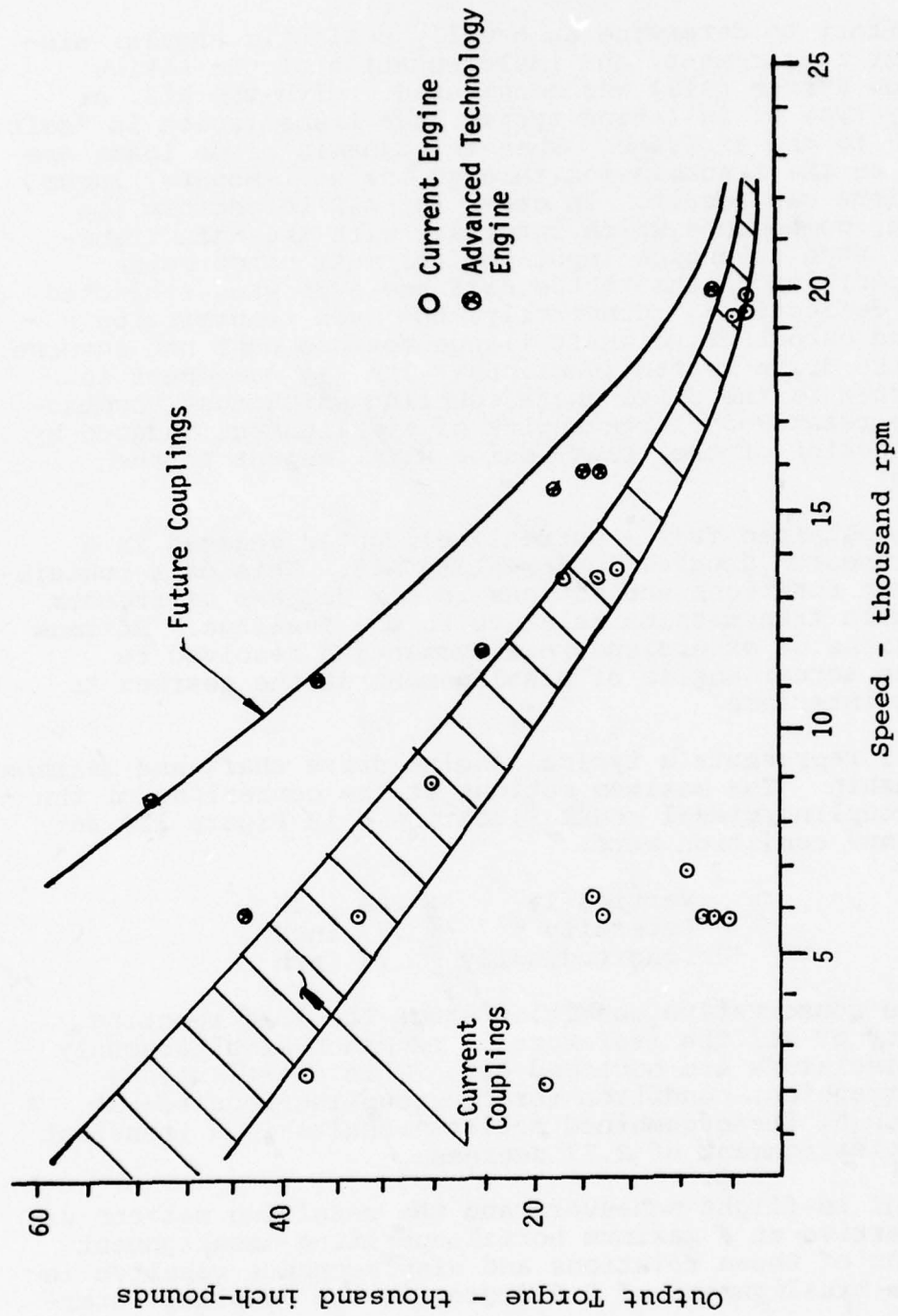


Figure 11. Torque versus Speed Trending, High-Speed Engine Couplings.

Angular Misalignment Requirement

In an effort to determine an equally realistic angular misalignment requirement, the implementation of the Active Isolation System (AIS) was considered. With the AIS, or with any type of isolation system, the transmission is "soft mounted" to the airframe. When aerodynamic blade loads are imposed on the transmission through the soft mounts, large deflections can result. In order for AIS to perform its function, components which interface with the main transmission, such as engine input shafts, must not provide significant load paths to the airframe even when subjected to high deflections. Conversely, the main transmission's input and output drive shaft flange motions must not adversely affect the drive system functions. The key component in this system is the drive shaft coupling which must accommodate the relatively large angles of misalignment induced by the deflection of the transmission with respect to the airframe.

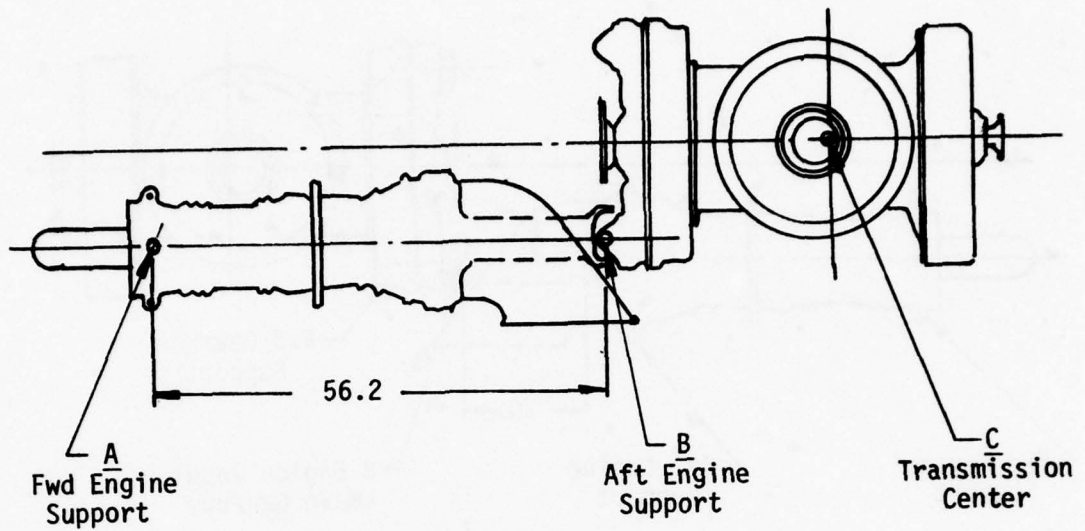
Data was obtained from a current helicopter engaged in a flight research program implementing AIS. This data contained maximum rotations and motions in six degrees of freedom of the main transmission relative to the fuselage. Maximum combinations of excursions were chosen and resolved to determine actual angles of misalignment at the gearbox to coupling interface.

Figure 12 represents a typical engine drive shaft and gearbox relationship. The maximum motions at the centerline of the engine coupling/gimbal mount (location B in Figure 12) for the maximum condition were:

Vertically	+ .66 inch
Laterally	+ .77 inch
Longitudinally	+ .74 inch

This is a conservative condition where the load reacting capability of all the isolators is exceeded simultaneously and the isolators are bottomed out. This constitutes a maximum transient condition for the coupling requirement. A resolution of these combined motions results in a transient angular misalignment of 2.77 degrees.

A study of in-flight maneuvers and the resulting motions was made to arrive at a maximum normal operating misalignment. Resolution of these rotations and displacements resulted in a maximum misalignment of 0.6 degree at the coupling interface.



Normal Installed Position

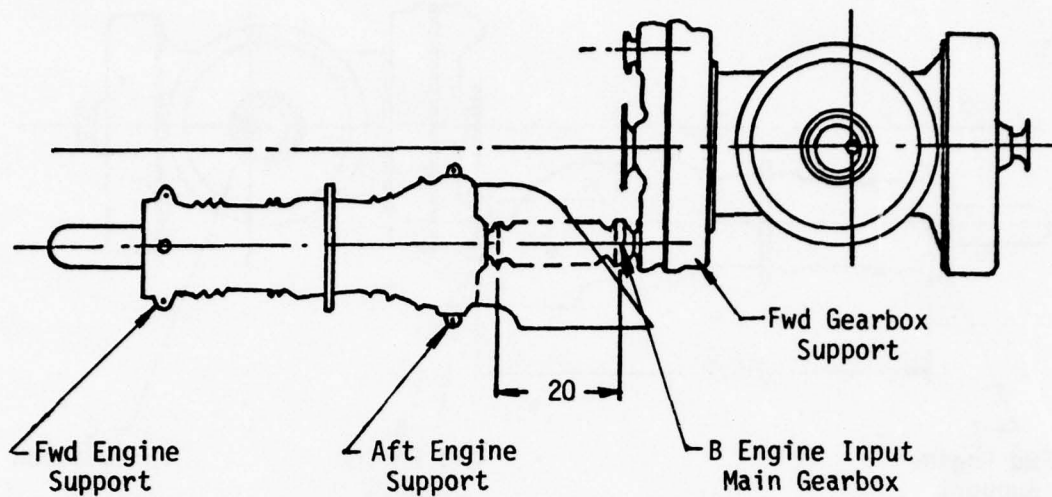
	<u>A</u>	<u>B</u>	<u>C</u>
STA.	218.42	274.65	302.75
WL.	268.82	266.86	246.60
B.L.	12.00	12.00	0.00

Maximum Rotated Position (Isolators Bottomed)

	<u>A</u>	<u>B</u>	<u>C</u>
STA.	219.18	275.39	302.75
WL.	268.82	267.52	246.60
BL.	12.00	12.67	0.00

Maximum change in angle at B - 2.77°

Figure 12. Engine/Gearbox Preferred Configuration, A.I.S. Motion Study.



Maximum operating displacement determined in study at location
 $B = .326$ inch.

Angular misalignment due to this displacement seen by coupling
 located at $B = 0.93^\circ$

Allowance for installation at $B = 0.33^\circ$

Maximum operating angle = 1.26°

Maximum operating requirement of coupling to be developed in the
 program = 1.50°

Figure 13. Engine/Gearbox Alternate Configuration,
 A.I.S. Motion Study.

It is observed that certain engine installations are self-supporting. That is, both engine and gearbox are independently mounted to the airframe and subsequently coupled together by a short drive shaft (see Figure 13). Applying identical input flange excursion to this particular mounting configuration results in a much greater operating angular misalignment requirement of .93 degree.

Upon the basis of these studies, a realistic but conservative coupling misalignment requirement of 1.5 degrees continuous and 3.0 degrees transient was established for a speed of 20,000 rpm. This point is plotted on the misalignment versus speed coupling curve of Figure 14 and shows the order of improvement to be achieved in attaining this program goal.

The following requirements definition was formulated as a result of the Future Requirements Study.

Requirements Definition

Mandatory Requirements

- . Torque 4727 in.-lbs (1500 hp)
- . Speed 20,000 rpm
- . Angular Misalignment
 - Continuous 1.5 deg
 - Transient 3.0 deg
- . Constant Velocity Ratio
- . No Lubrication or Service Requirement
- . Long Life 2500 hr MTBR
- . Fail-Safe Construction
- . Broad Environmental Application
 - Temperature Range -65°F to 250°F
 - Dust, Sand, Water, Salt Spray, Snow and Ice
 - (Qualification Test per MIL-STD-810B)

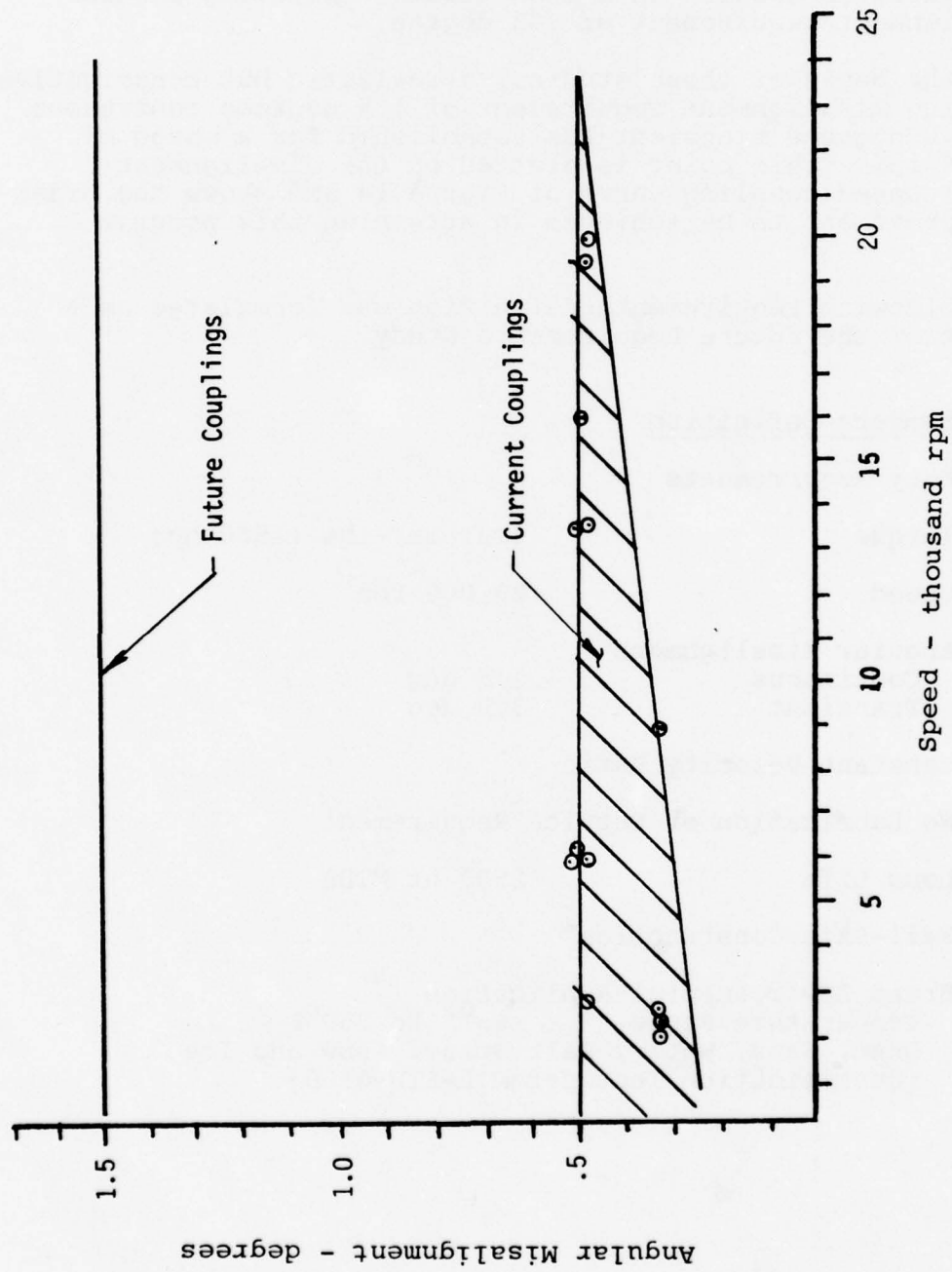


Figure 14. Angular Misalignment versus Speed, High-Speed Engine Couplings.

Design Goals

- . Light Weight 1 lb or less
- . Ease of Installation and Removal
- . Angular Misalignment
 - Continuous 3 deg
 - Transient 5 deg

Constant Velocity Ratio

The rotational velocity of the driving and driven member should remain constant during transmission at angular misalignments. It is important that cyclic torsional pulsations are not generated by the coupling, as they would have an adverse effect on engine or gearbox.

No Lubrication or Service Requirements

Some couplings have parts with moving contact that require lubrication and maintenance. The rubbing parts generate heat, are subject to wear, and the coupling performance rapidly deteriorates. Moreover, the lubricant seals limit the couplings' environmental and shelf life and make mandatory frequent inspection and service intervals. Future couplings should not require lubrication, so the above problems will not be encountered.

Substantial MTBR

Aircraft dynamic components have a mean-time-between-removal (MTBR) rate for scheduled removals for overhaul, repair, or inspection, and unscheduled removals for failures. Removals for modifications, cannibalization, or to facilitate other in-aircraft maintenance are excluded. Component MTBR has a direct influence on aircraft availability and readiness, maintenance burden, spares requirement, and reliability. The future coupling should have an MTBR substantially above state-of-the-art designs.

Fail-Safe Construction

A practical and sound safeguard against catastrophic failure from fatigue or other damage is a fail-safe structure. This is in keeping with present aircraft design philosophy which

dictates that the component must sustain approximately limit loads with any one of its elements failed. In the future coupling, the flexure element should be designed to cope with this requirement.

Broad Environmental Application

In military helicopter coupling applications, the operational environment runs to extremes. Temperatures vary ranging from arctic to equatorial. Combinations of moisture, sand, dust, salt, and ice adversely influence the surfaces in close proximity because the airframe normally provides little shelter from exposure to these elements. All parts must be treated for protective finishes, and insulation of dissimilar material becomes extremely important for the coupling and interface hardware in this rugged environment.

Care must be exercised in excluding the formation of natural pockets or crevices that will permit buildup of corrosive deposits of sand, salt, or moisture or provide physical obstruction which limits functional deflection of component parts.

COUPLING DESIGN

CONCEPTUAL DESIGN

The initial objective of the conceptual design phase of the program was to generate new and innovative coupling concepts that would enable the coupling design objectives to be met or exceeded. In addition, consideration was given to parameters such as envelope size, economy of fabrication, simplicity of construction, and overall adaptability to helicopter drive system constraints.

As a result of the patent data search, data from coupling fabricators, and engineering brainstorming sessions, several novel concepts began to emerge. Basically, the coupling envisioned was to have no moving parts and thus eliminate the necessity for servicing and lubrication (in other words, a flexure element coupling).

Research and prototype demonstration programs had already indicated potential for the use of fiber reinforced composite materials. The high strength, low modulus properties inherent in these composites are ideal for a coupling flexure member. Composites also offer additional attractive properties such as low weight, excellent fatigue properties, low cost, and ease of fabrication.

A composite material consists of reinforcing filaments (boron, graphite, glass, etc.) imbedded in a matrix (epoxy, resin, or aluminum) which supports and carries the reinforcement. A laminated composite consists of stacking several plies or layers in preferred orientations. This network of plies is subsequently cured, forming a single element having homogenous properties of stiffness and strength. Depending on the fiber orientation, the strength of the cured element can be different in each direction.

The use of composites also offers adaptability to construction by laying up the impregnated plies in various thicknesses to provide the precise section properties desired. Having decided to use a composite flexure element, the next step was to determine whether to use a composite tape or a continuous filament winding. In addition, each coupling configuration was considered individually for the type of composite to be used. This was determined analytically by applying the particular composite material properties to the geometry of the load, joint, and wrap applicable to each concept.

As a result of this conceptual design effort, seven concepts were conceived, all but one employing a composite flexure member. These concepts were subsequently analyzed and evaluated using the following design conditions where ϕ is the angular misalignment:

.	Speed	=	20,000 rpm
.	HP	=	1500
.	ϕ (continuous)	=	1.5 deg
.	ϕ (transient)	=	3.0 deg

Diaphragm Coupling

The diaphragm coupling shown in Figure 15 is attractive because of its simplicity and one-piece construction. This configuration eliminates load transfer joints and loose parts that affect balance and add weight.

The typical failure mode of the metallic diaphragm counterpart is fatigue crack initiation followed by rapid crack propagation leading to eventual complete loss of drive. The chance of this catastrophic type failure would be reduced in a composite diaphragm by virtue of ply orientation in the composite buildup which would increase crack propagation time.

Loop-Belt Coupling

The loop-belt concept shown in Figure 16 employs a flexure element fabricated of unidirectional composite tape. The three driving belts are the primary tension members connecting the alternate lobes of the input and output flange adapters.

The driving belts are constructed by winding tape in a fixture around fittings at the fastener locations until the desired thickness is obtained. A subsequent wrap of much thinner section in the form of a circumferential belt is employed to maintain proper spacial relationships and to combine the three belts into an assembly.

This concept features simplicity of construction utilizing unidirectional composite tape.

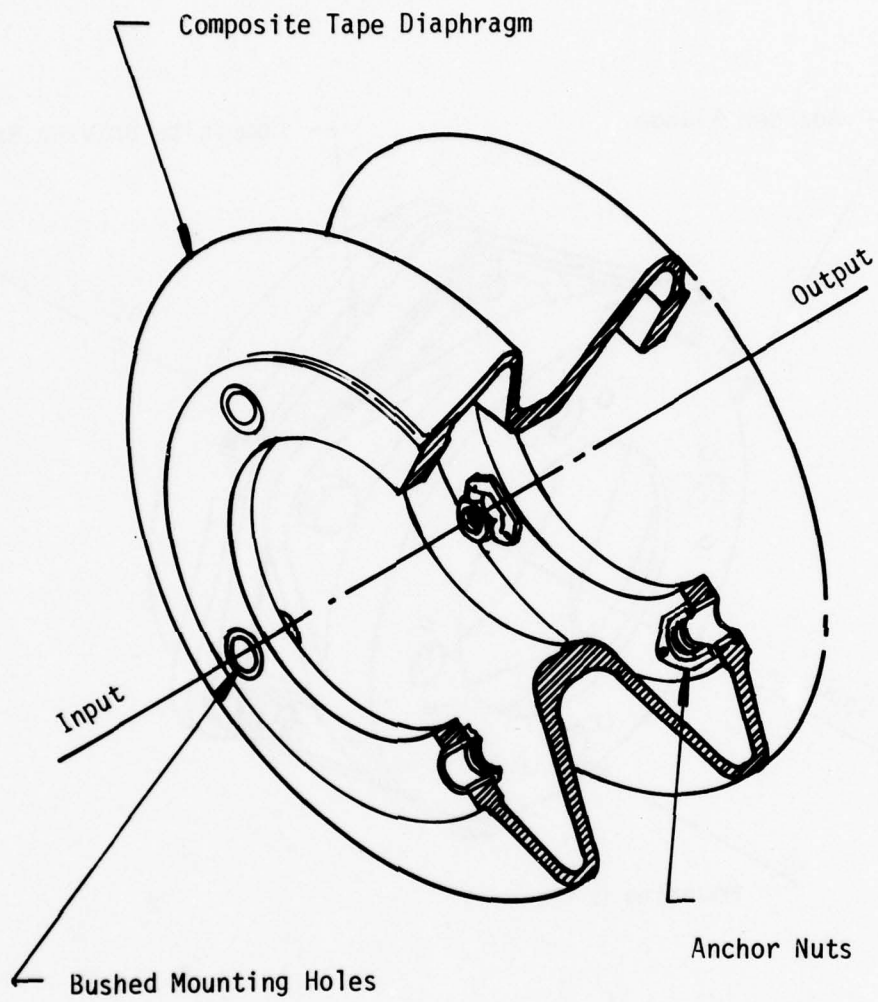


Figure 15. Diaphragm Coupling Concept.

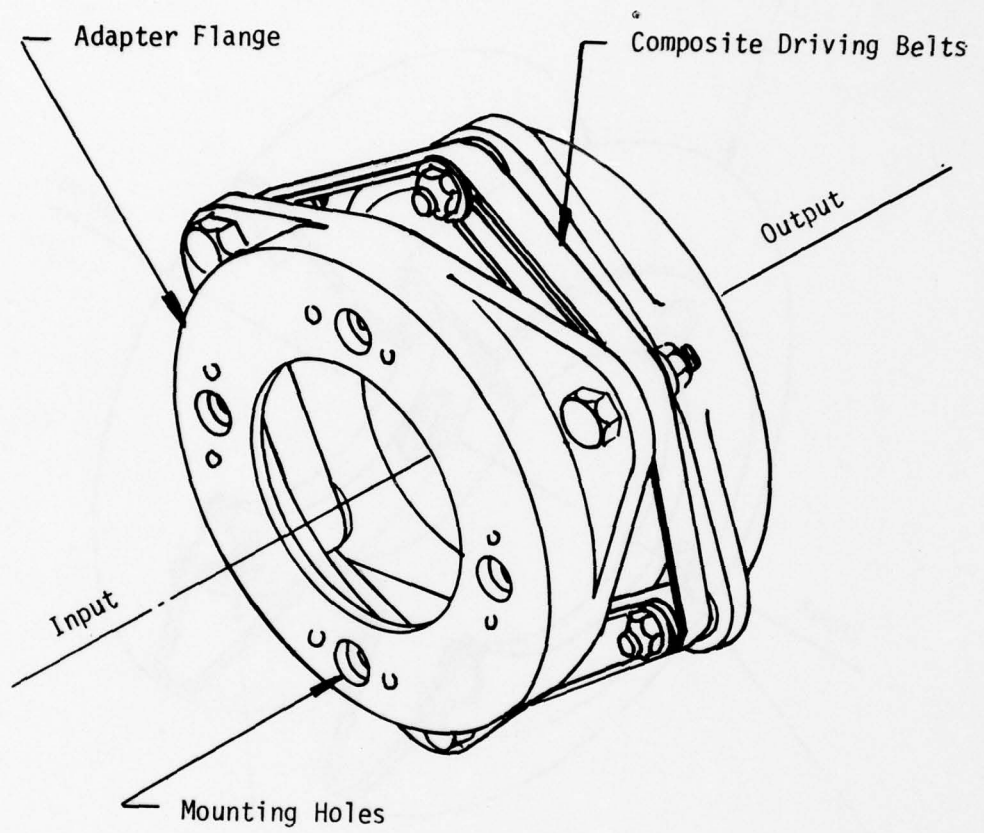


Figure 16. Loop-Belt Coupling Concept.

Circumferential Belt Coupling

Figure 17 illustrates the concept of a belt which utilized unidirectional composite tape wound over the alternating lobes of the input and output flange members. The circumferential strap, which carries the torque through tension, is reinforced by +45° cross plies at the load transfer joints. The cross section of the flexure segment can be optimized to provide load and angular misalignment capacity while maintaining acceptable stress levels.

The design is simple and compact and has economy of construction, low unit weight, and absence of loose parts. The design of the connection at the composite strap is the key to success of this coupling.

Elastomeric Coupling

The concept shown in Figure 18 is not new, but has been used with a measure of success in the helicopter industry. The elastomeric coupling has excellent misalignment and torque-carrying capacity but in the past has experienced rubber block and bond failures traceable to what in current technology is known as poor shape factor. Failure due to compression instability at certain combinations of torque and speed is the result.

A modification, as illustrated here, was considered a candidate concept for the coupling to be developed in the program.

Filament-Wound Coupling

The coupling shown in Figure 19 is comprised of four filament-wound composite flexure members, each being a separate unit wound around a half-spool fitting at either end. The members are secured by fasteners at alternate lobes of the driving and driven flange adapters.

The filament-wound coupling configuration lends itself to the use of a filament composite fiber as opposed to composite tape construction. The uninterrupted filaments wound around the load transfer fittings should prove beneficial in this critical area.

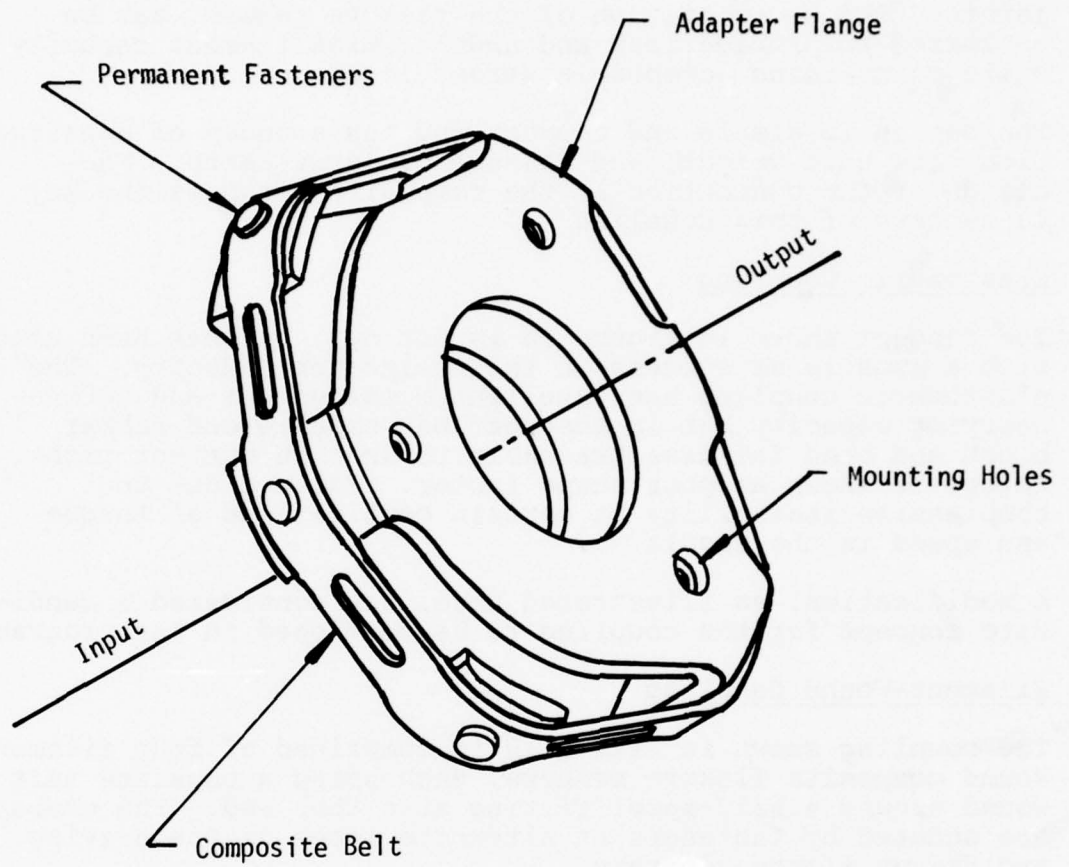


Figure 17. Circumferential Belt Coupling Concept.

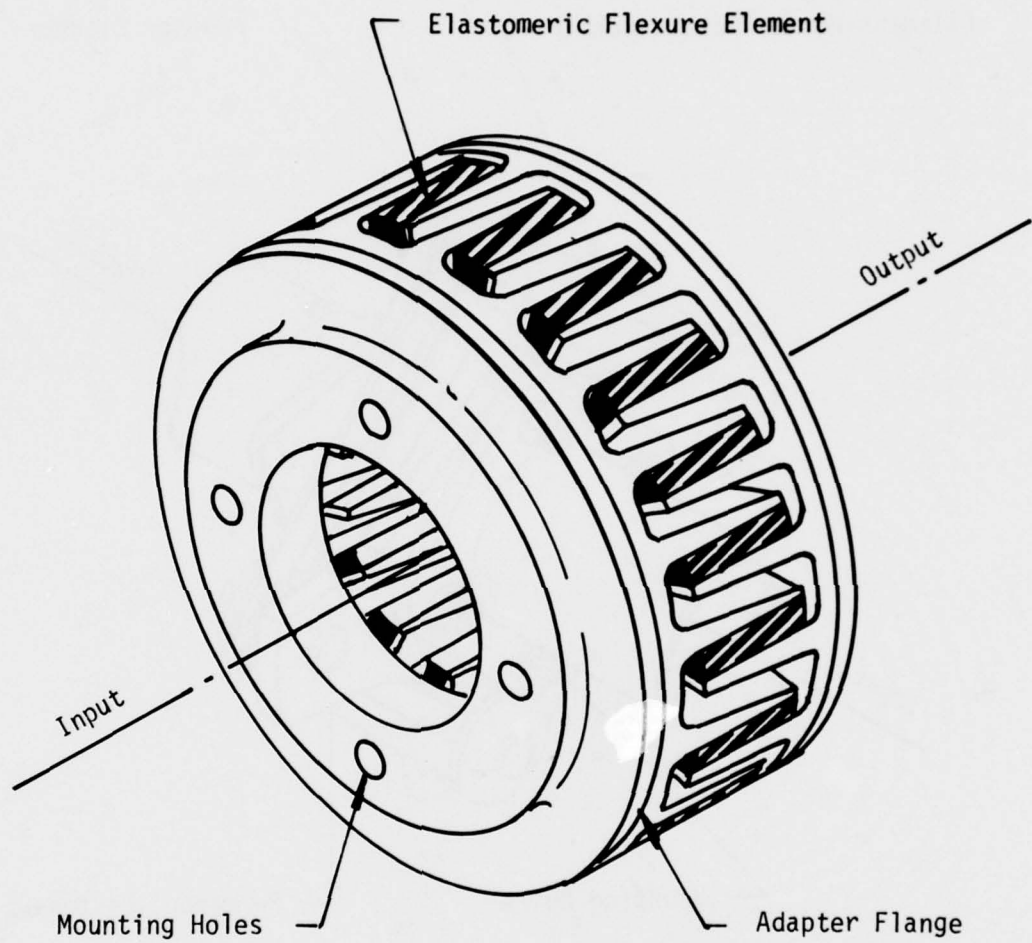


Figure 18. Elastomeric Coupling Concept.

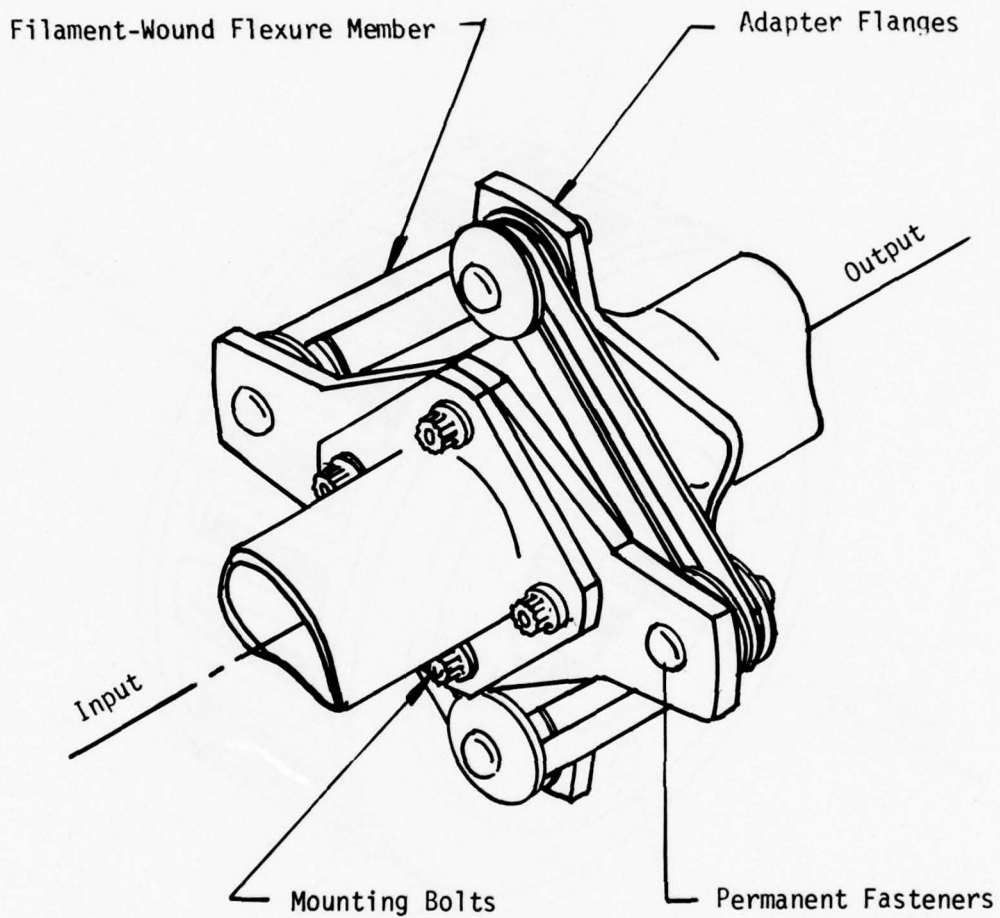


Figure 19. Filament-Wound Coupling Concept.

Tension Strap Coupling

The tension strap coupling shown in Figure 20 has four flexure members loaded in tension. In a conventional disk type coupling, alternate segments of the flexure member are loaded in tension and compression. Since the segment in tension is an order of magnitude stiffer than the segment in compression, the compression segment's contribution in the driving effort is negligible.

By eliminating the compression portion of the coupling, an additional driving member can be added. Each driving member is of greater length for the same coupling envelope size, which yields two benefits. First, the section can be made 25% thinner for the same axial stress because the load per member is reduced. Second, the length of each flexure element is substantially increased by virtue of the coupling geometry. This combination of a thinner and longer member provides for increased angular misalignment capability at the same low bending stress.

This coupling is designed to transfer torque primarily in one direction, which does not present a problem for helicopter applications.

Helical Strap Coupling

The concept of the helical strap coupling shown in Figure 21 is similar to that of the tension strap coupling of Figure 20, i.e., it is comprised of four flat helical cantilever tension members which act as driving/flexing members connecting the input and output flanges. The coupling is fabricated from unidirectional composite tape wound around an arbor until an annulus of the required proportion is formed. After the curing process, the helical straps are formed by machining four helical slots 180 degrees long phased 90 degrees apart. With this method of fabrication, the stresses at the ends of the slots are high. A better joint design can be obtained by building the coupling as a layup, but the manufacture becomes more expensive.

The unit construction eliminates joint load transfer problems, assembly procedures, and loose hardware.

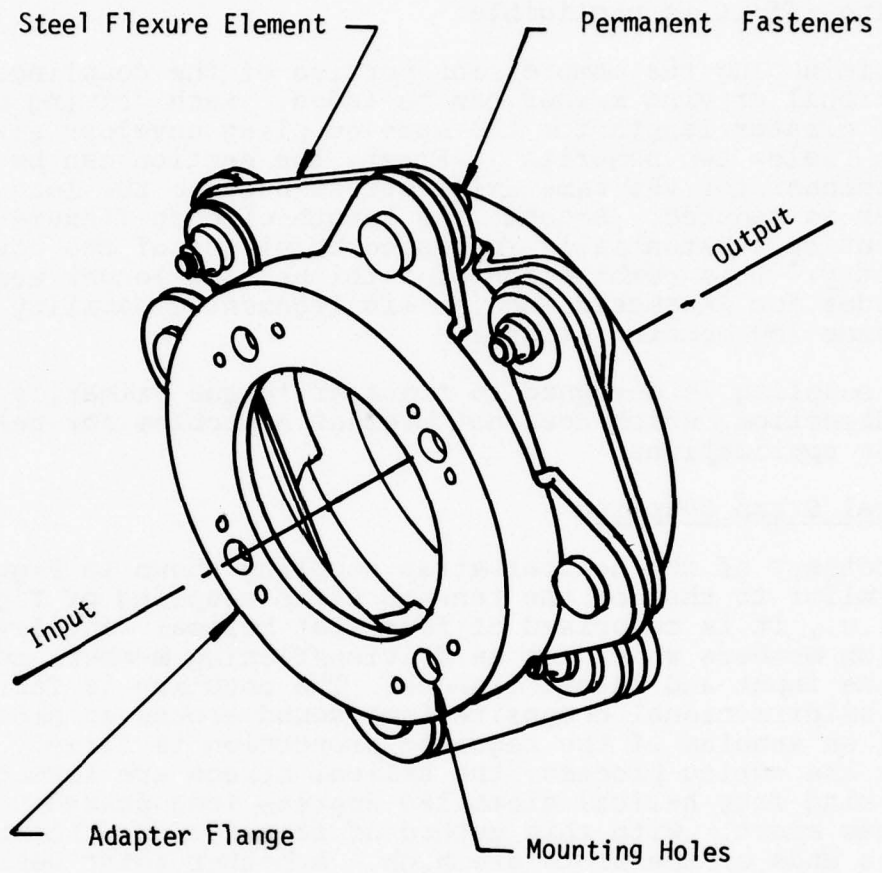


Figure 20. Tension Strap Coupling Concept.

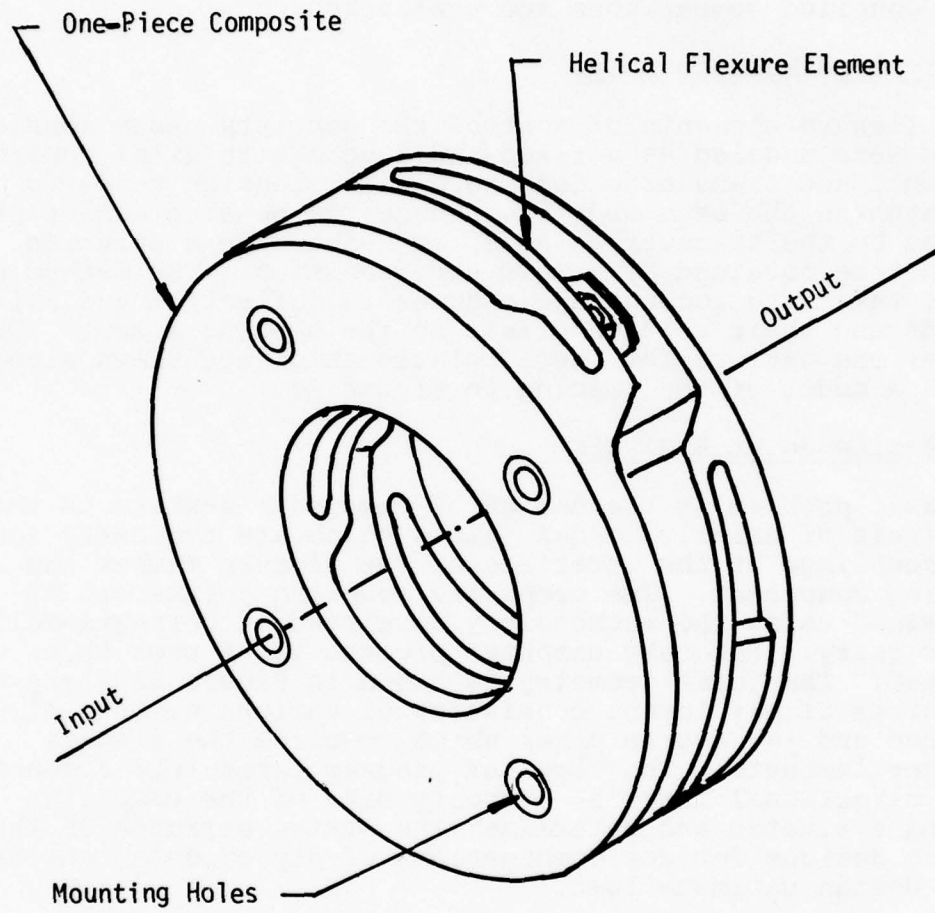


Figure 21. Helical Strap Coupling Concept.

PRELIMINARY DESIGN

During this portion of the program, the coupling concepts were analytically sized and evaluated using the future operational requirements. The following paragraphs discuss typical analytical procedures used which provided the basis for coupling comparisons and evaluation.

Basic Load Relationships

The flexure elements of most of the concepts under consideration were modeled as a fixed ended beam with axial tension, moment, and transverse loading. Axial tension tends to straighten the beam and thus reduce the bending moment produced by the transverse loads, in which case a solution cannot be obtained by simple superposition. The method used must take into account the changes in deflection and axial loads and their related effect on the bending moment. The equations derived for these relationships are shown along with a model of the loading in Figure 22.

Composite Joint Analysis

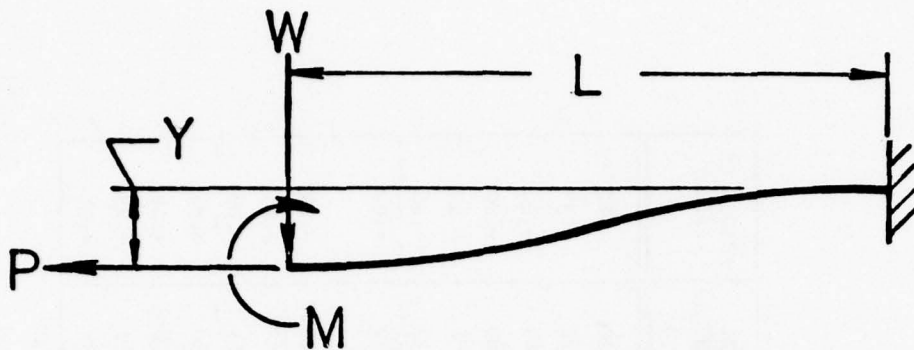
A basic problem in the design of composite members is the analysis of axially loaded joints which are typically found in couplings at the interface of the flexure member and its mating component. The composite coupling joints can be designed using the methodology developed at Carnegie-Mellon University. Sikorsky computer program Y205A uses this method. The joint geometry is shown in Figure 23 along with a matrix of ply layups consisting of various numbers of 0 degree and +45 degree plies which comprise the flexure member laminate. The computer program takes into account the directional material property data of the composite being evaluated and determines the static strength of the joint designs for any combinations of ply orientations at the design ultimate load.

Bearing failure tends to be the critical failure mode in Kevlar due to its low compressive strength (40,000 psi) in the fiber direction. All the designs shown in Figure 23 are critical in bearing. The mixture of 0 degree to +45 degree plies indicated in these joints was based on information obtained from previous computer runs. The equation for the Margin of Safety is

$$M_S = \frac{F \text{ allowable}}{F} \quad (3)$$

where

$$F = \text{stress in psi}$$



$$M = \frac{W (\cosh KL - 1)}{K (\sinh KL)} \quad (4)$$

$$Y = \frac{W}{P} \left[KL - \tanh KL - \frac{(\cosh KL - 1)^2}{\sinh KL \cdot \cosh KL} \right] \quad (5)$$

$$K = \sqrt{\frac{P}{EI}} \quad (6)$$

WHERE:

M = BENDING MOMENT, IN-LB

Y = DEFLECTION, IN.

W = TRANSVERSE LOAD, LB.

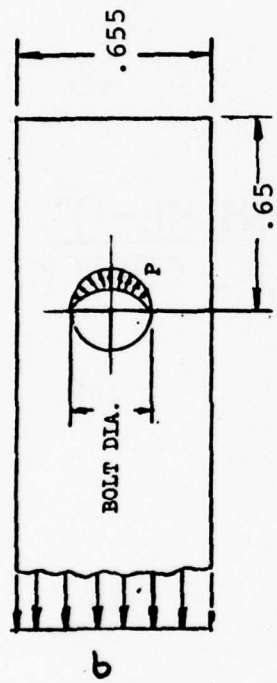
P = TORQUE LOAD, LB.

E = MODULUS OF ELASTICITY

I = MOMENT OF INERTIA, IN.⁴

L = LENGTH OF FLEXURE ELEMENT, IN.

Figure 22. Basic Load Model.



Joint Number	Bolt Dia. (in.)	Number ±45° Plies	Thickness ±45° Plies (in.)	Number 0° Plies	Thickness 0° Plies (in.)	Total Thickness (in.)	Margin of Safety
1	0.25	16	.088	24	.132	.220	-.42
2	0.25	18	.099	26	.143	.242	-.35
3	0.25	20	.110	28	.154	.264	-.28
4	0.25	22	.121	30	.165	.286	-.20
5	0.25	24	.132	32	.176	.308	-.13
6	0.25	26	.143	34	.187	.330	-.06
7	0.25	28	.154	36	.198	.352	+0.02
1	0.3125	16	.088	24	.132	.220	-.24
2	0.3125	18	.099	26	.143	.242	-.15
3	0.3125	20	.110	28	.154	.264	-.06
4	0.3125	22	.121	30	.165	.286	+0.04
5	0.3125	24	.132	32	.176	.308	+0.14
6	0.3125	26	.143	34	.187	.330	+0.23
7	0.3125	28	.154	36	.198	.352	+0.31

Figure 23. Composite Joint Model and Ply Mix Matrix.

Material Selection

Normally the stresses developed by the operating torque alone have only a secondary effect upon the endurance of any coupling. The prime source of failure is fatigue damage incurred by the alternating stresses resulting from angular misalignment. Consequently, the ideal material for the coupling flexure member has three basic mechanical properties: high strength, low bending modulus, and high fatigue endurance. Of all the fibers examined, Kevlar 49 embodies the best combination of these basic properties. Table 5 gives material properties for some typical composites. Figure 24 is an S/N curve comparison of Kevlar with two other low modulus composites: E- and S-Glass/Epoxy. Boron and graphite have excellent strength and fatigue properties, but have a relatively high bending modulus. It should be noted that these curves represent unidirectional fibers with a minimum to maximum stress relationship of $R = .1$.

The data on Kevlar 49 is presented in Figure 25 as a Goodman diagram which is a convenient form for the design analyst. An allowable working stress for the material is found by multiplying the mean allowable by the reliability factor ($R = .61$ for three sigma).

Typical Coupling Sizing

In preparation for comparing each of the seven coupling designs and selecting two for fabrication and test, a preliminary analysis was conducted to determine the size and weight of each design. The primary consideration in this effort was to obtain the impact of the flexure element configuration on the coupling.

The following examples are typical of the procedures used in this effort.

TABLE 5. UNIDIRECTIONAL COMPOSITE ALLOWABLES

Material and Ply Orientation	Strength Properties						Elastic Properties							
	Ult Tens (ksi)	Ult Compr (ksi)	Yield Compr (ksi)	Ult Shear (ksi)	E Tension (msi)	E Compr (msi)	G Shear (msi)	Poisson Ratio	Density (lb/in. ³)	E Tension (msi)	E Compr (msi)	G Shear (msi)	Poisson Ratio	Density (lb/in. ³)
Graphite/ Epoxy 0°/90° +45°	160	160		10	17		.6	.21	.055					
	87	88			9.5									
	22	22		50	2.2		4.5	.76						
Kevlar 49/ Epoxy 0°/90° +45°	189	34	30	8	10.8	10.5	.3	.34	.050					
	49	21		13	4.0	3.8	.3							
	26	15	5.5	27	1.1	1.0	3.0							
E-Glass/ Epoxy 0°/90° +45°	147	83		2.5	5.7	4.6	.45		.065					
	39	45		14	2.8									
	20	12		36	1.9		1.6							
Boron/Alum 0°/90° +45°	137	182			32									
	81				19									
	20												.53	

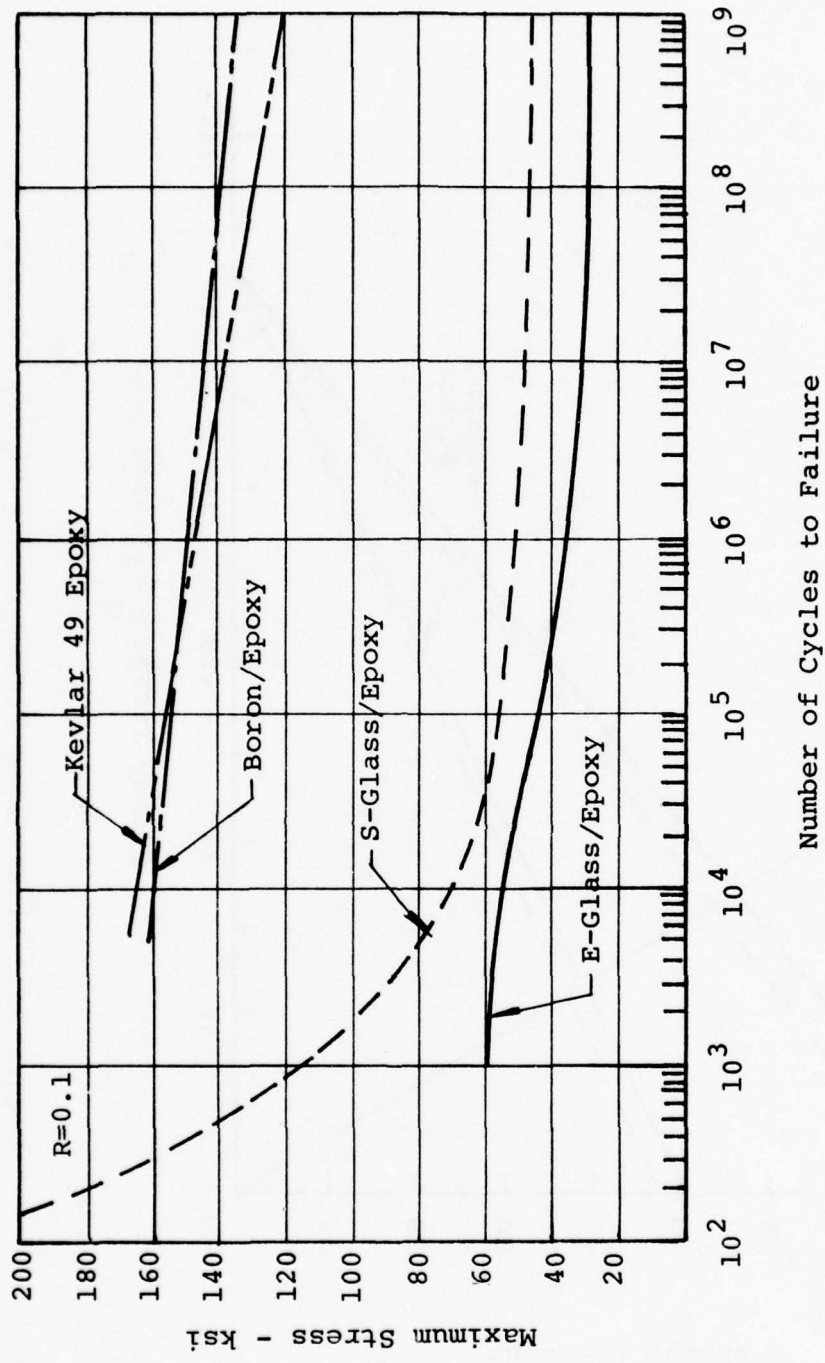


Figure 24. Stress versus Cycles - Unidirectional Composites
Tension - Tension Fatigue.

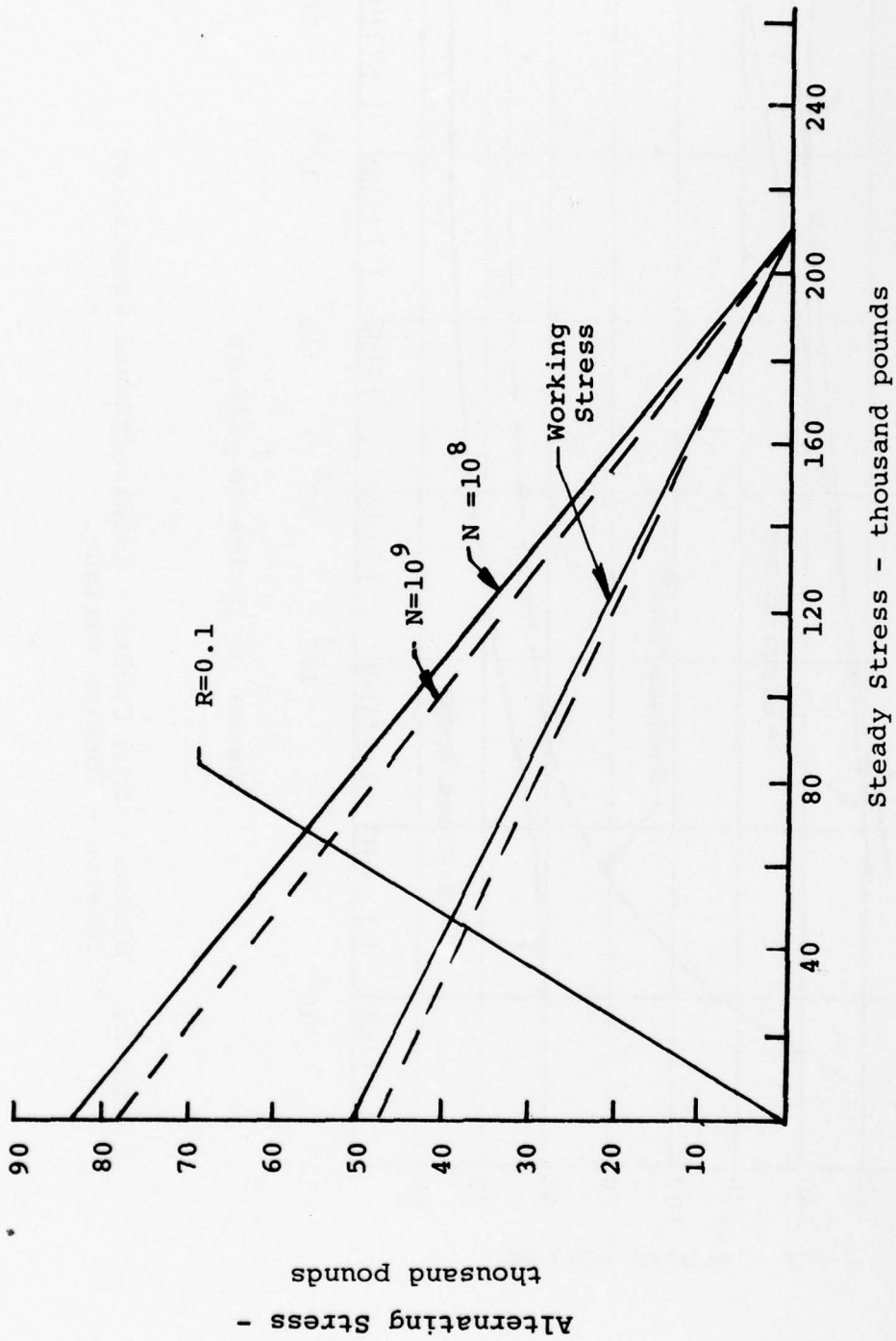


Figure 25. Alternating Stress versus Steady Stress, Unidirectional Kevlar 49/Epoxy Composite.

Circumferential Belt Coupling

In examining the basic relationships established in Figure 22, it is seen that the load, P , deflection, Y , effective length, L , and moment, M , are all a function of the coupling radius. By choosing a radius at random and calculating the maximum stress, a curve of stress versus radius is derived and is shown in Figure 26. Using the plot of alternating stress versus steady stress in Figure 25 along with Figure 26, a satisfactory solution for the flexure element can be made and the coupling size determined.

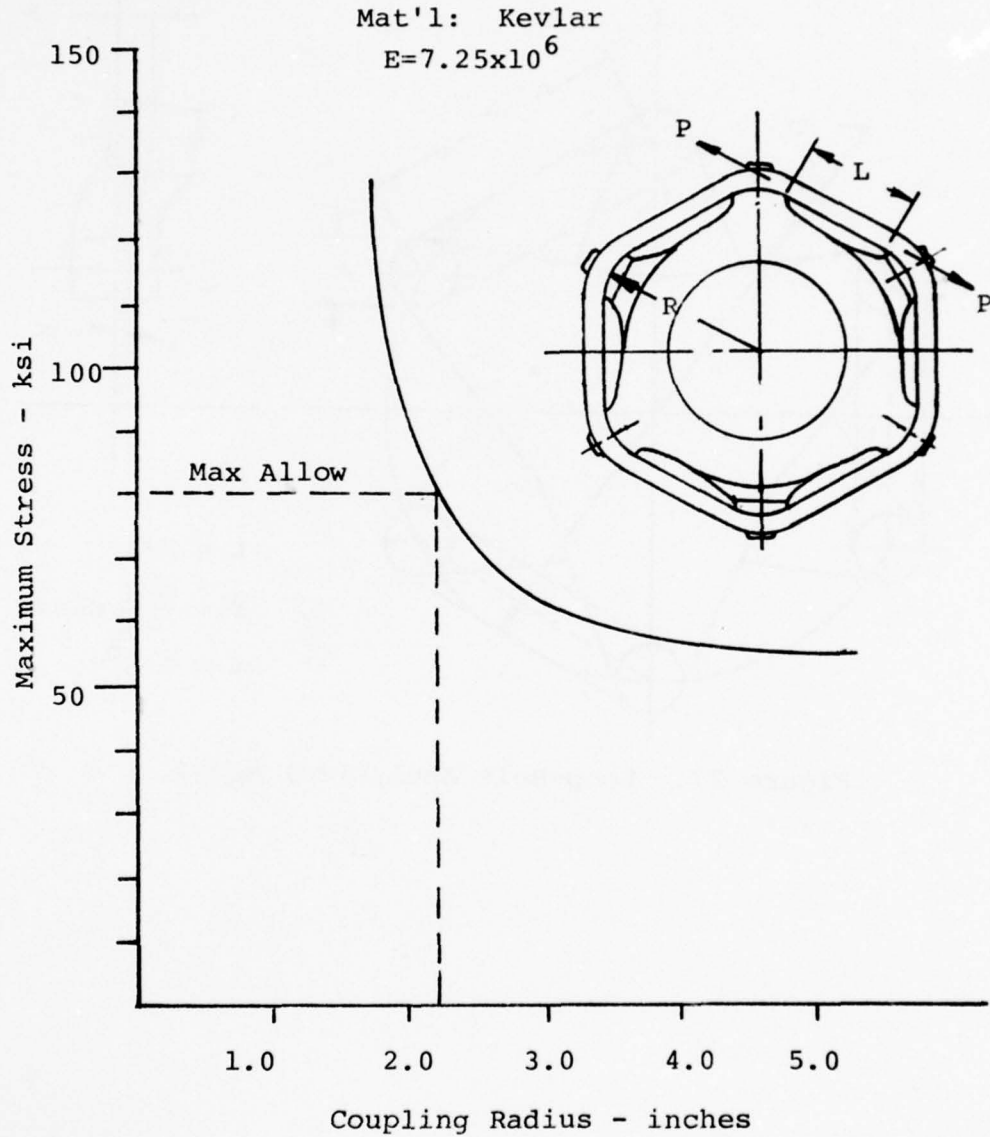


Figure 26. Maximum Stress versus Coupling Radius, Circumferential Strap Design.

Loop-Belt Coupling

The loop-belt coupling can be represented by two tri-lobe flanges connected by flexible elements. As the driven and driving flanges are rotated with respect to each other through an angle (representing angular misalignment), the flexible elements are bent and twisted. The coupling can thus be idealized as shown in Figure 27.

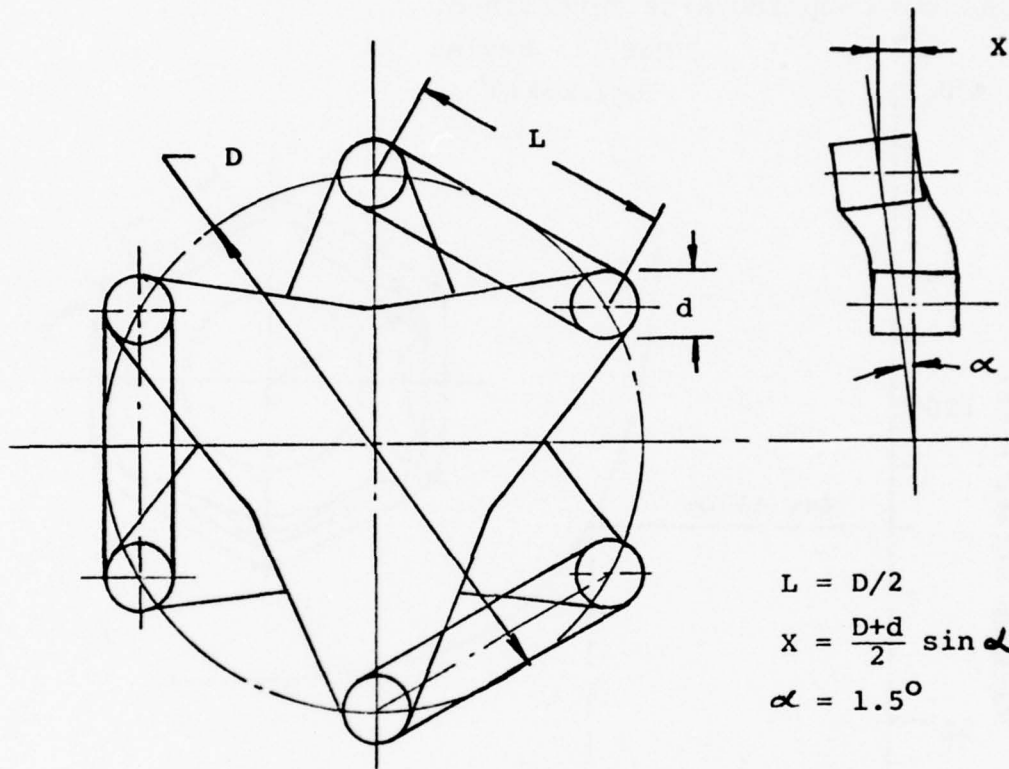


Figure 27. Loop-Belt Analytical Model.

The loads transmitted by the coupling are

$$hp = 1500 @ 20,000 \text{ rpm}$$

$$T = \frac{(63,025)(1500)}{20,000} = 4730 \text{ in.-lbs}$$

The driving loads transmitted by the flexible elements are

$$F_t = \frac{2T}{3D \cos 30^\circ} = \frac{(2)(4730)}{3D \cos 30^\circ} = \frac{3640}{D} \quad (7)$$

and each element transmits one half of the total.

$$P = \frac{1820}{D}$$

Figure 28 shows the isolated elements with loads.

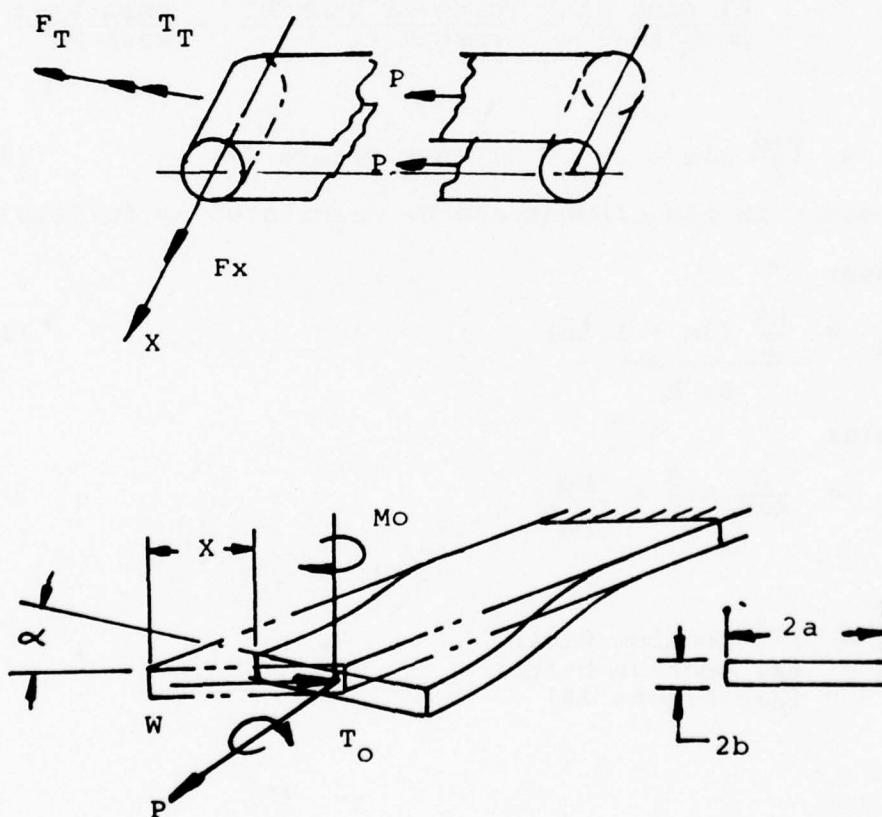


Figure 28. Loop-Belt Analytical Model Isolated Elements.

From an analysis of this flexible element, the following equations can be derived:

$$x = \frac{M_o}{P} \left(\frac{1}{\cosh kl} - 1 \right) - \frac{W}{kP} (\tanh kl - kl) \quad (8)$$

$$M_o = \frac{W}{k} \frac{\cosh kl - 1}{\sinh kl} \quad (9)$$

$$T_o = \frac{KG}{L} \quad (10)$$

where

$$k = \sqrt{\frac{P}{EI}} \quad (11)$$

Combining equations (8) and (9),

$$M_o = \frac{PX}{\frac{kl \sinh kl}{\cosh kl - 1} - \frac{\sinh kl \tanh kl}{\cosh kl - 1} - \frac{\cosh kl - 1}{\cosh kl}} \quad (12)$$

where

$$x = \frac{D+d}{2} \sin \alpha \quad (\text{see Figure 27}) \quad (13)$$

The stresses in the element can be calculated as follows:

Shear

$$S_s = \frac{KG}{L} \frac{(3a + 1.8b)}{8a^2 b^2} \quad (14)$$

Axial

$$S_t = \frac{P}{4ab} \times \frac{3}{4} \times \frac{M_o}{ba^2} \quad (15)$$

where

$$\begin{aligned} a &= 1/2 \text{ section width} \\ b &= 1/2 \text{ section height} \\ &(\text{See Figure 28}) \end{aligned}$$

Figure 29 is a series of curves for various loop-belt coupling diameters showing steady and vibratory stress as a function of belt thickness for a constant width.

All seven couplings were subjected to this preliminary type of sizing analysis to formulate an equitable baseline for comparison. Drawings of each of the seven concepts are shown in Figures 30 through 36.

COUPLING SELECTION PARAMETERS

After completion of the Preliminary Design Phase of this program, a decision point had been reached. This milestone involved the selection of two coupling designs to pursue through fabrication and test. As a guide in making these design choices, a relative ranking by a weighted factor method was chosen to provide an objective evaluation of the seven coupling concepts to be considered.

Four criteria were chosen to evaluate the coupling design: weight, cost, reliability, and operational limits. These four factors were given a weighted value, the sum of which became the individual coupling's rating of merit, with 100% being a perfect rating.

The four ranking criteria were assigned the following values based on engineering judgment, and they represent the relative importance of each factor to the overall coupling design.

1.	Reliability	40%
2.	Operational Limits	30%
3.	Weight	20%
4.	Cost	10%
		<u>100%</u>

Each of these four basic criteria were subsequently subdivided where applicable into subcategories.

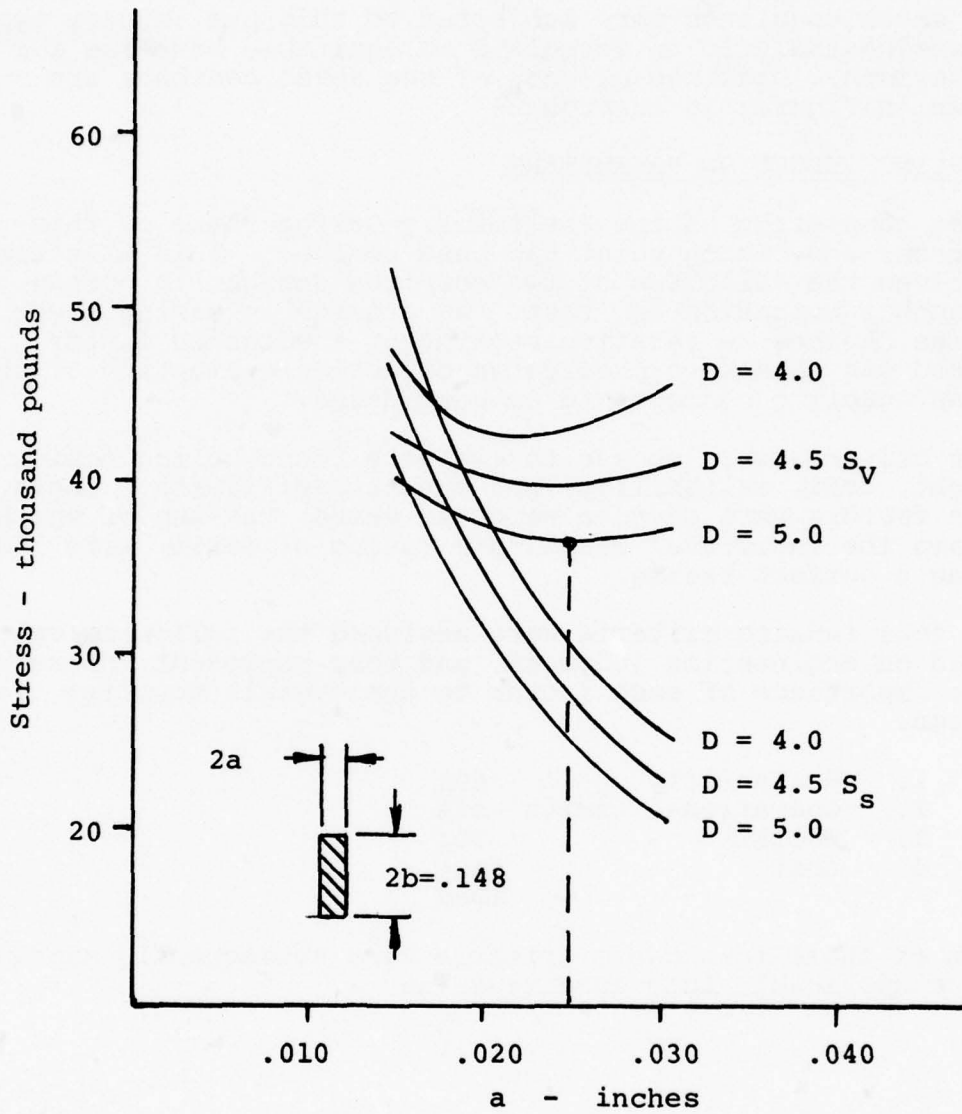
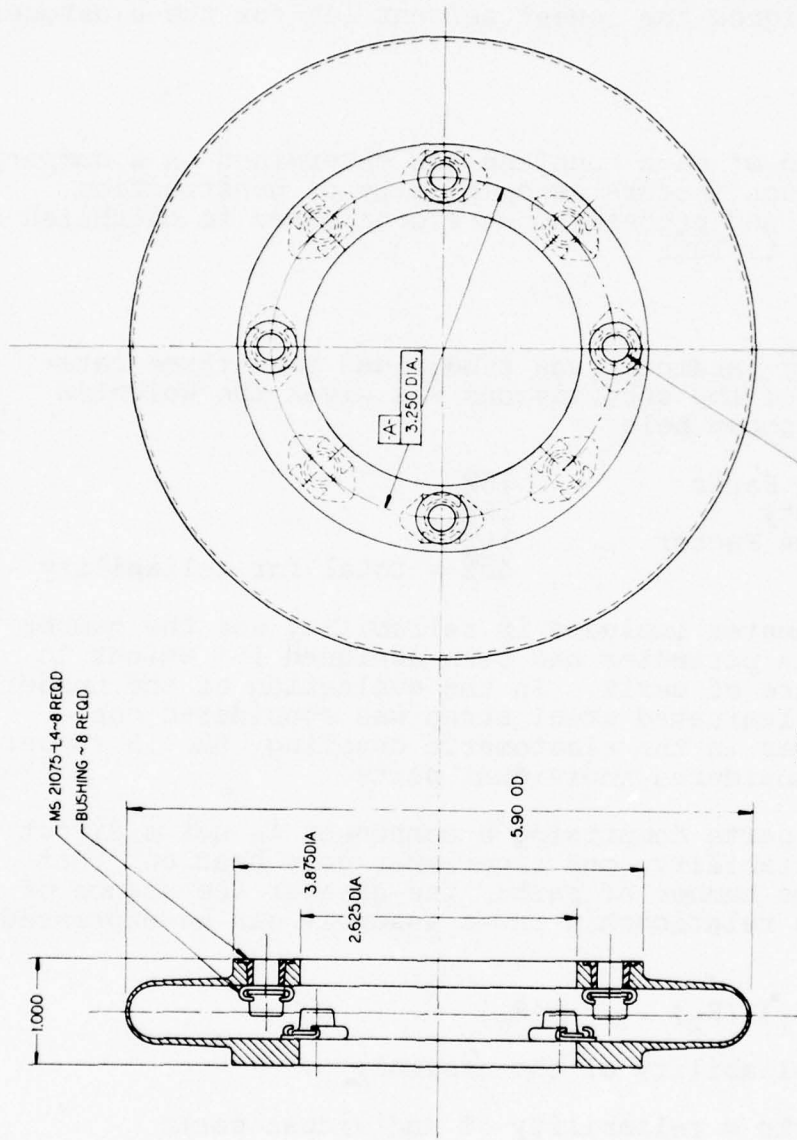


Figure 29. Maximum Stress versus Section Thickness, Loop-Belt Coupling Diameter.



COMPOSITE DIAPHRAGM CPLG.	
ADVANCED COUPLING	
DEVELOPMENT PROGRAM	
E 78286	38012-10001
REV. 4.1	DATE

Figure 30. Diaphragm Coupling Design.

Weight

The weight of each of the designs shown in Figures 30 through 36 was determined by calculating the volume for each component and multiplying by the appropriate density.

The coupling with the lowest weight was assigned 20% in the weight ranking criteria, while the coupling with the highest weight was assigned the lowest percent (4% for the elastomeric coupling).

Cost

The cost rating of each coupling was determined on a comparative basis. Such factors as complexity of construction, material cost, and processing were considered to establish a rating from 1% to 10%.

Reliability

The reliability parameter was subdivided into three categories. Each of the subdivisions was given the weighted percentage as shown below:

Number of Parts	15%
Fail Safety	15%
Confidence Factor	10%
	40% = total for reliability

The first parameter included in reliability was the number of parts. This parameter has been assigned 15% weight to the total figure of merit. In the evaluation of the number of parts, the laminated steel strap was considered one element, whereas in the elastomeric coupling, the 15 rubber blocks were considered individual parts.

The number of parts comprising a component is not a direct measure of reliability, but experience does bear out that the greater the number of parts, the greater the chance of failure. This relationship in an assembly can be expressed as

$$R_A = (R_1) (R_2) \dots (R_N)$$

R_A = reliability of the assembly

$R_1, R_2, \text{ etc}$ = reliability of individual parts

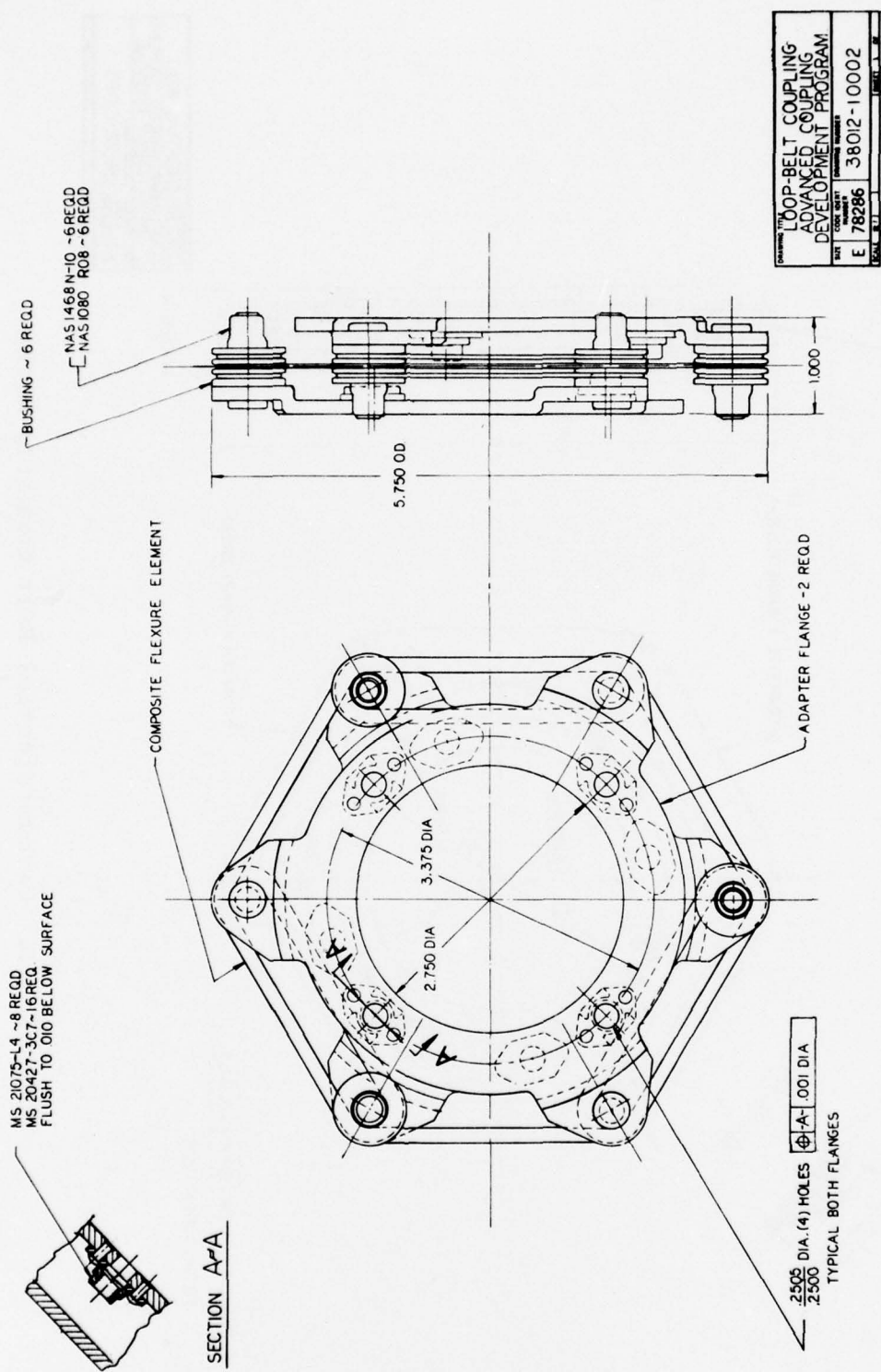


Figure 31. Loop-Belt Coupling Design.

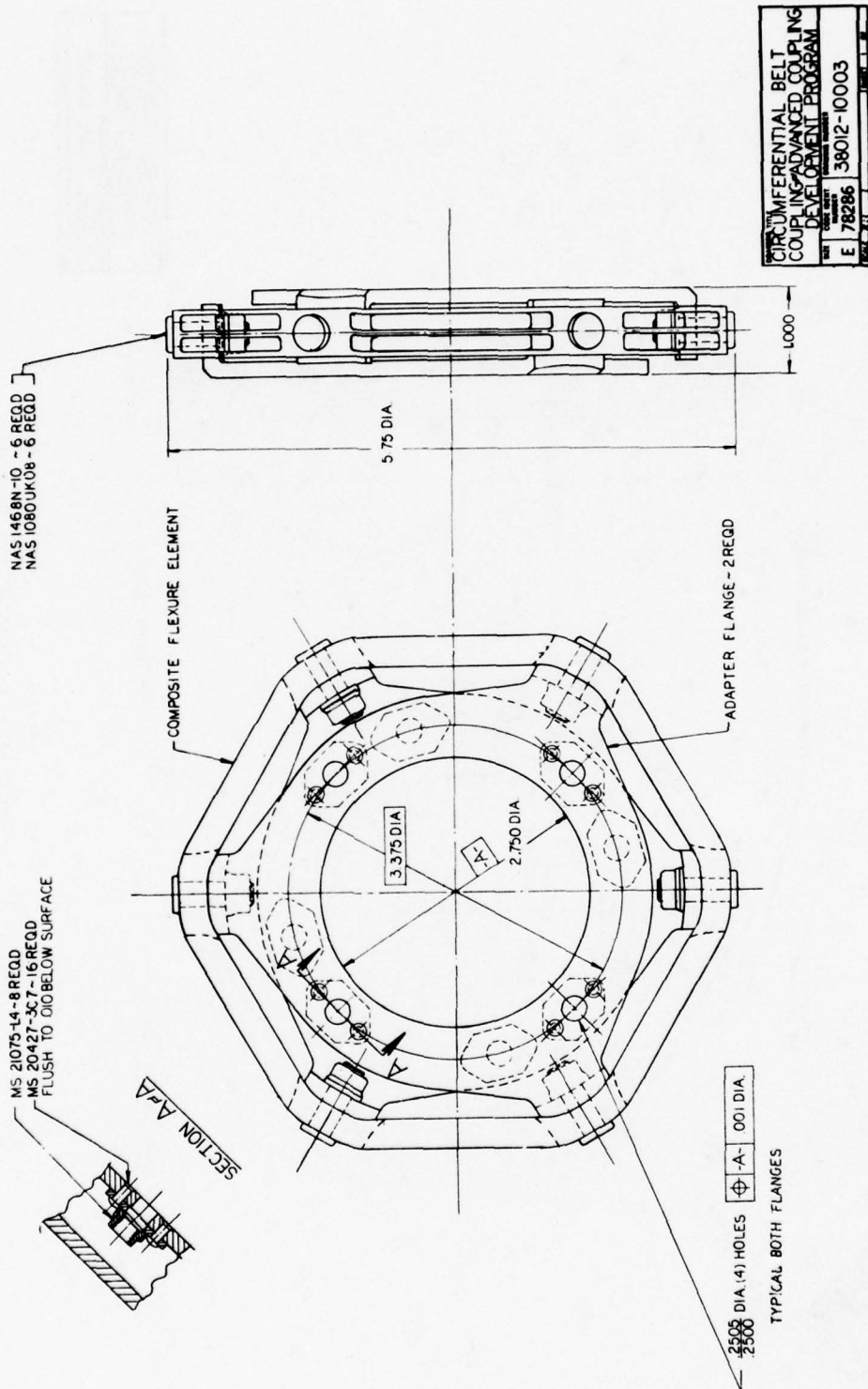


Figure 32. Circumferential Belt Coupling Design.

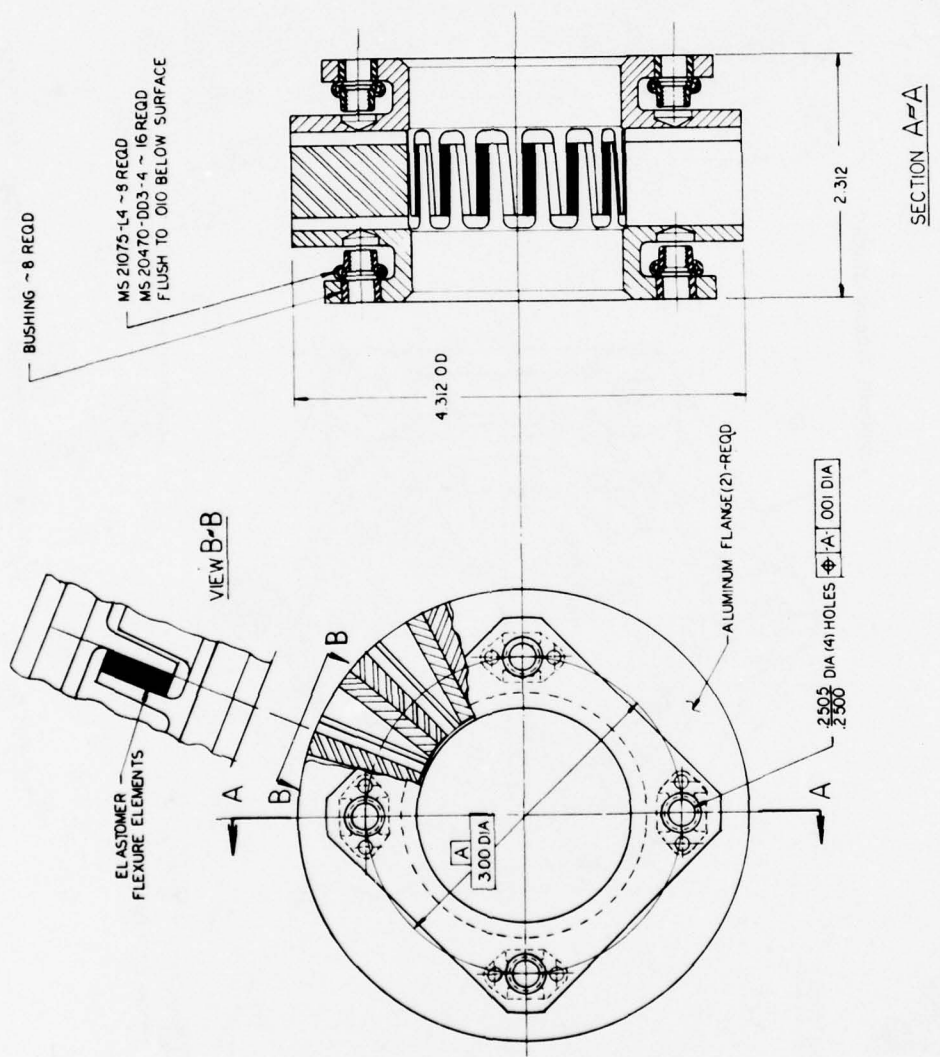


Figure 33. Elastomeric Coupling Design.

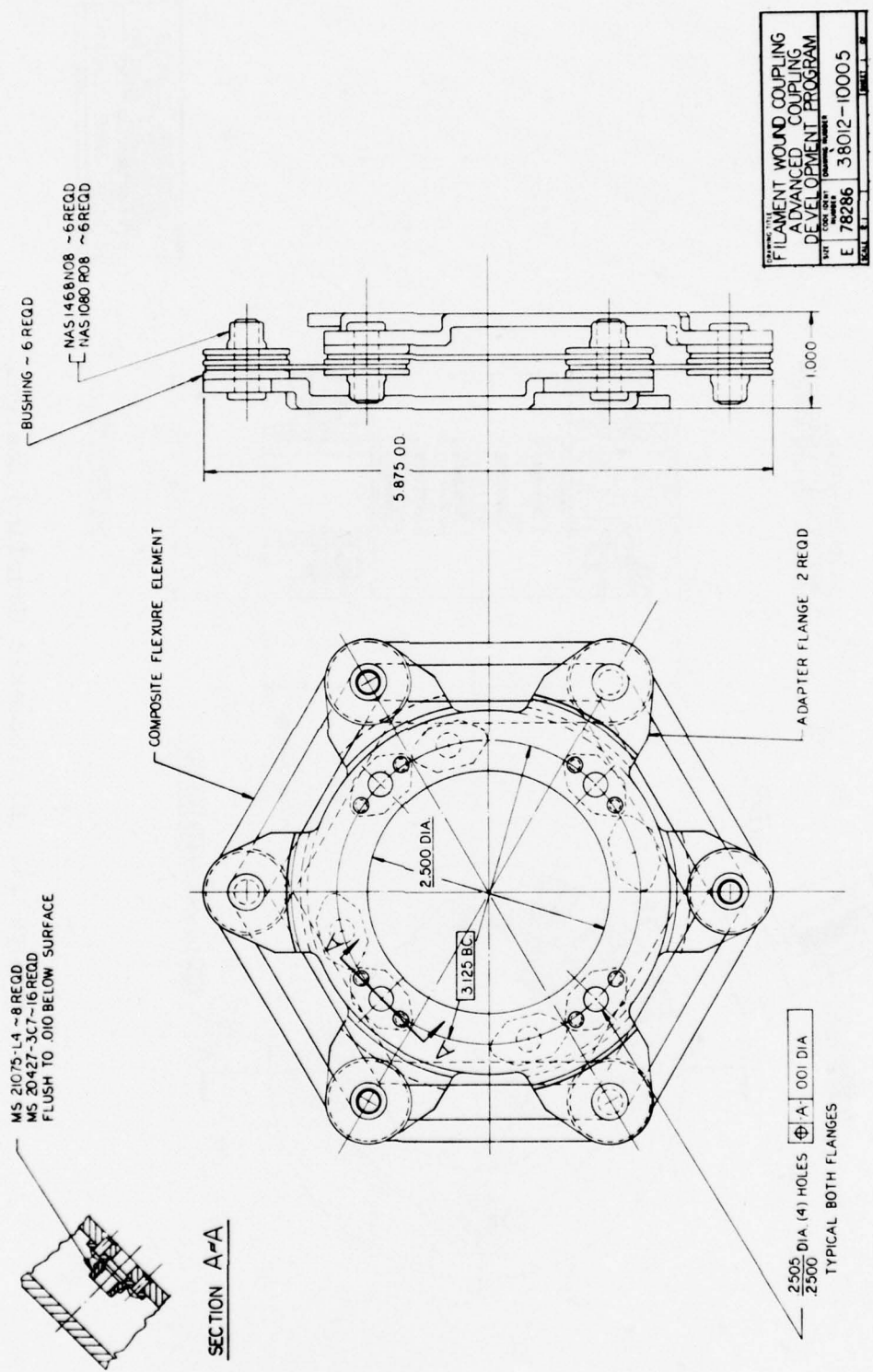
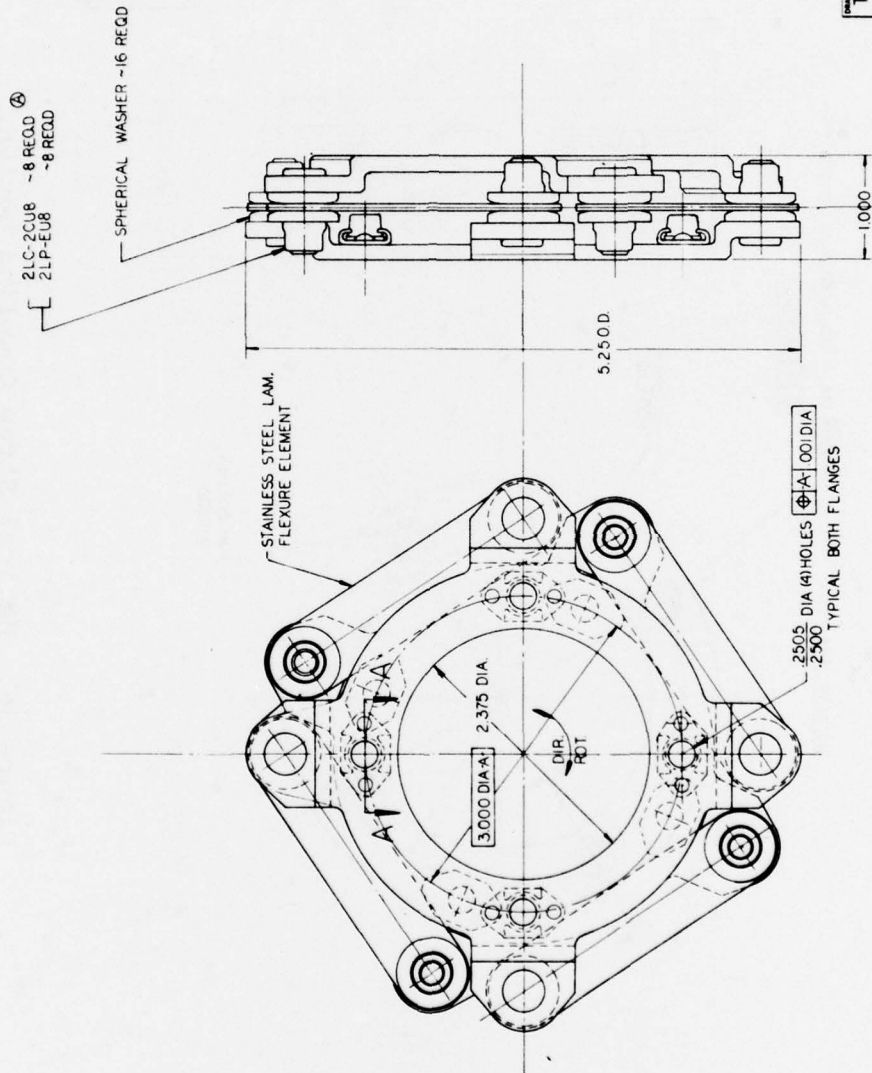


Figure 34. Filament-Wound Coupling Design.



TENSION STRAP COUPLING
 ADVANCED COUPLING
 DEVELOPMENT PROGRAM
 E 78286 38012-10006

Figure 35. Tension Strap Coupling Design.

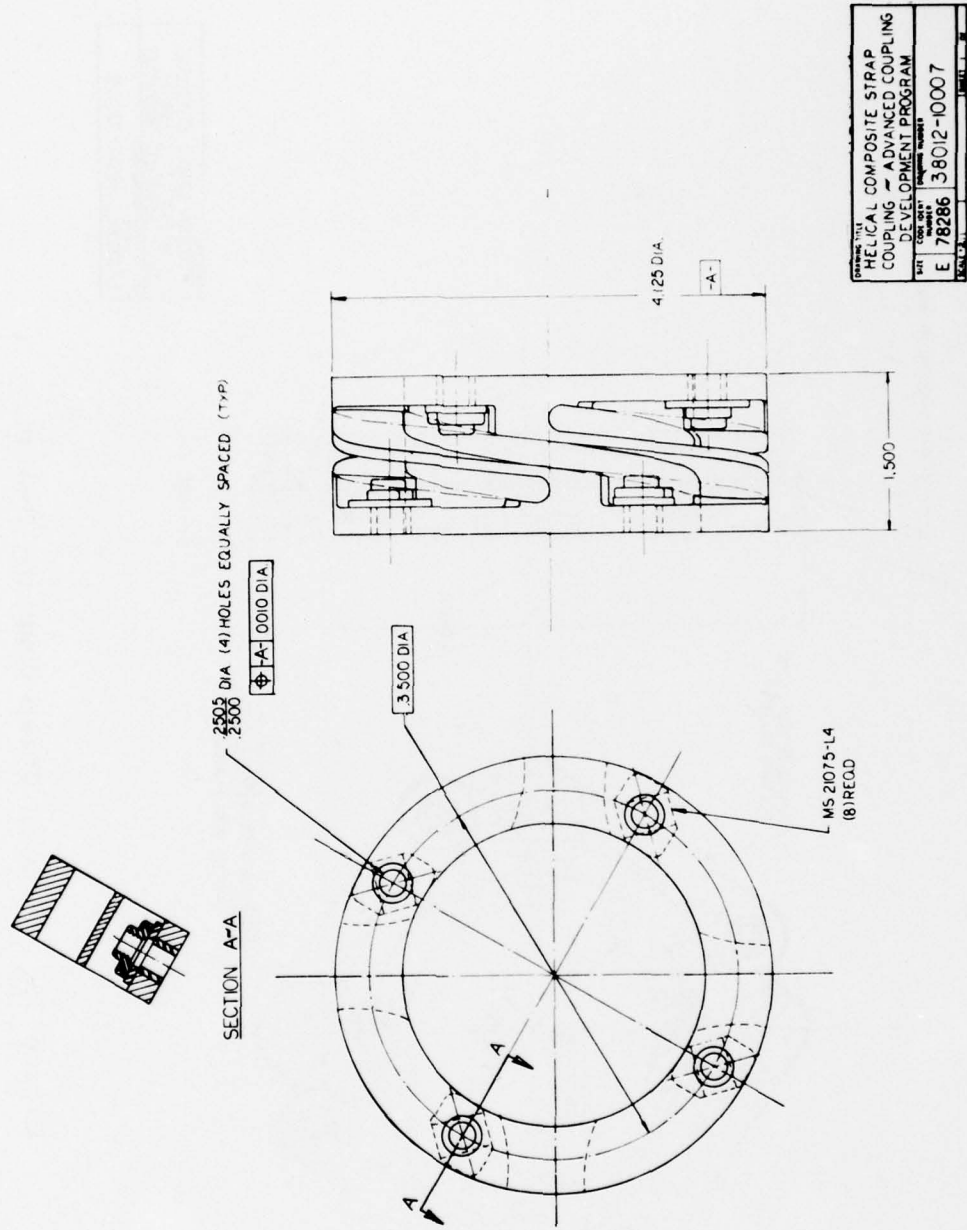


Figure 36. Helical Strap Coupling Design.

Therefore, assuming no change in the individual component reliabilities, the assembly with the greater number of parts will have a lower reliability.

In arriving at the actual ratings for the individual coupling, a linear relationship is used. The coupling with the lowest number of parts was given a rating of 100% of the 15% for number of parts, while the coupling with the greatest number of parts was given a rating of 50% of the 15%.

The factor for reliability based on the number of parts can be expressed as

$$F_N = 46.875N - 46.645 \quad (16)$$

The coupling with the lowest number of parts approaches the maximum rating of 15% using the above equation.

The second reliability rating factor is fail safety, which is also assigned a value of 15%. The most common mode of failure is assumed to be fatigue of the flexure element under conditions such as those represented by the fastener interface with the flange. The coupling is then rated on its ability to perform with as many failed elements as possible. Thus, torque path redundancy is used as a measure of the fail-safe rating and can be expressed as follows:

$$\frac{1}{R_T} = \frac{1}{R_1} + \frac{1}{R_2} + \dots + \frac{1}{R_N}$$

The coupling with the most redundant paths was given a rating of 90% of the 15% assigned for fail safety and that with the least, a rating of 50% of the 15%. This can be presented as

$$F = .165 - .09P \quad (17)$$

where

$$P = \text{number of load paths}$$

The third and final factor to be considered was the reliability confidence factor which was assigned a total of 10%. The couplings being evaluated were new concepts, and obviously no field usage data could be used directly to establish these values. However, by similarity to couplings in use, and a knowledge of the individual coupling's sensitivity observed in the analysis, an objective ranking can be made. This third factor is given a maximum weight of 10% to that coupling rated with the highest confidence level.

The relative reliability ratings for the seven couplings based on a total value of 40% of the total figure of merit are shown below in Table 6.

TABLE 6. RELIABILITY RATING				
Coupling	No. of Parts 15%	Fail Safe 15%	Confidence Factor 10%	Total Reliability 40%
Diaphragm	.15	.09	.09	33
Loop-Belt	.08	.13	.09	29
Circumferential	.15	.09	.07	31
Elastomeric	.08	.14	.05	27
Filament Wound	.10	.09	.07	26
Tension Strap	.13	.14	.10	37
Helical Strap	.15	.09	.09	33

Operational Limits

The limits of operation factor is assigned a total weight of 30% of the total figure of merit and is divided into three subcategories: torque, speed, and misalignment. This factor is used to measure the coupling's potential to meet the needs of the helicopter coupling usage spectrum.

The torque limit is assumed to be that which would be encountered in a heavy lift helicopter, i.e., 8000 hp at 11,000 rpm or 46,000 in./lbs. The torque limit factor is given an individual rank of 10% of the total figure of merit.

The potential speed limit is established in the basis of the proposed STAGG engine concept which has a maximum rating of 800 hp at 30,000 rpm. An assessment of the individual coupling's ability to operate at these high speeds is a measure of its adaptability to this environment and forms the basis for the 10% speed factor rating.

The misalignment factor is also given a weight of 10%. This parameter is a measure of the coupling's ability to transmit torque with a high degree of misalignment. A summary of the rankings for operational limits is presented in Table 7.

TABLE 7. OPERATIONAL LIMITS RATING

Coupling	Torque 10%	Speed 10%	Misalignment 10%	Operational Limit 30%
Diaphragm	.10	.08	.09	.27
Loop-Belt	.06	.06	.06	.18
Circumferential	.07	.06	.06	.19
Elastomeric	.05	.05	.05	.15
Filament Wound	.06	.06	.05	.17
Tension Strap	.09	.07	.09	.25
Helical Strap	.09	.10	.10	.29

The resulting total figure of merit for each of the coupling concepts is shown in the coupling selection matrix chart of Table 8.

COUPLING SELECTION

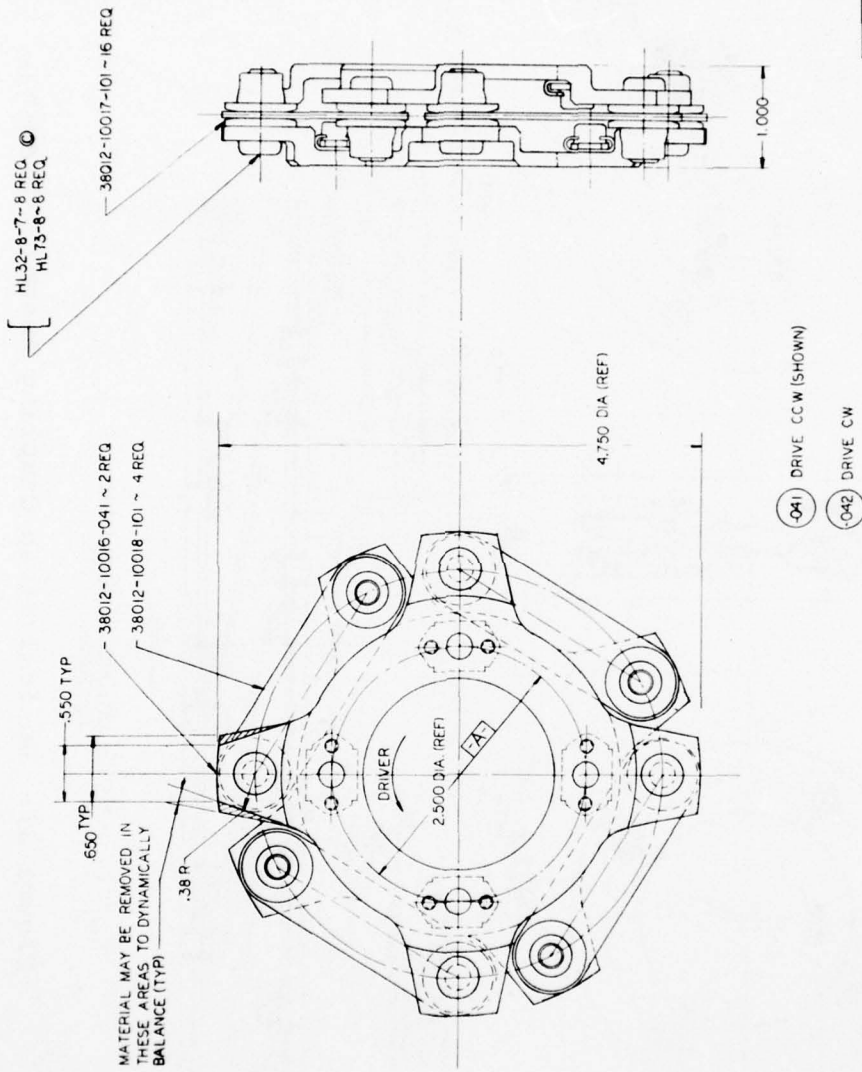
It was decided that two designs would be selected for fabrication and testing. The two designs selected were the composite helical strap coupling and the tension strap coupling. The diaphragm coupling, although placing second in the figure of merit (see Table 8), was not selected for final design. This design required analytical methodology that was not yet available and that would increase the development cost of the program. The tension strap coupling running a close third was chosen as the second design to develop for fabrication.

The final designs of both the composite helical strap coupling and the tension strap coupling are shown in the assembly drawings, Figures 37 and 38 respectively.

Particular attention was given to the selection of a manufacturer to fabricate the composite helical strap coupling. An appraisal of five sources and their recommended approach to composite layup and processing procedures was conducted. A team comprising representatives from purchasing, manufacturing, engineering, structural materials, and design engineering was consulted in making the vendor selection.

TABLE 8. COUPLING DESIGN SELECTION MATRIX

	Wt 20%	Cost 10%	Reliability 40%		Confidence 10%	Operational Limits 30%			Overall Rating 100%
			No. Parts 15%	Fail Safe 15%		Torque 10%	Speed 10%	Misalign- ment 10%	
Diaphragm 38012-10001	19.9	10	15.	9.	9.	10.	8.	9.	89.9
Loop-Belt 38012-10002	15.4	8.	8.	13.	9.	6.	6.	6.	70.4
Circumferen- tial Belt 38012-10003	16.1	7.	15.	9.	7.	7.	6.	6.	73.1
Elastomeric 38012-10004	3.9	5.	8.	14.	5.	5.	5.	5.	50.9
Filament Wound 38012-10005	15.3	8.	10.	9.	7.	6.	6.	6.	66.3
Tension Strap 38012-10006	15.5	8.	13.	14.	10.	9.	7.	9.	85.5
Helical Strap 38012-10007	19.9	9.	15.	9.	9.	9.	10.	10.	90.9



PROJECT TITLE	COUPLING TENSION STRAP
PROJECT NUMBER	ADVANCED COUPLING DEVELOPMENT PROGRAM
REV	E 78286
DATE	38012-10006

Figure 38. Tension Strap Coupling Assembly Drawing.

The fabrication of the tension strap coupling was comparatively simple, and the component parts were assigned to local manufacturers for fabrication. The final assembly was performed at Sikorsky.

Photographs of the two couplings fabricated in this effort are shown in Figures 39 and 40.

In addition to the test specimens, hardware had to be designed and fabricated to modify the test facility to accommodate the test requirements. This consisted of changes to provide incremental angular misalignment at the coupling flanges up to 6°, adapter shafts for the two different couplings, and provisions for a high-speed telemetry slip ring.



Figure 39. Helical Strap Coupling Specimen.

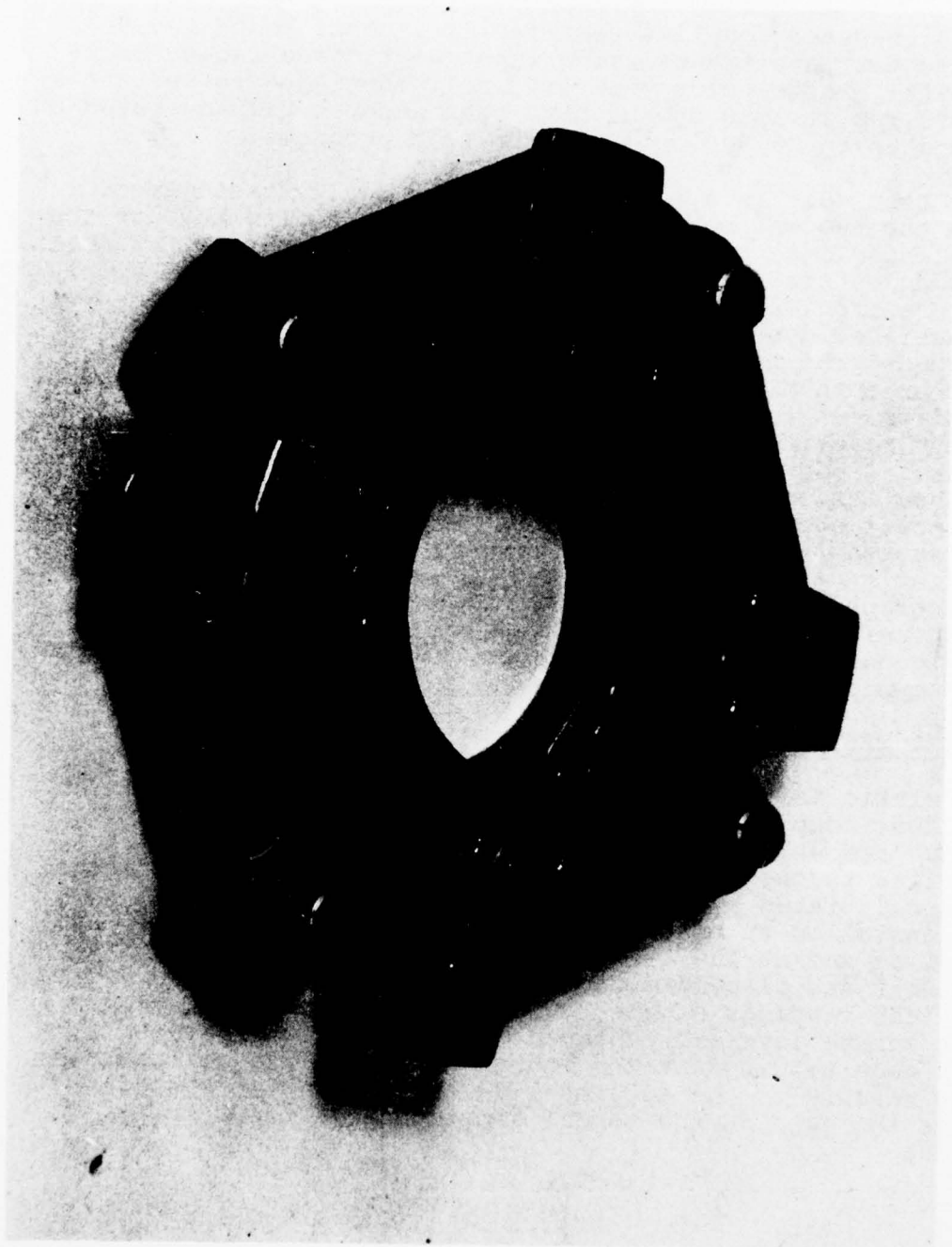


Figure 40. Tension Strap Coupling Specimen.

TEST FACILITY

DYNAMIC TEST FACILITY

The high-speed coupling test facility consists of two H-3 helicopter main transmission input sections arranged back-to-back. These units were originally designed to operate at 18,900 rpm at 1750 hp and have been successfully operated at speeds up to 26,500 rpm in prior test programs.

This test unit is a four square regenerative arrangement with the two end boxes connected by dual shafts through the couplings to be tested. A portion of the coupling torque is introduced statically through the closed gear loop. Hydraulic pistons provide means whereby the required test torque can be achieved dynamically after the operating speed has been reached. The location of the end boxes relative to one another determines the shaft coupling misalignment. Angular misalignment is introduced through adjusting jacks located at the mounting feet of the slave gearbox. A 150-hp electric motor and eddy-current clutch drives the unit through a matched set of multiply V-belts at the rotor brake flange. The power supplied by the motor is only required to overcome the system friction.

Photographs of the test unit, Figures 41 through 45, show the general arrangement and some details of the angular misalignment adjustment features, vibration instrumentation, and coupling test shaft containment provisions.

STATIC TEST FACILITY

The static test fixture comprises a reaction member to which the test coupling is secured by its driven flange, and a torque arm which is fastened to its input flange. Torque is supplied to the system through a pulley and cable arrangement by a calibrated hydraulic load cell. Dial indicator gages are installed at both input and output flanges of the test coupling and at the test rig torque arm. A photograph of the unit and placement of the indicators is shown in Figure 46. The readings of all three gages are recorded as each test torque level is achieved. The difference between the dial gage readings at the input and output flange locations is a measure of the torsional deflection in the coupling, while the gage on the torque arm indicates total system windup.

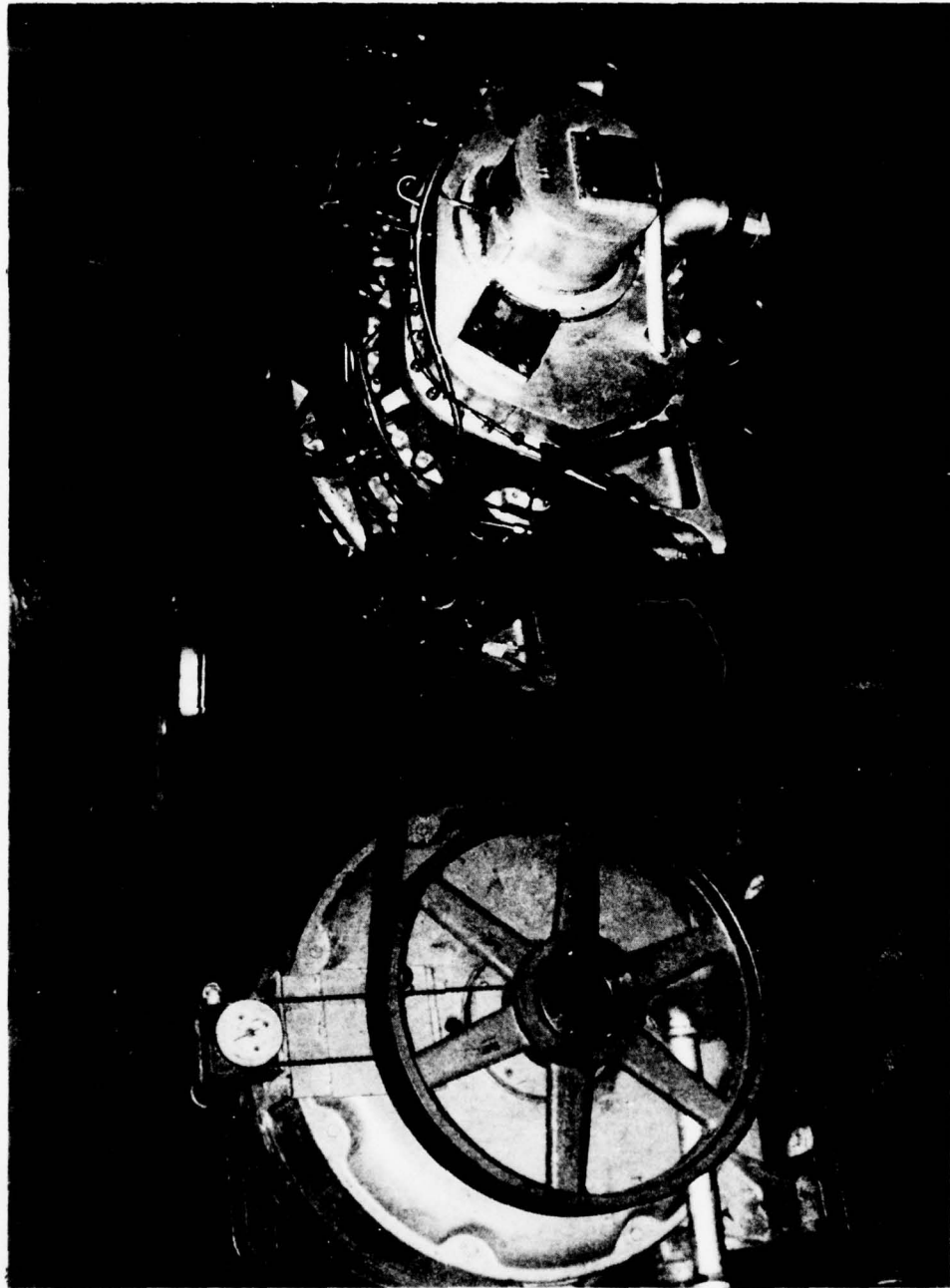


Figure 41. High-Speed Test Facility, Motor/Clutch and Gearbox Arrangement.



Figure 42. High-Speed Test Facility, Back-to-Back Input Gearboxes.

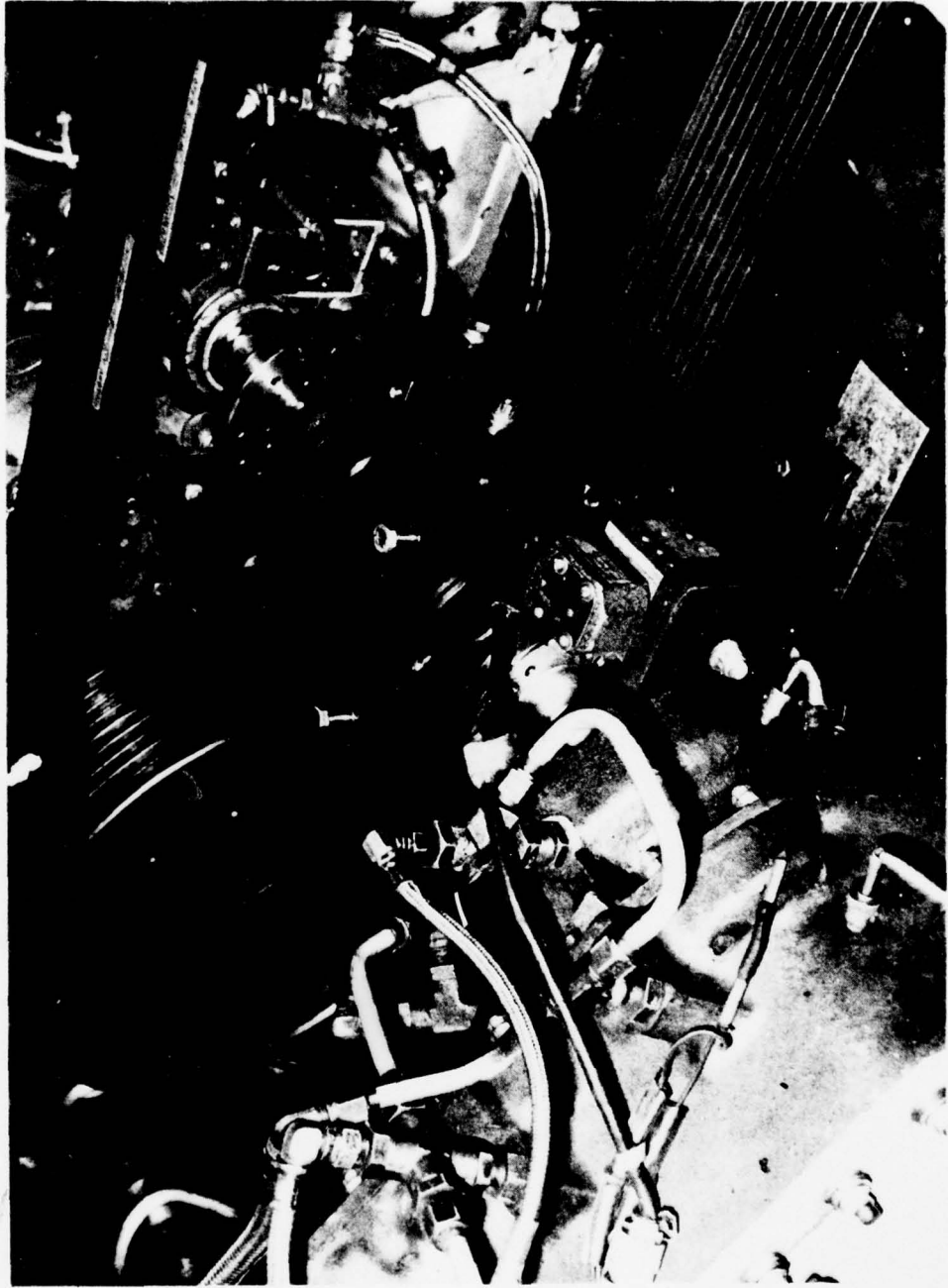


Figure 43. High-Speed Test Facility, Dummy Box Input, Test Shaft Side.

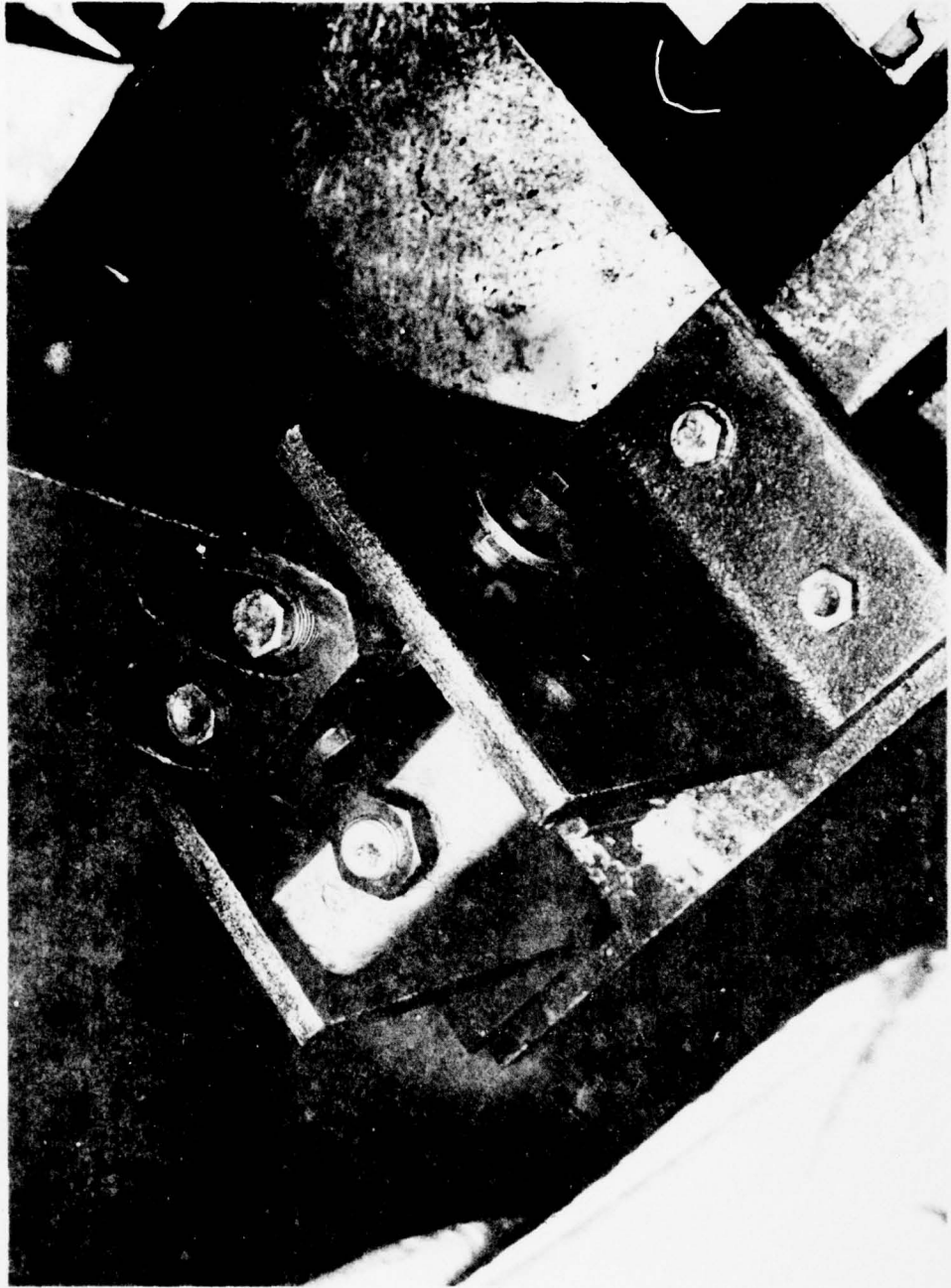


Figure 44. High-Speed Test Facility, Angular Misalignment Adjusting Jack.

AD-A064 296

UNITED TECHNOLOGIES CORP STRATFORD CT SIKORSKY AIRCR--ETC F/G 1/3
ADVANCED COUPLING DEVELOPMENT PROGRAM.(U)

OCT 78 R A STONE

DAAJ02-74-C-0054

UNCLASSIFIED

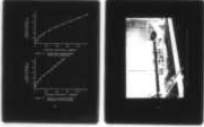
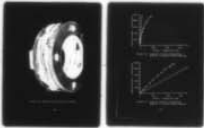
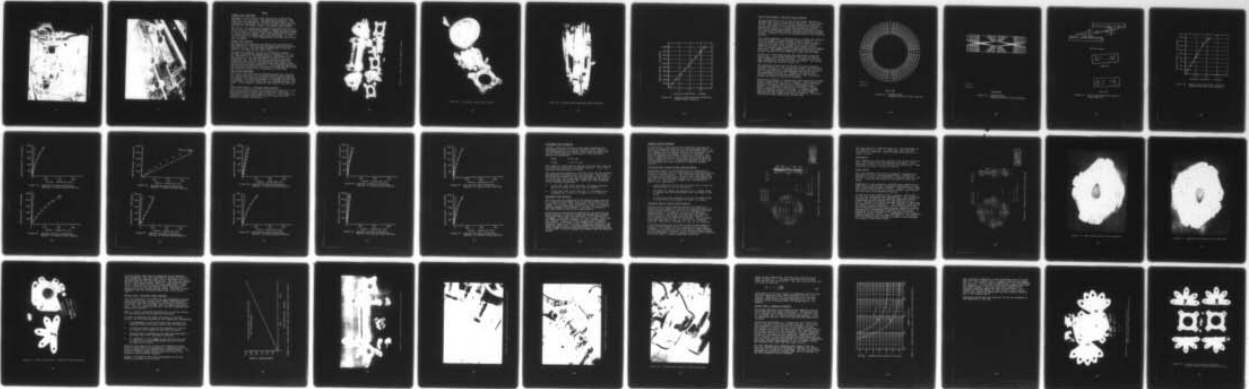
SER-510004

USARTL-TR-78-40

NL

2 OF 2

AD
A064 296



END
DATE
FILMED
4 --79,
DDC

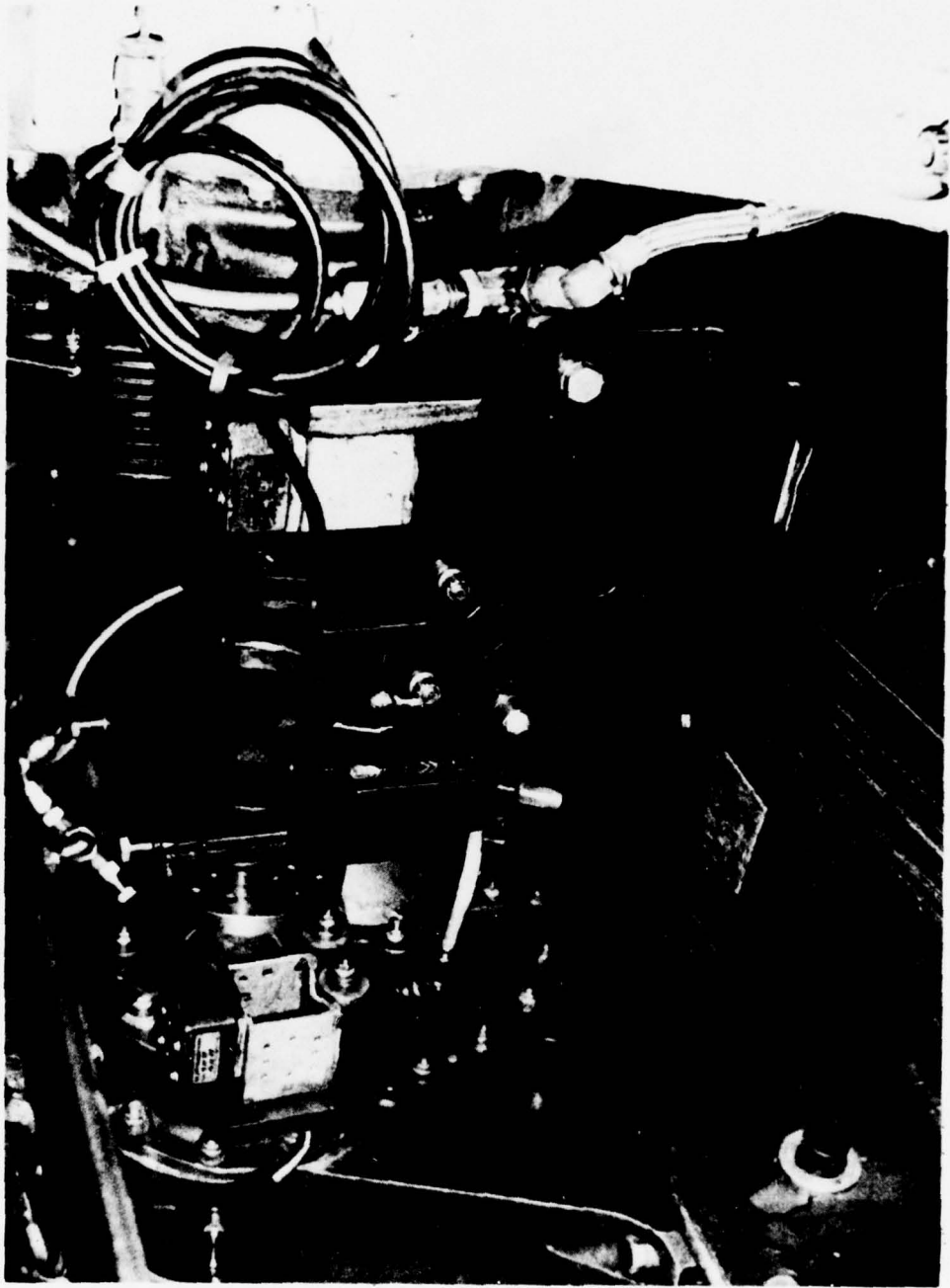


Figure 45. High-Speed Test Facility, Test Shaft Containment System.

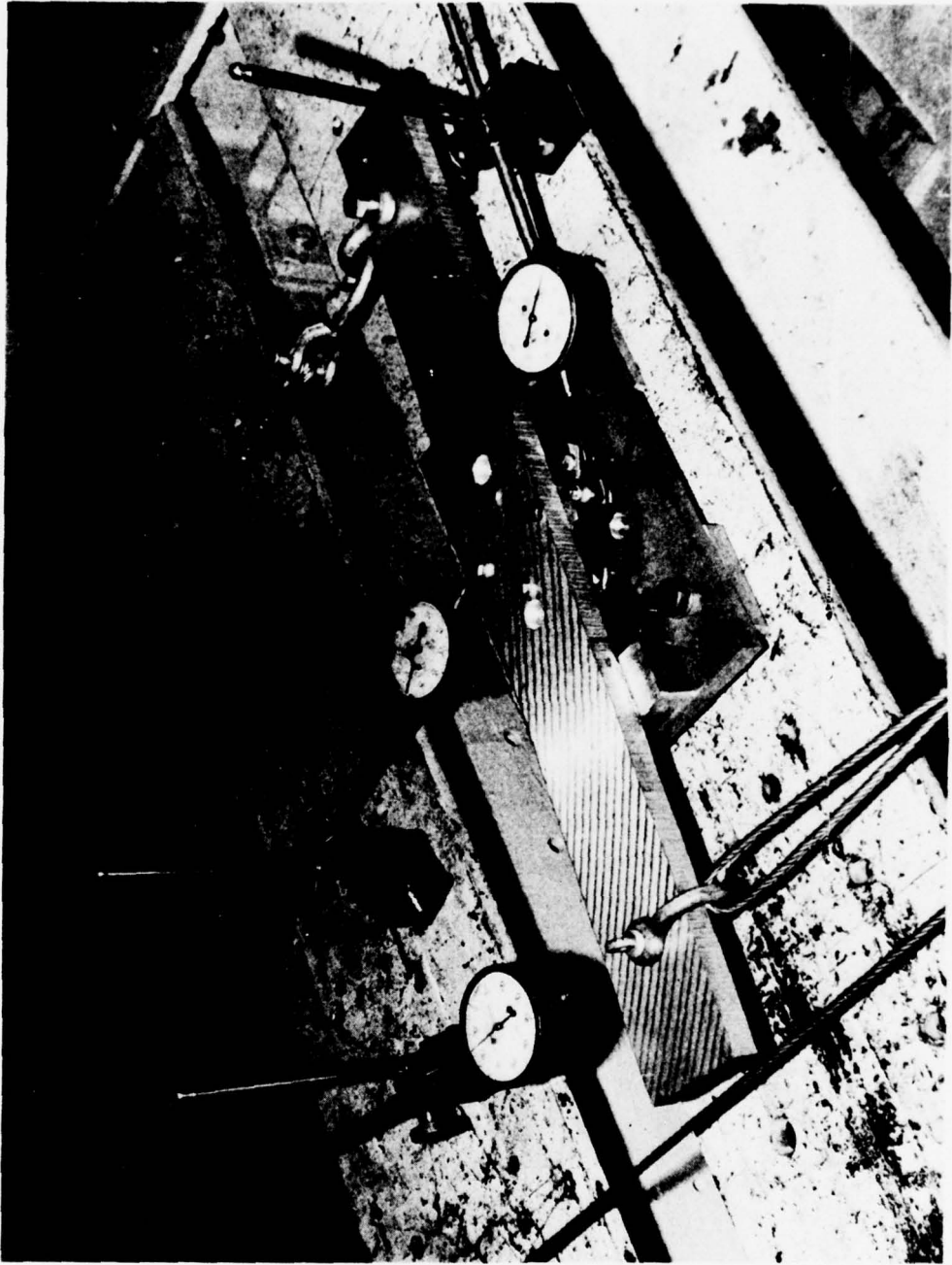


Figure 46. Static Overtorque Test Fixture.

TESTS

DYNAMIC TEST PROCEDURE

Specimens of the tension strap coupling were fabricated, mounted on the test shaft, and dynamically balanced. The first test was designed to validate the performance of the couplings by operating for 10 hours or until first signs of distress at 100% speed, torque, and angular misalignment.

The initial run consisted of operation at 2000 rpm with "0" torque and "0" angular misalignment. Speed was then increased in increments of 2000 rpm until the final operating speed of 20,000 rpm was reached. Each test condition was held for 15 minutes prior to advancing to the next speed. At each level of speed, oil flow, temperatures, and vibration levels were monitored.

Dynamic Test Results

The tension strap coupling was tested with the procedure outlined above. When the coupling speed attained the designated 20,000 rpm, the test shaft experienced a coupling fracture, aborting further test effort.

The coupling assembly, as well as the facility adapter flanges, sustained the damage shown in Figures 47, 48, and 49. Examination of the fractured parts indicated a static type failure of the coupling flange at the root of the attachment lug. Further analysis of the test components showed that the fracture was caused by centrifugal force acting at the eccentric distance between the flange centerline and tension strap centerline. It was further determined that without modification, the coupling flange design limited the operational speed of the coupling to 16,000 rpm.

STATIC TEST PROCEDURE

The static test consisted of subjecting each test coupling to a torque equivalent to twice the design torque condition. One side of the coupling was fixed while torque was applied in increments of 1100 inch-pounds to a maximum value of 9900 inch-pounds. Torsional deflection was recorded at each load level. A photographic record was also made of the test set-up.

Static Test Results - Tension Strap Coupling

The tension strap coupling was successfully tested to a load above the design ultimate torque without any permanent deformation or any other signs of distress. The results are plotted in Figure 50 relating the test torque with the measured torsional deflection.

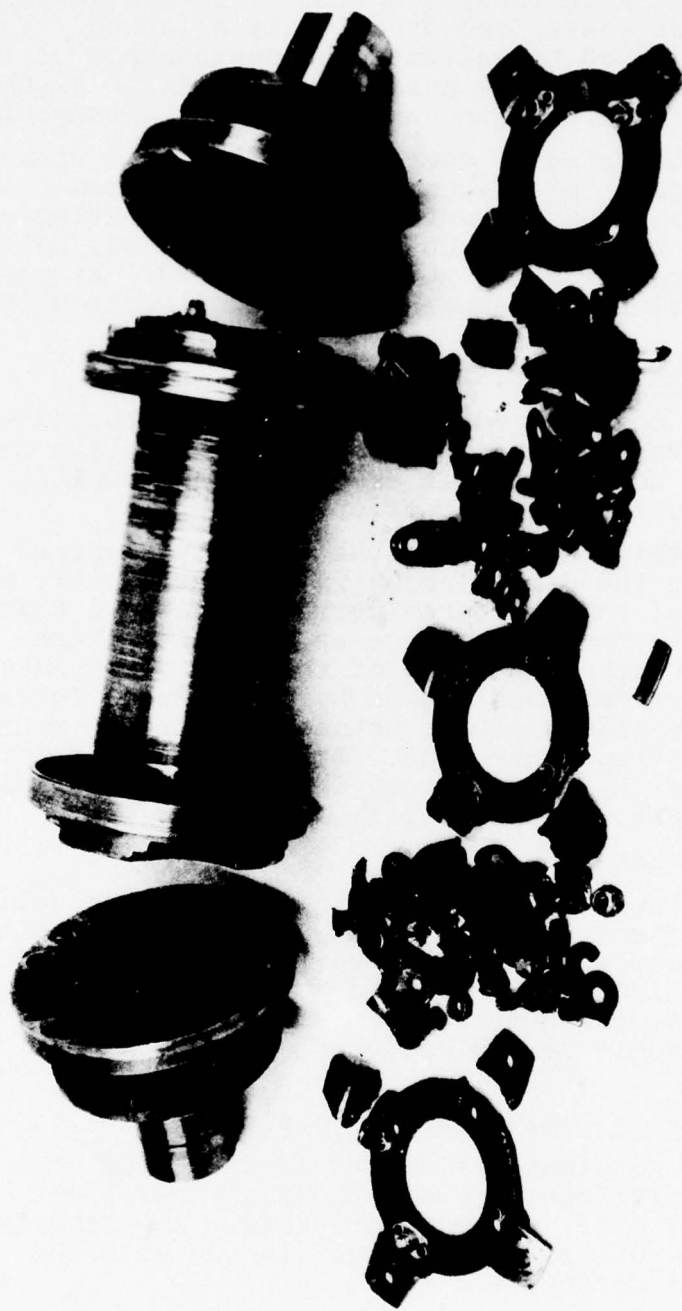


Figure 47. Test Shaft and Adapter Flanges.



Figure 48. Test Shaft and Coupling Parts.

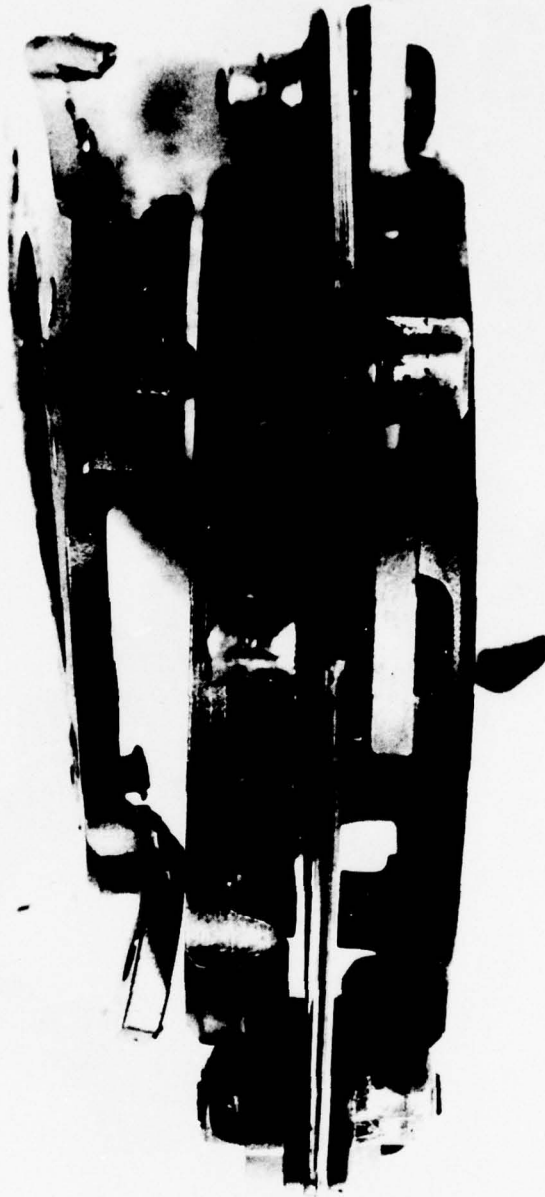


Figure 49. Coupling Test Specimen Flange Fracture.

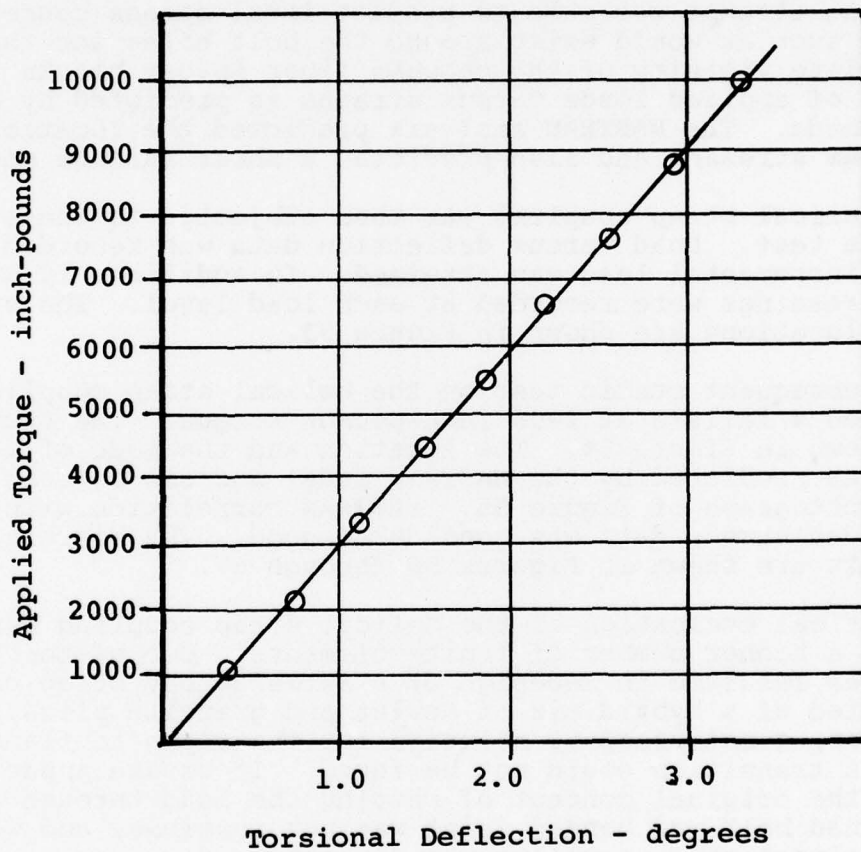


Figure 50. Torque versus Torsional Deflection, Tension Strap Coupling.

Static Test Results - Helical Strap Coupling

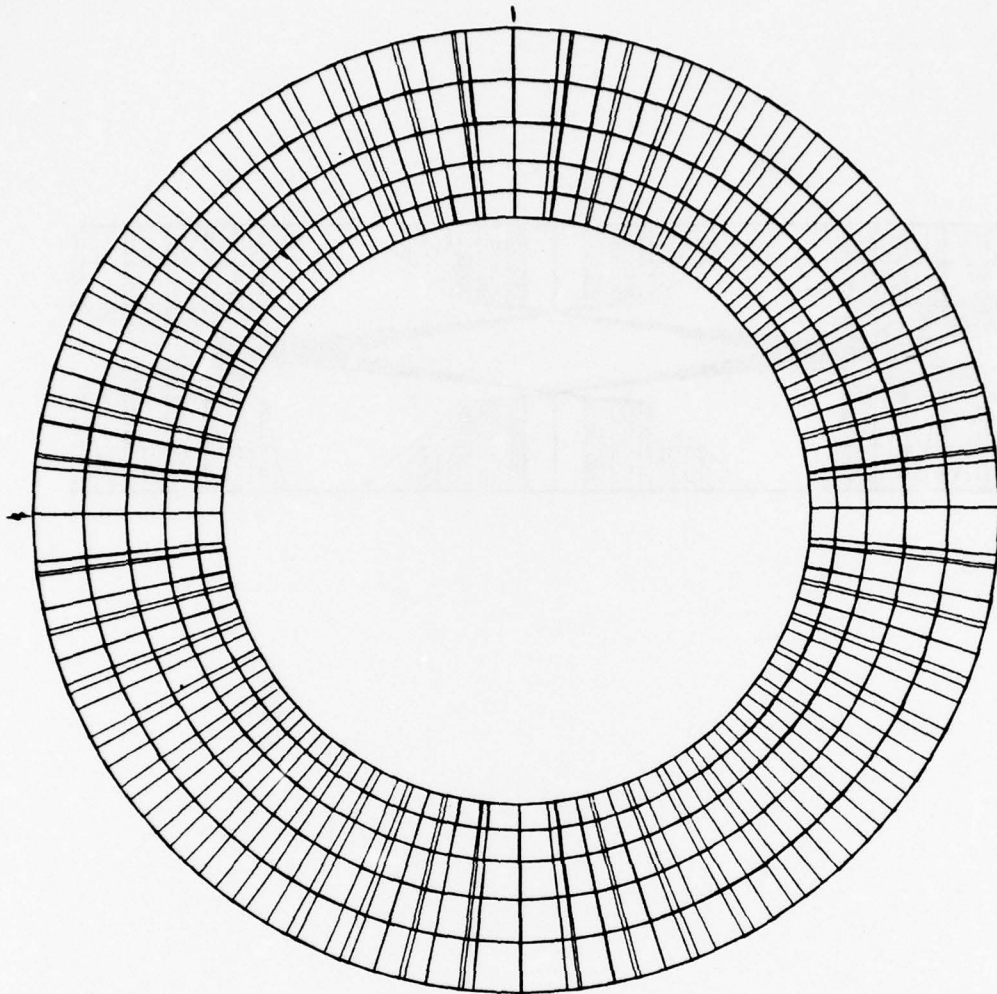
Prior to the static test of the helical strap coupling, a NASTRAN model of this coupling was generated. It was observed that the complex nature of this coupling configuration did not lend itself to a closed-form analytical solution in determining states of stresses and deformation patterns. The finite element approach was employed to generate a model of orthotropic elements capable of both bending and membrane actions. Figures 51 and 52 are NASTRAN plots of the coupling geometry.

The initial approach to the problem was to model the coupling such that general stress patterns could be defined. No initial attempt was made to predict local stress concentrations such as would exist around the bolt holes and the immediate vicinity of the chopped fiber spacer blocks. Plots of applied loads versus strains as predicted by NASTRAN were made. The NASTRAN analysis predicted the location of maximum stresses and also predicted a shear failure mode.

The helical strap coupling was then subjected to the over-torque test. Load versus deflection data was recorded as each incremental load was attained. In addition, 12 strain gage readings were recorded at each load level. The strain gage locations are shown in Figure 53.

The subsequent static test on the helical strap coupling induced a failure at 1900 inch-pounds torque. The test data is shown in Figure 54. The location and the mode of failure were as predicted by the NASTRAN model and can be seen in the photograph of Figure 55. NASTRAN correlation with recorded stress data was considered good. The correlation results are shown in Figures 56 through 67.

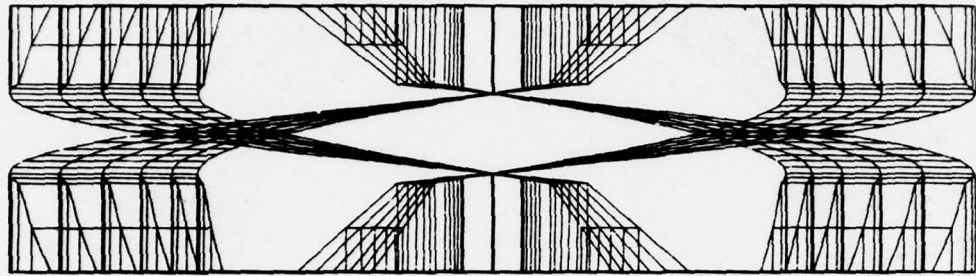
Analytical evaluation of the helical strap coupling continued using a higher number of finite elements. Use of these procedures resulted in redesign of a satisfactory strap constructed of a hybrid mix of Kevlar and graphite plies. However, a satisfactory solution for the strap to flange annulus transition could not be found. It became apparent that the original concept of sharing the load through a combined bolt and bonded joint was not feasible, and work on the helical strap coupling was discontinued.



HELICAL COUPLER
UNDEFORMED SHAPE

PLAN VIEW

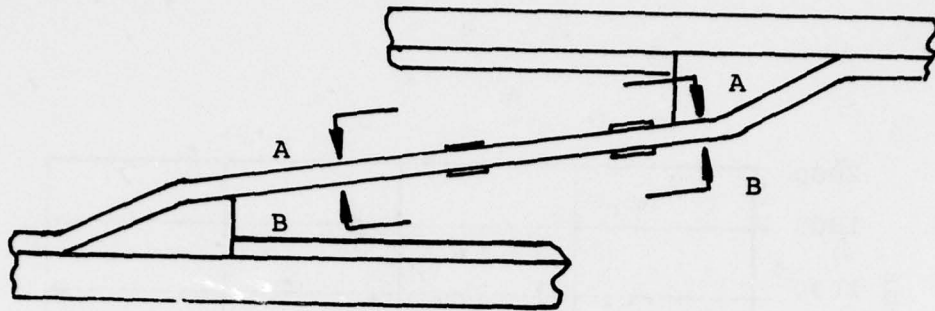
Figure 51. NASTRAN Model,
Composite Helical Strap Coupling.



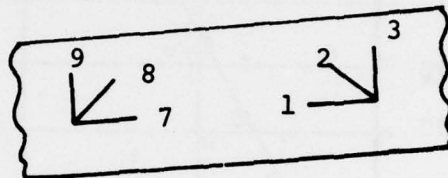
HELICAL COUPLER
UNDEFORMED SHAPE

ELEVATION

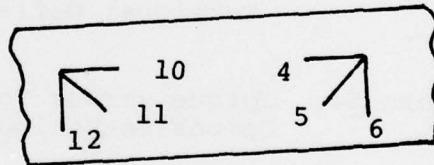
Figure 52. NASTRAN Model,
Composite Helical Strap Coupling.



Helical Strap



View A-A



View B-B

Figure 53. Strain Gage Locations, Helical Strap Coupling.

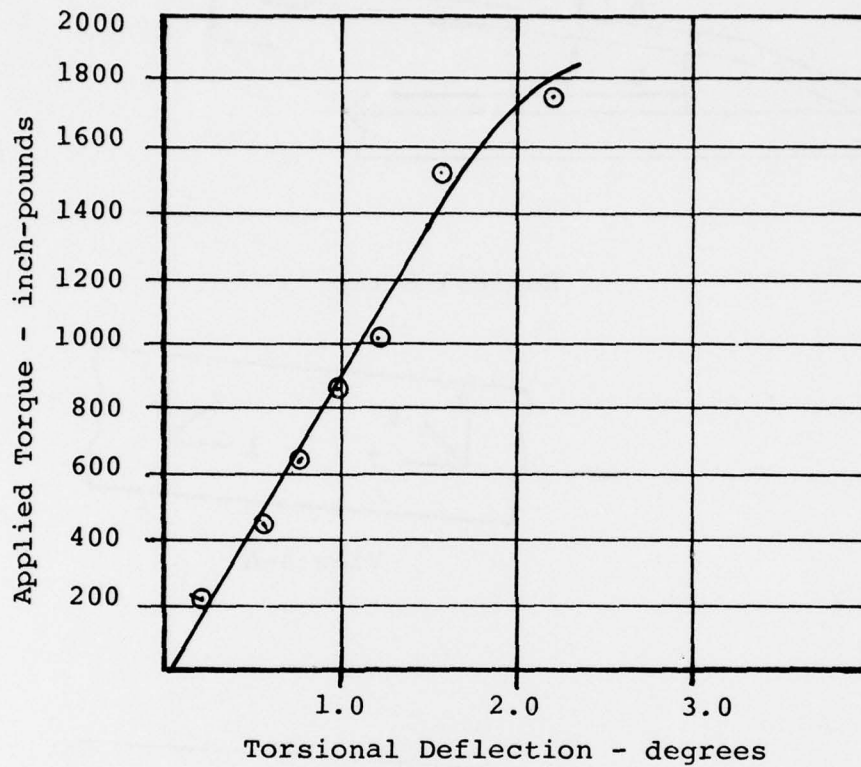


Figure 54. Torque versus Torsional Deflection, Composite Helical Strap Coupling.

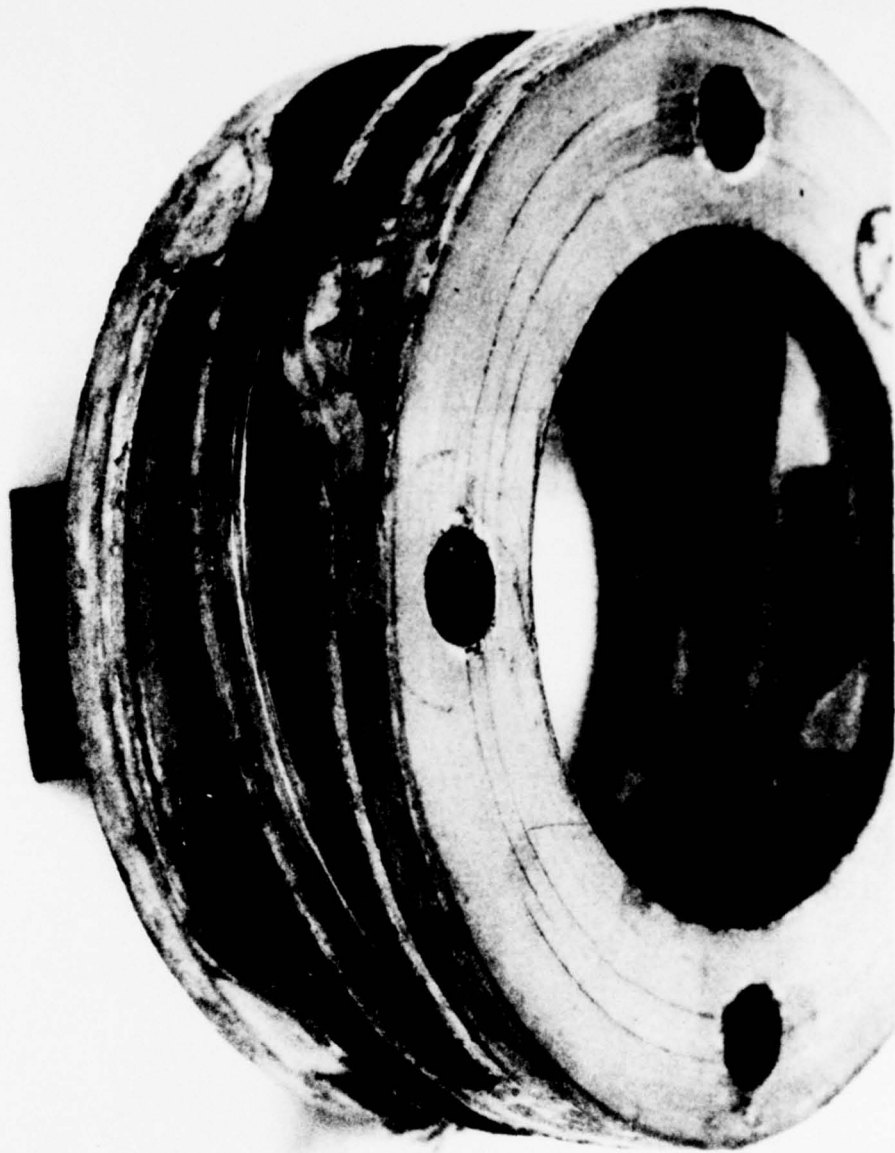


Figure 55. Helical Strap Coupling Fracture.

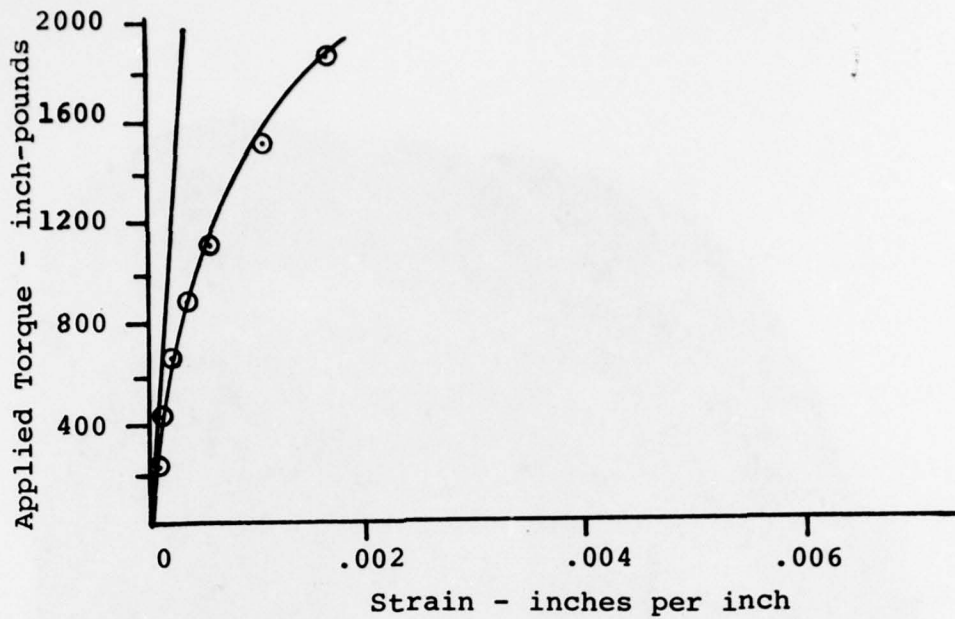


Figure 56. Analysis and Test Correlation, Gage No. 1, Helical Strap Coupling.

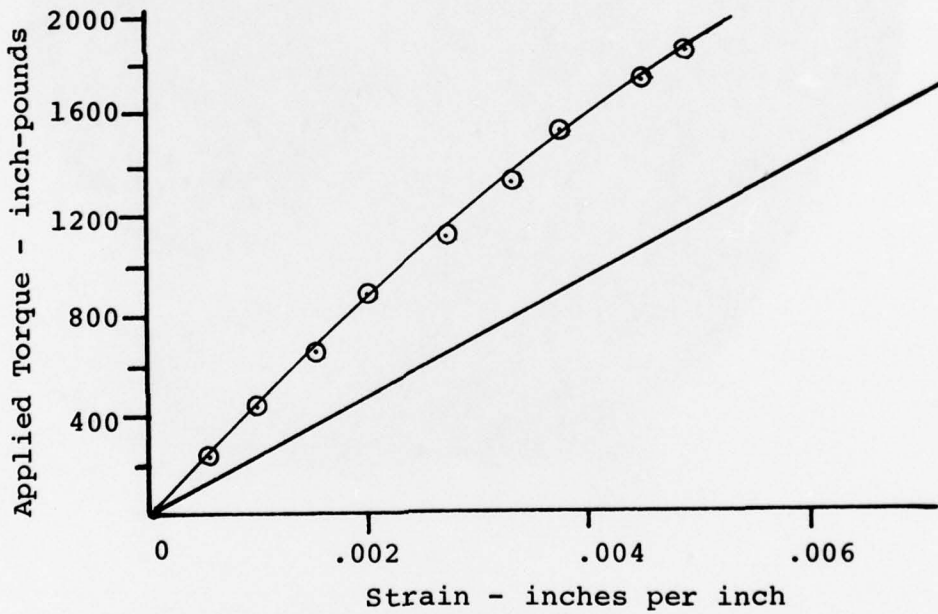


Figure 57. Analysis and Test Correlation, Gage No. 2, Helical Strap Coupling.

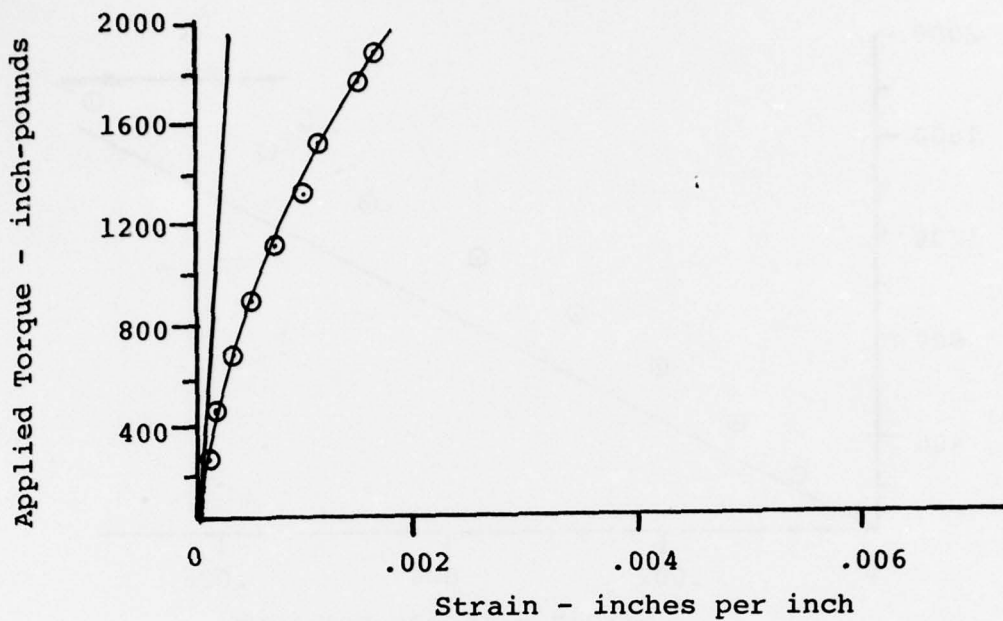


Figure 58. Analysis and Test Correlation, Gage No. 3, Helical Strap Coupling.

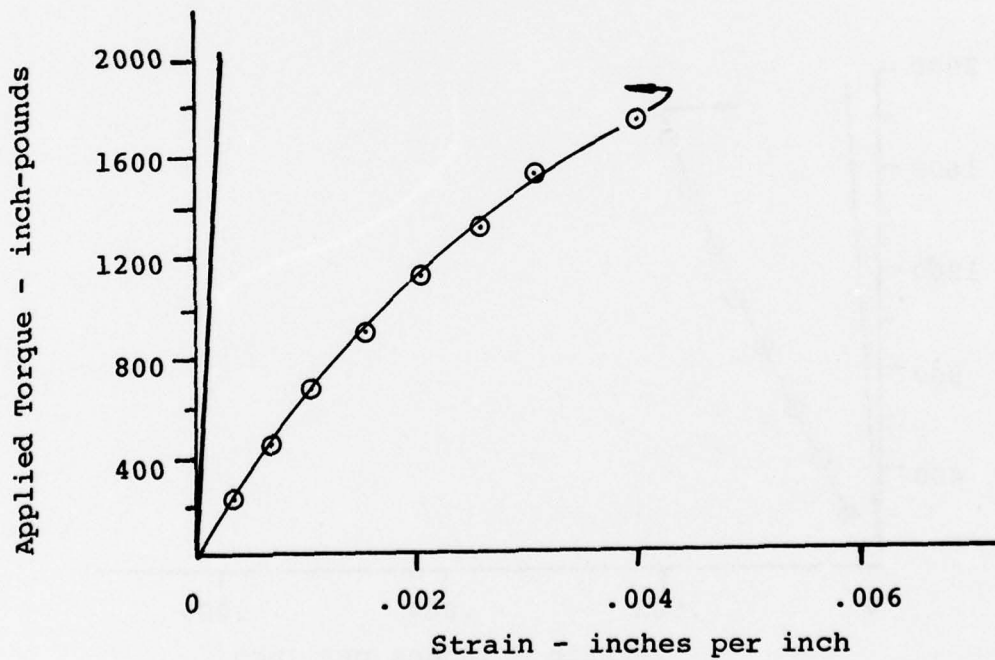


Figure 59. Analysis and Test Correlation, Gage No. 4, Helical Strap Coupling.

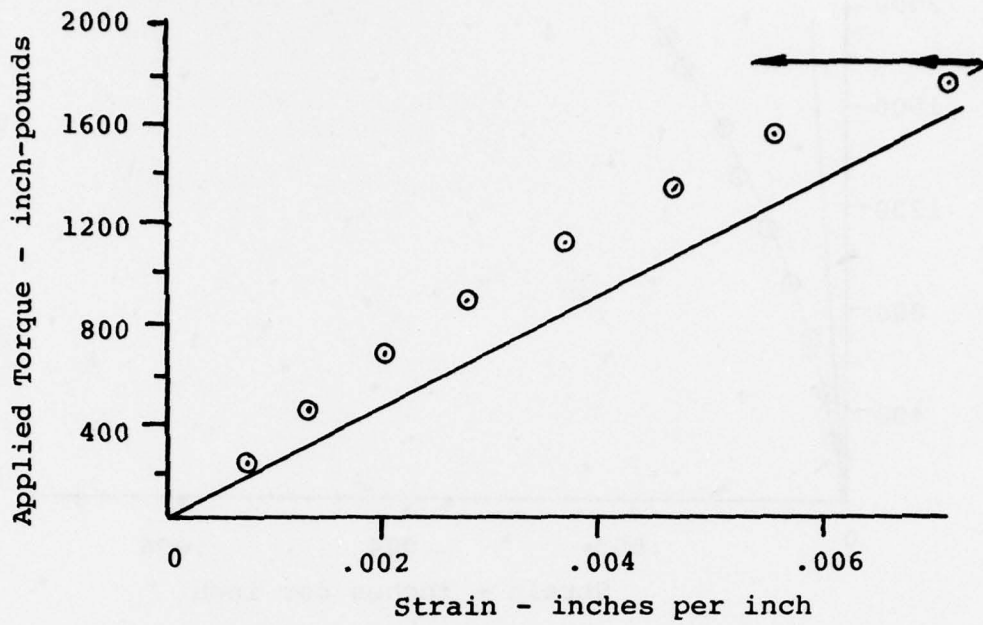


Figure 60. Analysis and Test Correlation,
Gage No. 5, Helical Strap Coupling.

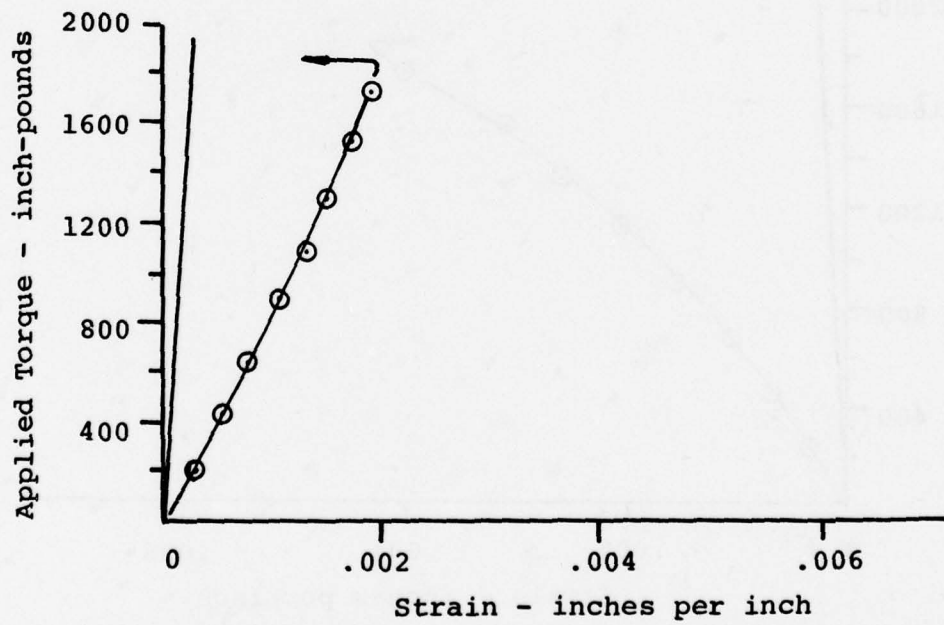


Figure 61. Analysis and Test Correlation,
Gage No. 6, Helical Strap Coupling.

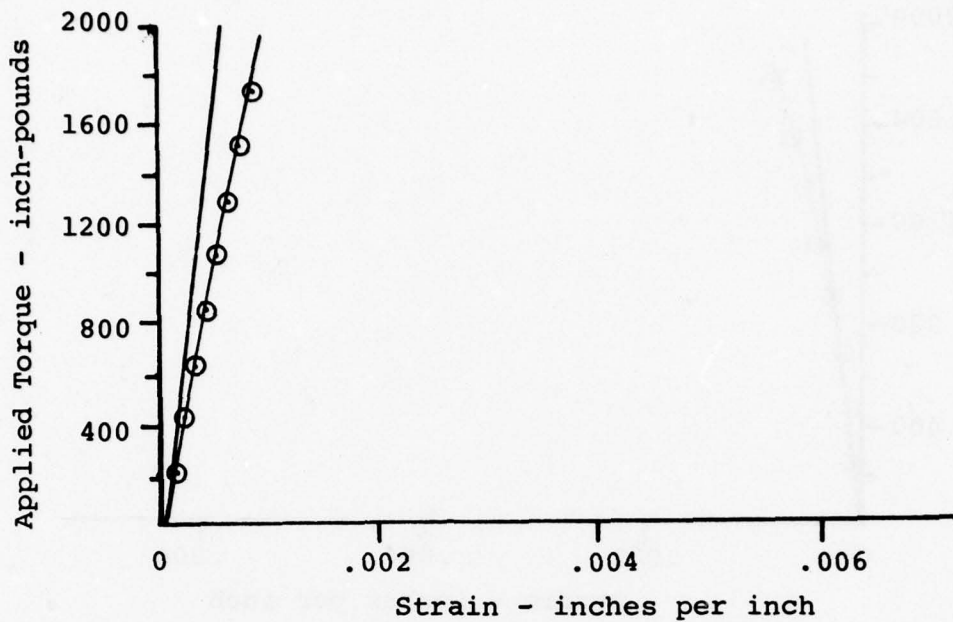


Figure 62. Analysis and Test Correlation, Gage No. 7, Helical Strap Coupling.

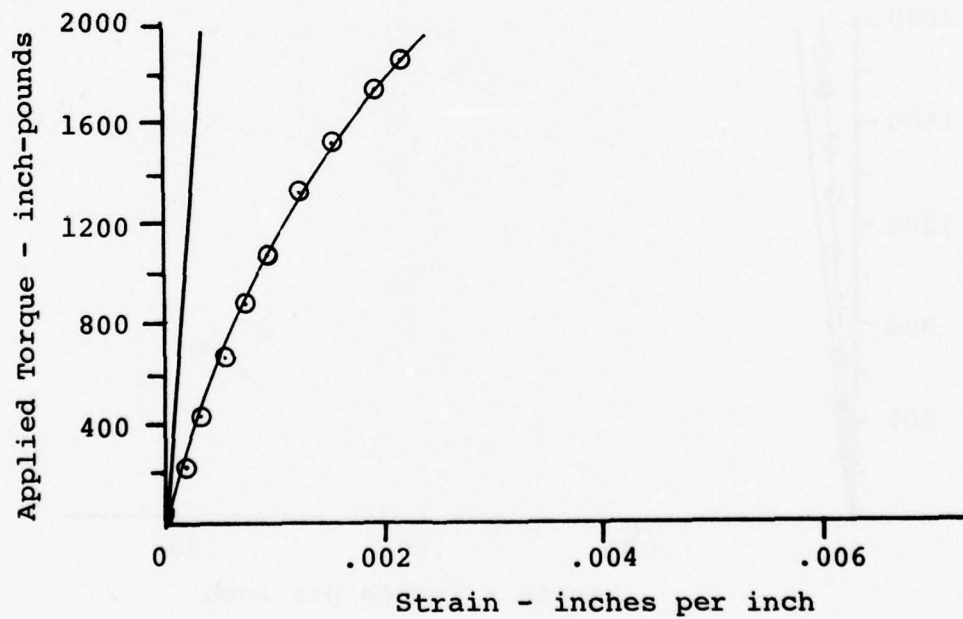


Figure 63. Analysis and Test Correlation, Gage No. 8, Helical Strap Coupling.

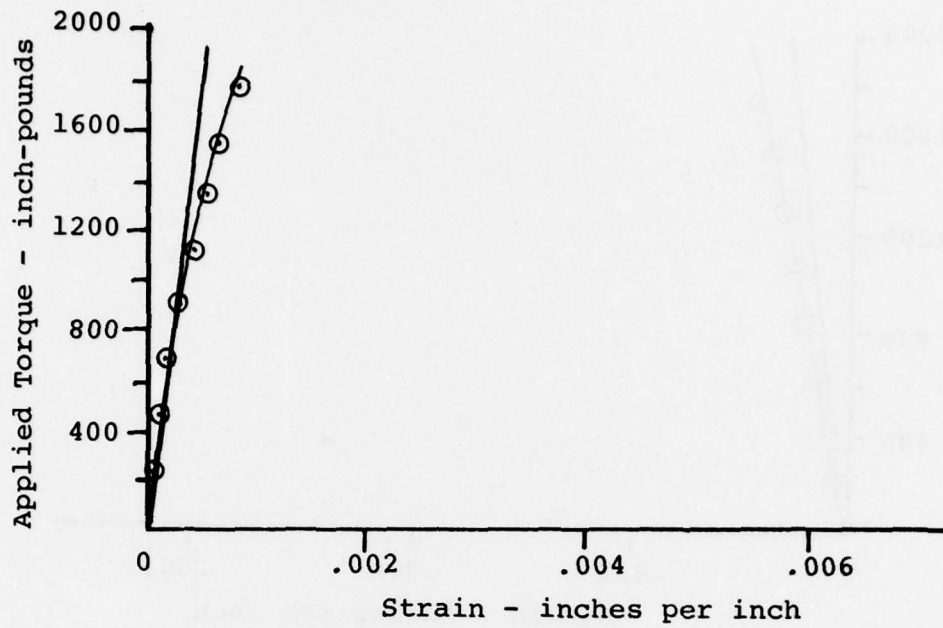


Figure 64. Analysis and Test Correlation, Gage No. 9, Helical Strap Coupling.

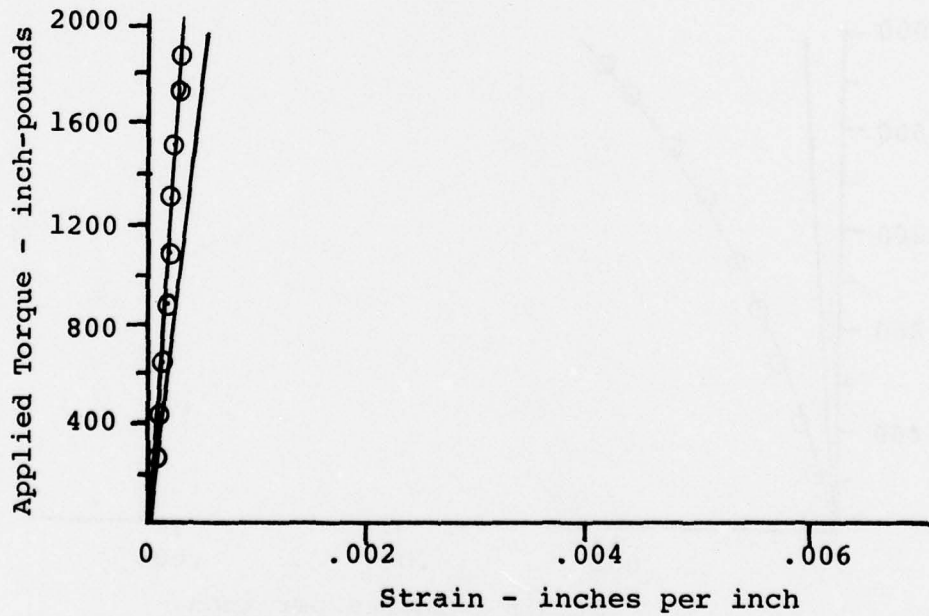


Figure 65. Analysis and Test Correlation, Gage No. 10, Helical Strap Coupling.

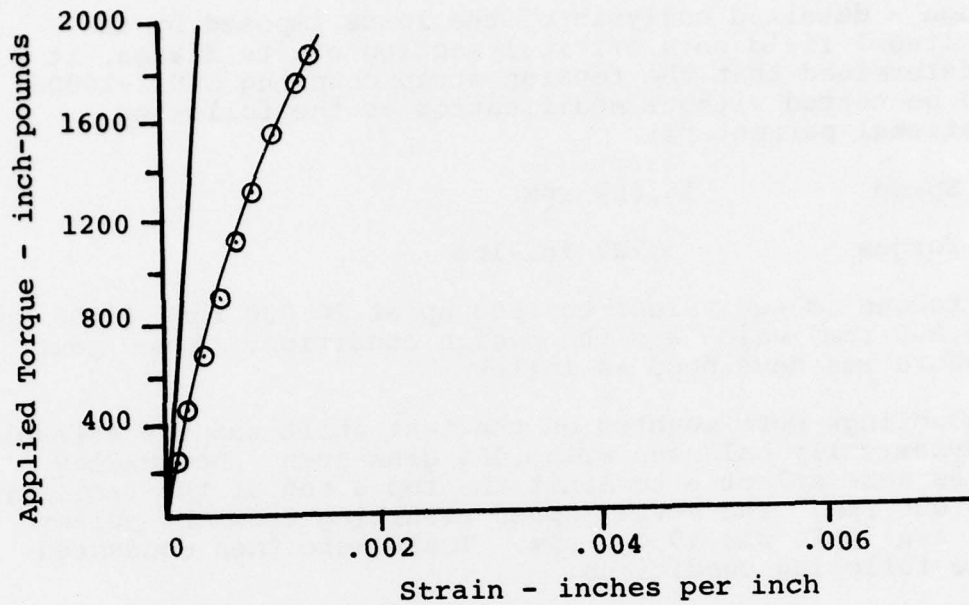


Figure 66. Analysis and Test Correlation,
Gage No. 11, Helical Strap Coupling.

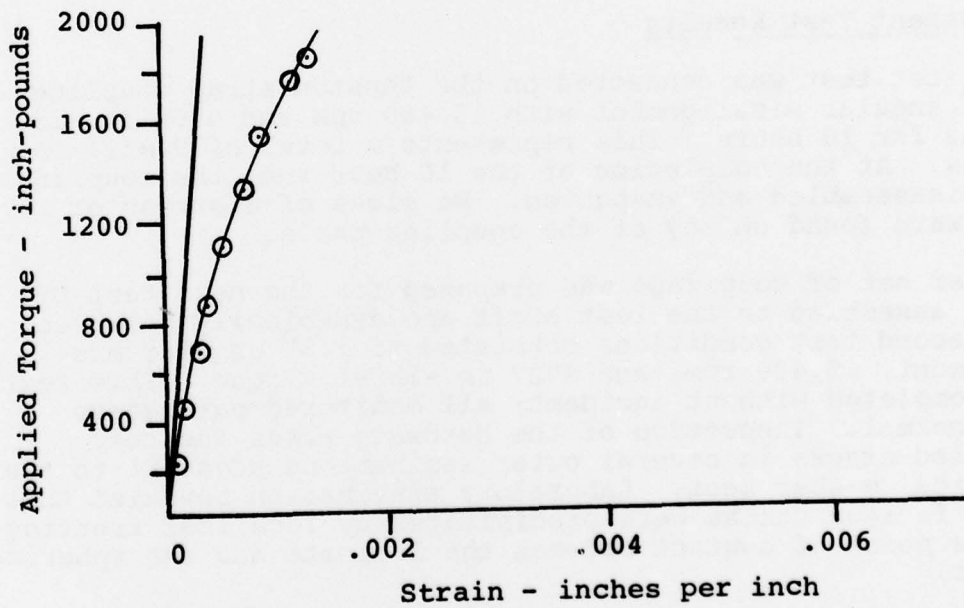


Figure 67. Analysis and Test Correlation,
Gage No. 12, Helical Strap Coupling.

ASSESSMENT TEST PROCEDURE

Through a detailed analysis of the loads imposed by the centrifugal field on a critical section of its flange, it was determined that the tension strap coupling 38012-10006 could be tested without modification at the following operational parameters:

Speed	16,000 rpm
Torque	4,727 in.-lbs

This torque is equivalent to 1500 hp at 20,000 rpm, (1200 hp at 16,000 rpm) which was the design condition. A new test procedure was developed as follows.

The couplings were mounted on the test shaft and the assembly was dynamically balanced with .403 gram-inch. New pulley sheaves were selected to limit the top speed of the facility to 16,000 rpm. The actual speed resulting from the pulley sizes available was 15,400 rpm. Tests were then conducted at the following conditions.

- a. 15,400 rpm, 4000 in-lb (977 hp), 1° angular misalignment for a total of 10 hours (9×10^6 cycles).
- b. 15,400 rpm, 4727 in-lb (1155 hp), $1\text{-}1/2^{\circ}$ angular misalignment for a total of 10 hours (9×10^6 cycles).

Assessment Test Results

The first test was conducted on the tension strap coupling at 1° angular misalignment with 15,400 rpm and 4000 in.-lb torque for 10 hours. This represents a total of 9 million cycles. At the completion of the 10-hour run, the coupling was disassembled and inspected. No signs of distress or wear were found on any of the coupling parts.

Another set of couplings was prepared for the next test by being assembled to the test shaft and dynamically balanced. The second test conditions consisted of 1.5° angular misalignment, 15,400 rpm, and 4727 in.-lb of torque. This test was completed without incident; all monitored parameters were normal. Inspection of the hardware after the test revealed cracks in several outer laminations adjacent to the spherical washer seat. Laboratory examination revealed that these fatigue cracks were precipitated by localized fretting at the point of contact between the laminate and the spherical washer.

INTERIM COUPLING PROGRAM

At this point in the program both candidate couplings had failed to successfully pass the initial performance test. It was evident that the program could not proceed as was originally planned and an alternate approach was necessary. A plan was proposed and adopted to develop, fabricate, and test two modifications of the tension strap coupling 38012-10006. These new designs would maximize usage of existing coupling hardware (i.e., flanges and laminated straps) and the techniques developed to design a composite flexure element.

Stainless Steel Tension Strap Coupling Design

The primary effort in this redesign was to substantially reduce or eliminate the fretting condition which precipitated an earlier fatigue failure. The redesigned coupling shown in Figure 68 was improved to obtain a calculated mean allowable continuous misalignment capability at rated torque and speed of 2°. The following changes were implemented to achieve this improvement:

- a. Silver plate was used on the stainless steel straps and radius blocks as a fretting barrier.
- b. The spherical washer was replaced with a radius block to improve the load distribution over the width of the strap.
- c. A radius block was designed to control the bend radius of curvature of the strap at the point of contact.

Composite Tension Strap Coupling Design

The new tension strap coupling required the design of a composite strap element to satisfy the required flexure and load carrying capabilities as well as accommodate existing flange geometry. A parametric study of six different graphite/epoxy strap designs was conducted and stiffness, static strength, and fatigue strength were compared. A five-element strap was selected as optimum. This composite strap was comprised of 50%, 0°, and 50%, +45° graphite laminate, with overall thickness of .022 in. per laminate.

A detailed analysis was conducted of the bolted connection using a finite element method to examine the bolt/strap interface. In conjunction with the finite element analysis, a static and fatigue analysis of the mating titanium flange lug was performed. Positive margins of safety were established in all cases at maximum operating conditions.

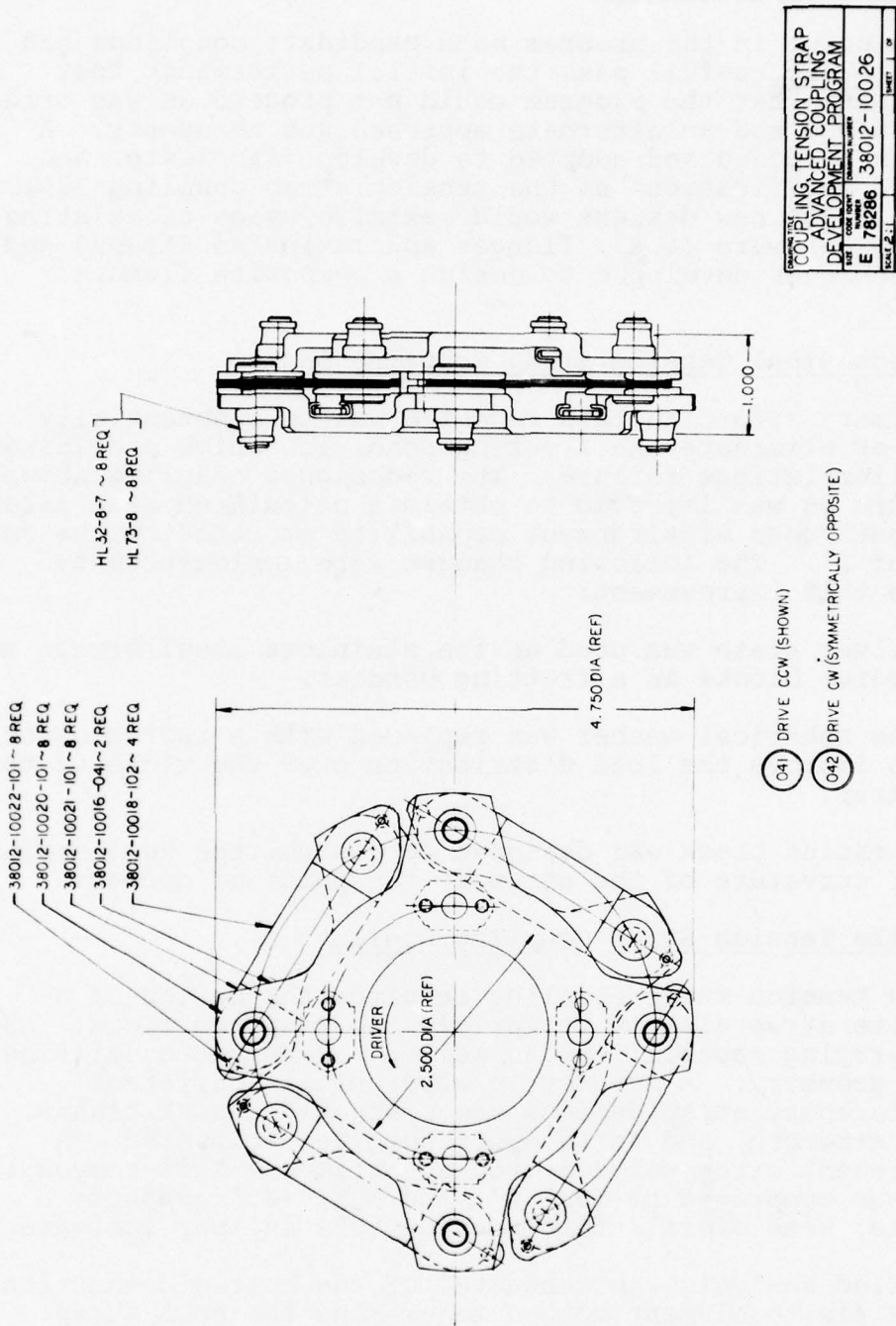


Figure 68. Steel Strap Coupling Redesign.

The final design is shown in Figure 69. The advantages of the composite strap over its steel counterpart are the elimination of fretting, reduced weight, and reduction in number of parts.

Fabrication

Upon completion of the detail design, both new and modified parts were released for fabrication and assembly. Four specimens of each of the two designs were fabricated. These couplings are shown in Figures 70 and 71.

Static Tests

Both the stainless steel and the composite couplings were subjected to static overload torque tests. Torque was applied in 1100 in.-lb increments to a minimum value of 9900 in.-lb. Torsional deflection was recorded at each load level.

Examination of the respective couplings upon completion of these tests revealed that no permanent deformation or other signs of distress had been incurred. Figures 72 and 73 show the results of this test as a plot of torque versus deflection for each of the modified couplings.

In the case of the composite strap coupling, 38012-10027, the test was repeated on the same specimen. The second test was run both up and down at identical increments and the load/deflection data checked for repeatability at each point. Excellent correlation between readings at each point was observed on this second run. The composite coupling was noticeably stiffer torsionally. At the conclusion of the static overload test, the graphite/epoxy composite coupling was partially disassembled to examine the detail parts. A photograph of the stainless steel coupling in the test fixture is shown in Figure 74. A photograph of the composite coupling after the test is shown in Figure 75. No indications of distress were observed in either of the couplings as a result of the static tests.

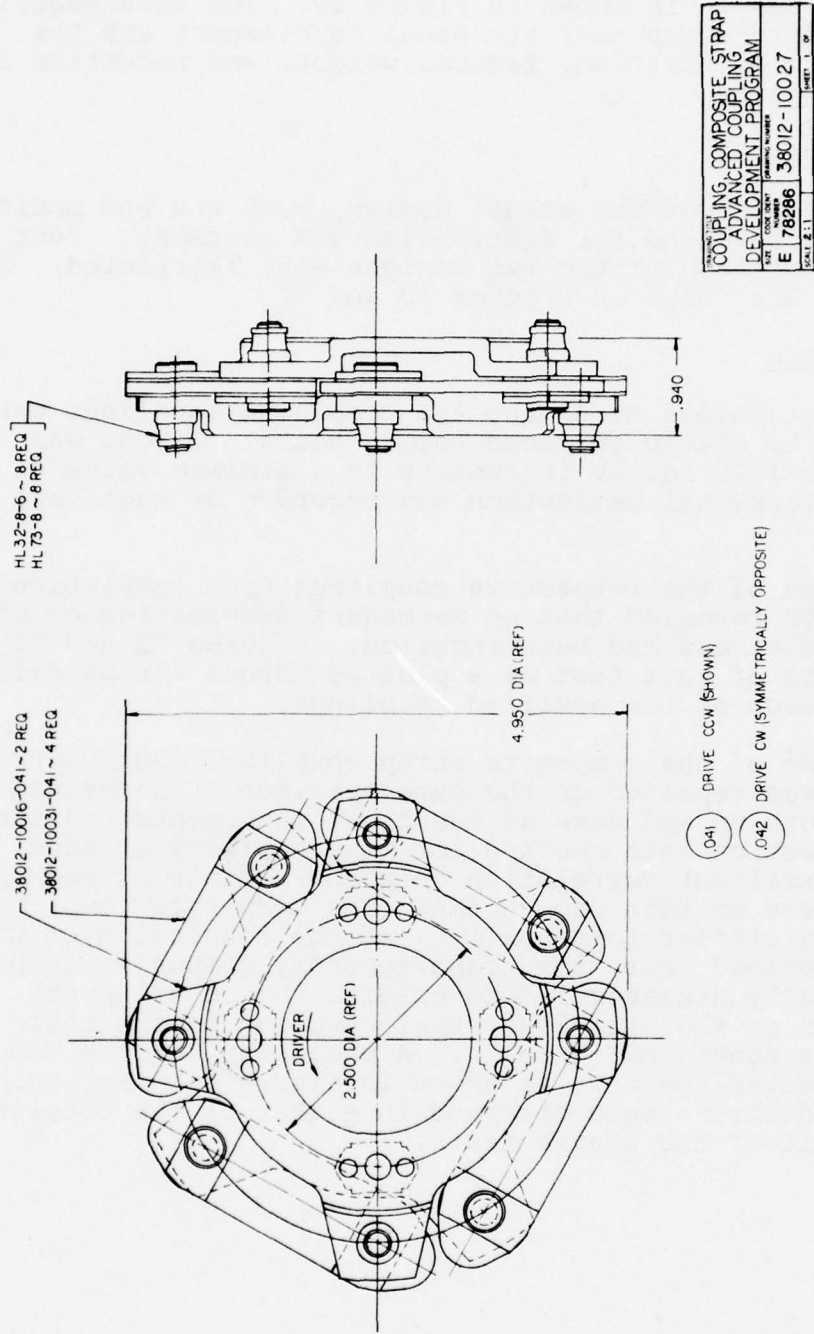


Figure 69. Composite Strap Coupling Redesign.



Figure 70. Steel Strap Coupling Test Specimen.



Figure 71. Composite Strap Coupling Test Specimen.

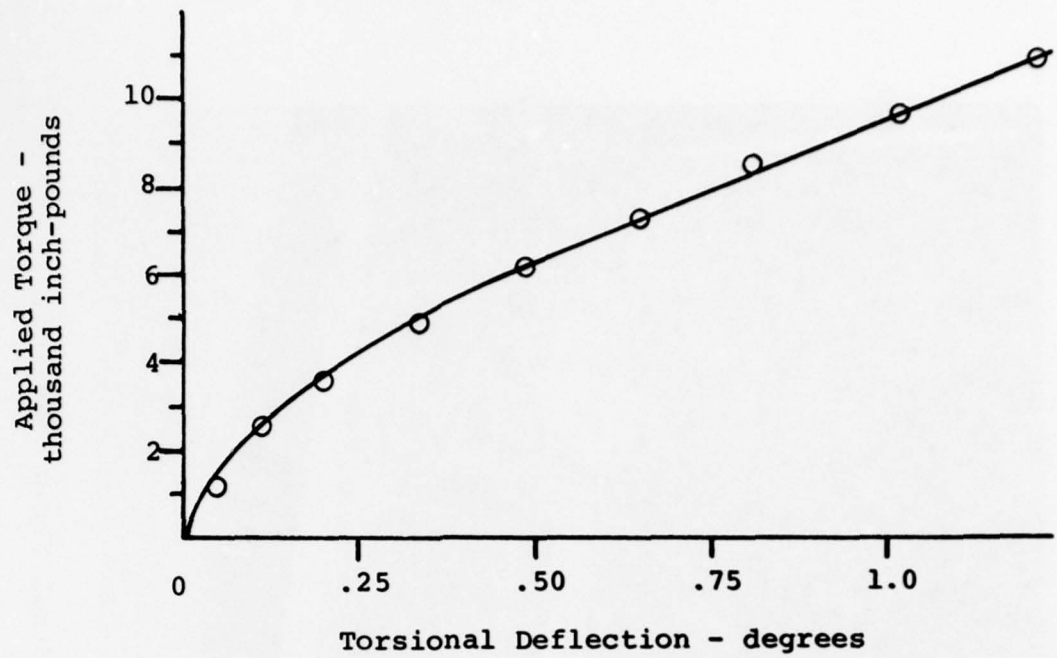


Figure 72. Deflection versus Torque, Steel Strap Coupling.

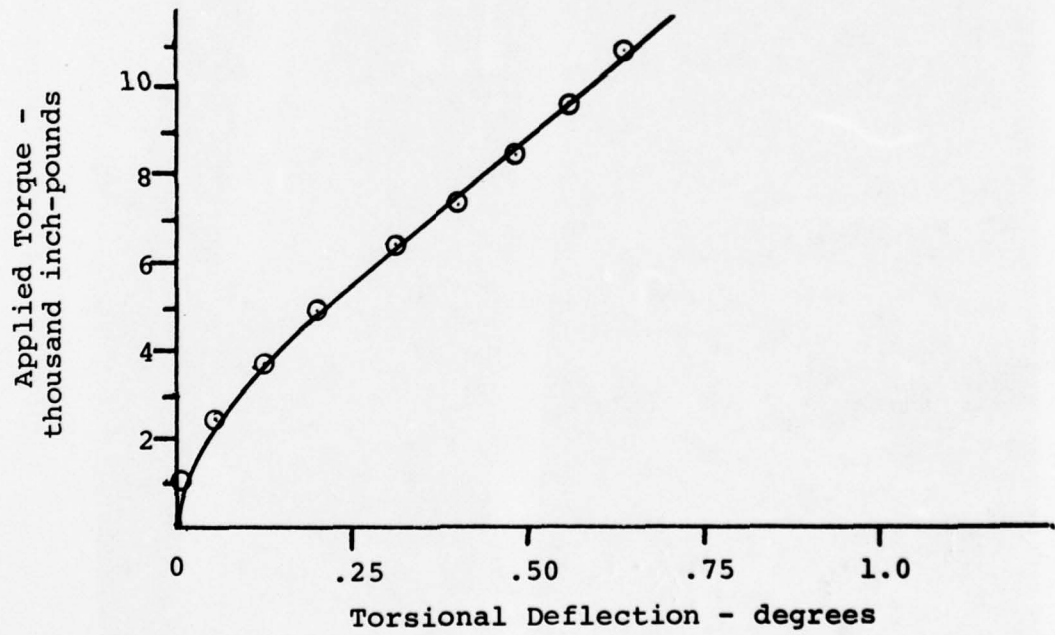


Figure 73. Deflection versus Torque, Composite Strap Coupling.

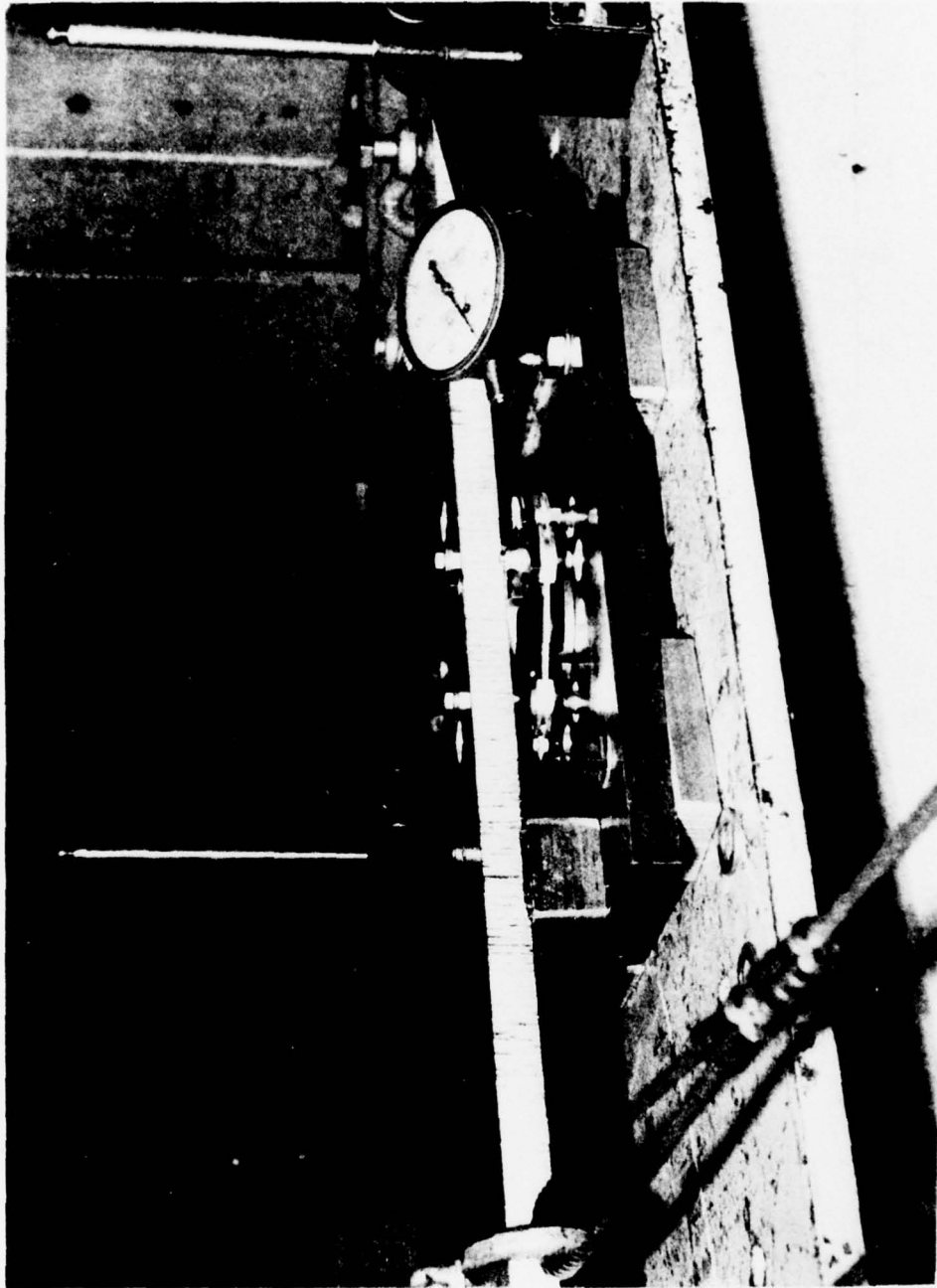


Figure 74. Static Torque Test, Steel Strap Coupling.



Figure 75. Static Torque Test - Composite Strap Coupling.

An axial spring rate test was conducted on the composite strap coupling. This test consisted of fixing one side of the coupling and applying axial load to the other side to a maximum value of .130 axial deflection. The test was conducted on a DU-10 deflectometer, which is a test machine that gives a continuous plot of load versus deflection. Figure 76 is a curve of axial deflection versus load showing a spring rate of 201 lb per inch per strap. This was in good agreement with the calculated spring rate of 210 lb per inch.

Dynamic Test - Stainless Steel Coupling

The first coupling to be tested was the redesigned stainless steel tension strap coupling, part number 38012-10026-041. The dynamic test plan consisted of 10 hours of operation at 15,400 rpm, 4727 in.-lb torque, and 1.5° angular misalignment. Prior to conducting the test, the test couplings were dynamically balanced.

After 7.5 hours, which was equivalent to 7.2 million cycles, the coupling failed and testing was terminated.

In order to determine the cause and origin of the test failure, the following procedures were immediately implemented:

1. A photographic record of the test shaft assembly was made both before and after removal from the facility.
2. A check was made on the facility geometry to confirm the angular misalignment at the time of testing.
3. A metallurgical examination and study was undertaken to determine the origin and mode of failures.
4. An assessment of the damage to the test facility and the work to be accomplished before testing could be resumed was initiated.

Metallurgical examination of the parts indicated fatigue cracks in each case had originated in a localized area of fretting damage in the stainless steel flexure element. The coupling titanium flange lug failures were found to be secondary static bending fractures.

Figures 77 through 80 show some photographs of the test hardware and stand after the test.

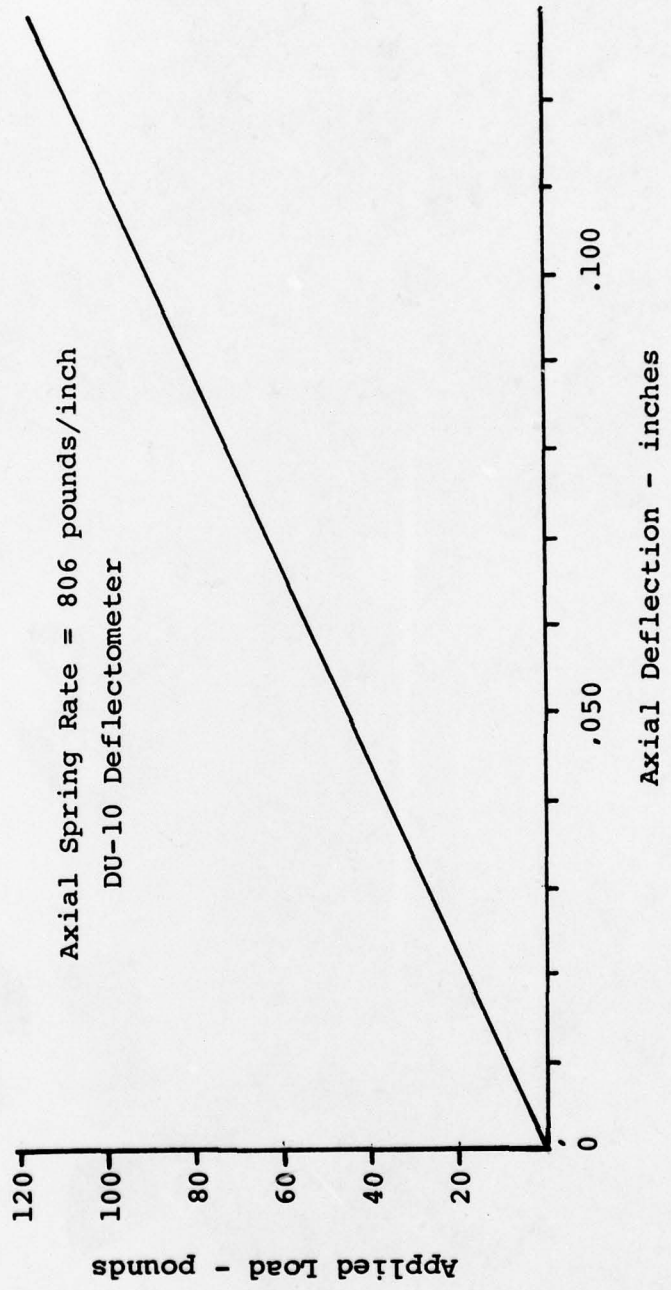


Figure 76. Axial Deflection versus Load, Composite Strap Coupling.

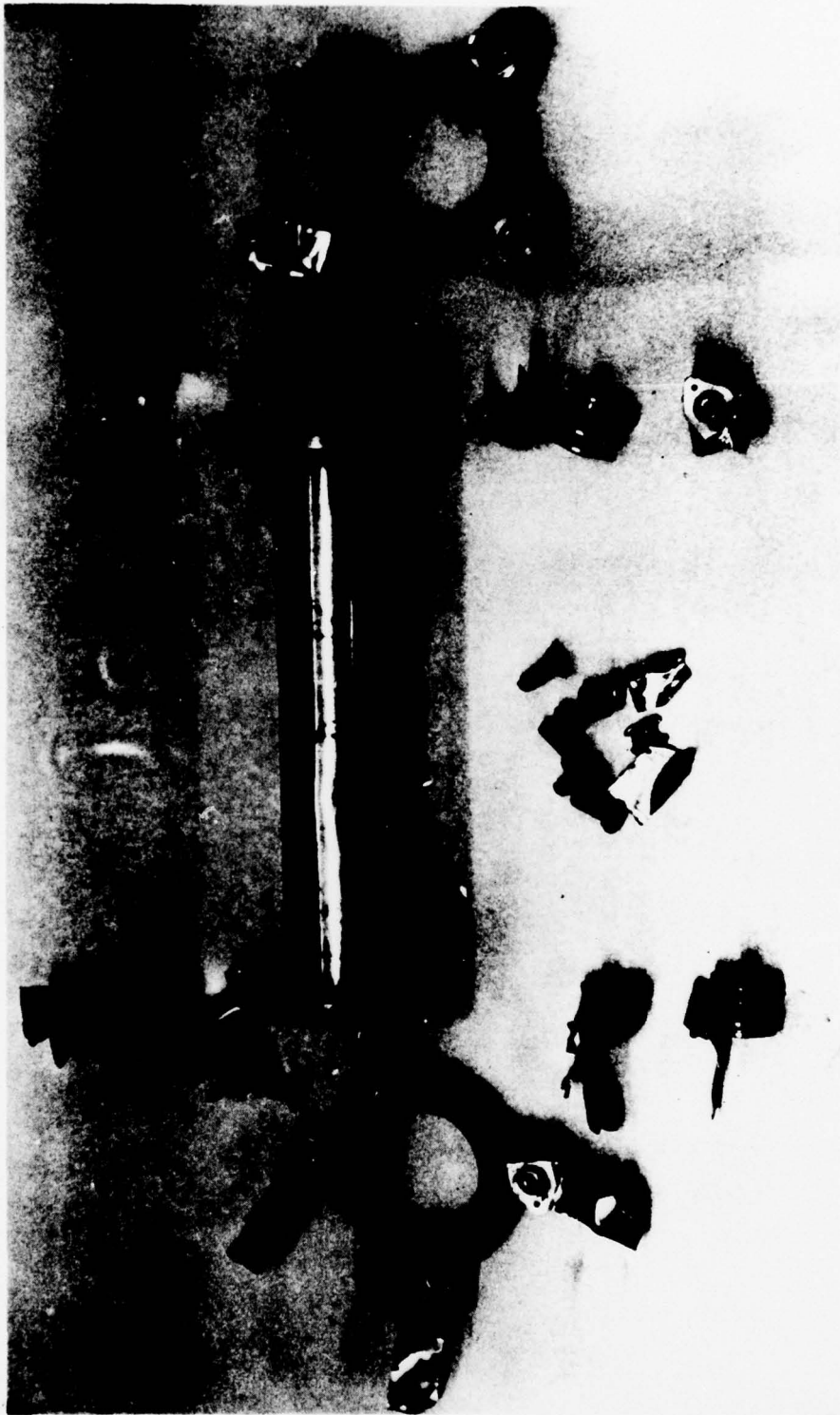


Figure 77. Dynamic Test Fracture, Steel Strap Coupling.

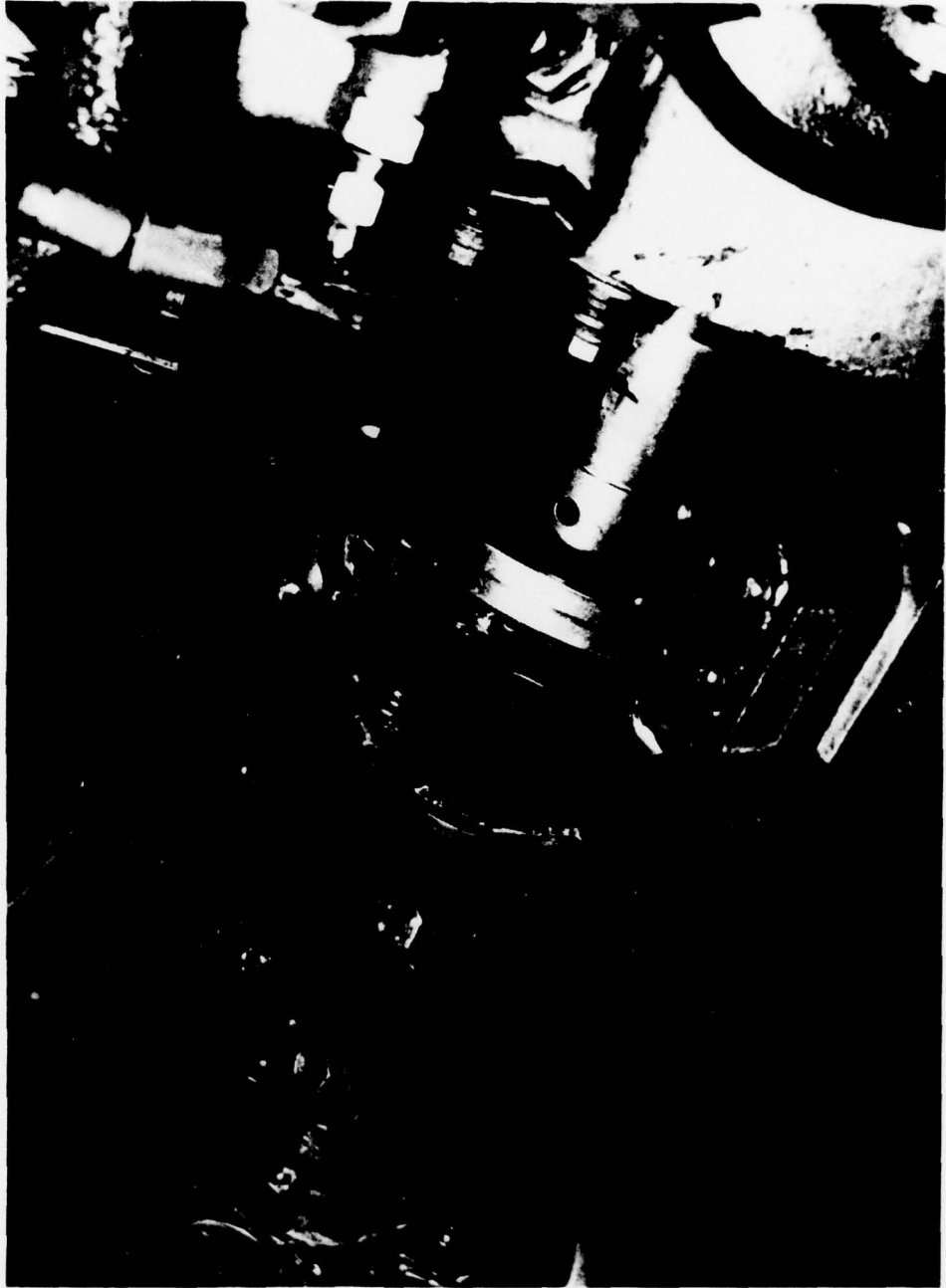


Figure 78. Dynamic Test Fracture, Test Shaft Containment.

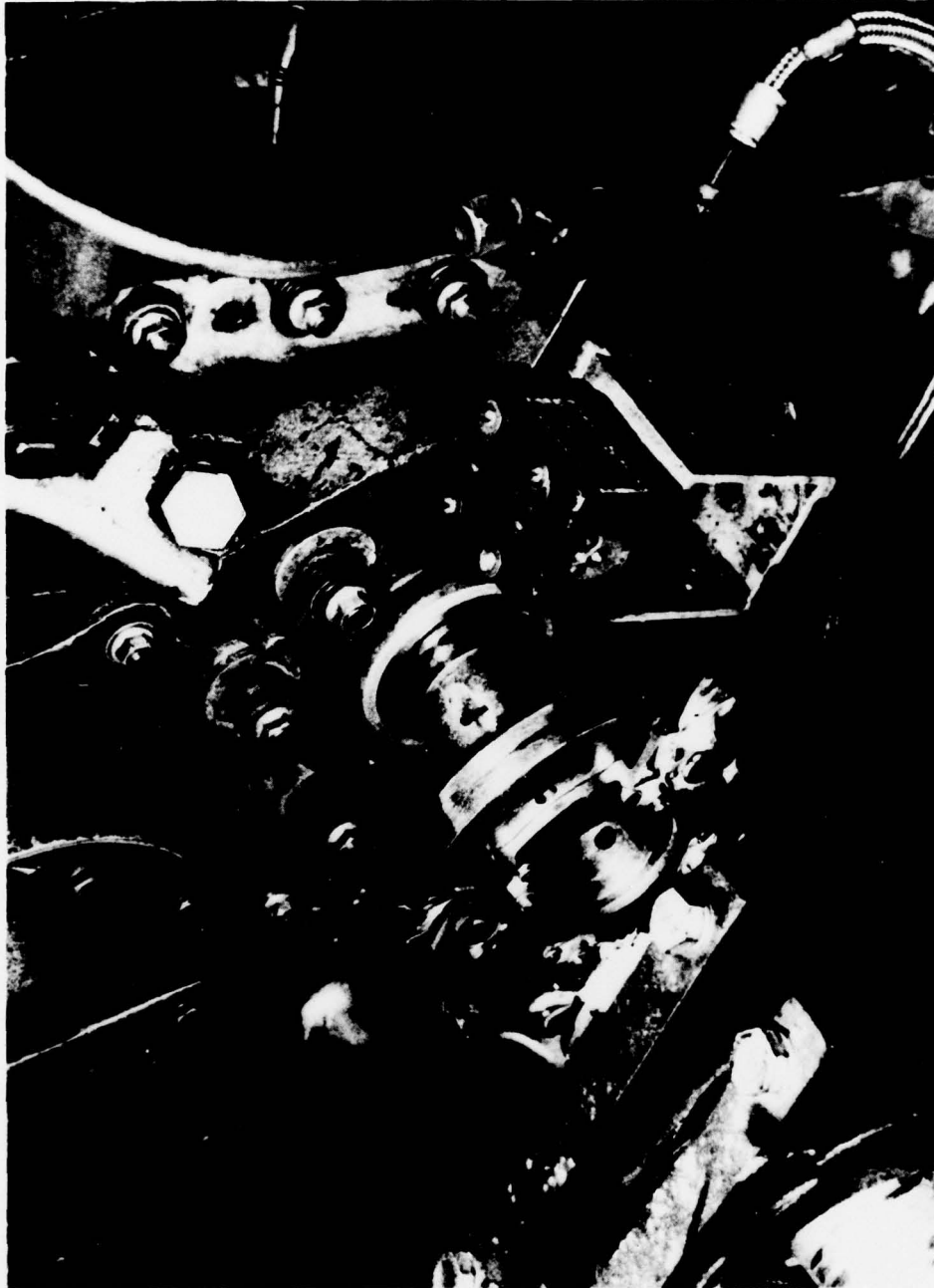


Figure 79. Dynamic Test Fracture, Test Box Flange.



Figure 80. Dynamic Test Fracture, Slave Box Flange.

Using fatigue methodology, the test point was plotted as shown in Figure 81. A standard shape S-N curve was then drawn through the failure point. For steel with chafing, the S-N curve is given by

$$\frac{S}{E} = 1 + \frac{.527}{N^{.666}} \quad (18)$$

Substitution of the test values of S=2degrees and N=7.2 into the above equation gives a mean endurance limit of 1.752 degrees. Applying an 80% reliability factor to the mean endurance limit gives a working endurance limit of 1.40 degrees, which is slightly below our design goal of 1.50 degrees.

Dynamic Test - Composite Coupling

The second coupling to be tested was the composite tension strap coupling, part number 38012-10027. The dynamic test plan consisted of 10 hours of operation at 15,400 rpm, 4727 in.-lb torque, and 1.5 degrees angular misalignment. Prior to conducting the test, the test couplings were dynamically balanced.

Testing was interrupted at 7.5 hours into the 10-hour test due to a failure of the test facility gearbox. The failure which resulted in rupturing the facility gear case was attributed to a fatigue failure at the web/gear interface. The failure occurred on the test shaft side, imposing inordinately high loads on the test couplings. This was evidenced by the bent condition of both shafts and flanges immediately adjacent to the coupling test specimens. Markings on the outer laminates of the test specimen couplings indicated that the test shaft excursion had caused the couplings to experience equivalent angular misalignments of up to 4 degrees during the shutdown cycle after the test stand failure.

The test specimens were examined after removal from the facility, and the decision was made to complete the 10-hour cycle with this same set of couplings. The test facility was subsequently restored to running order and the remainder of the test completed without incident.

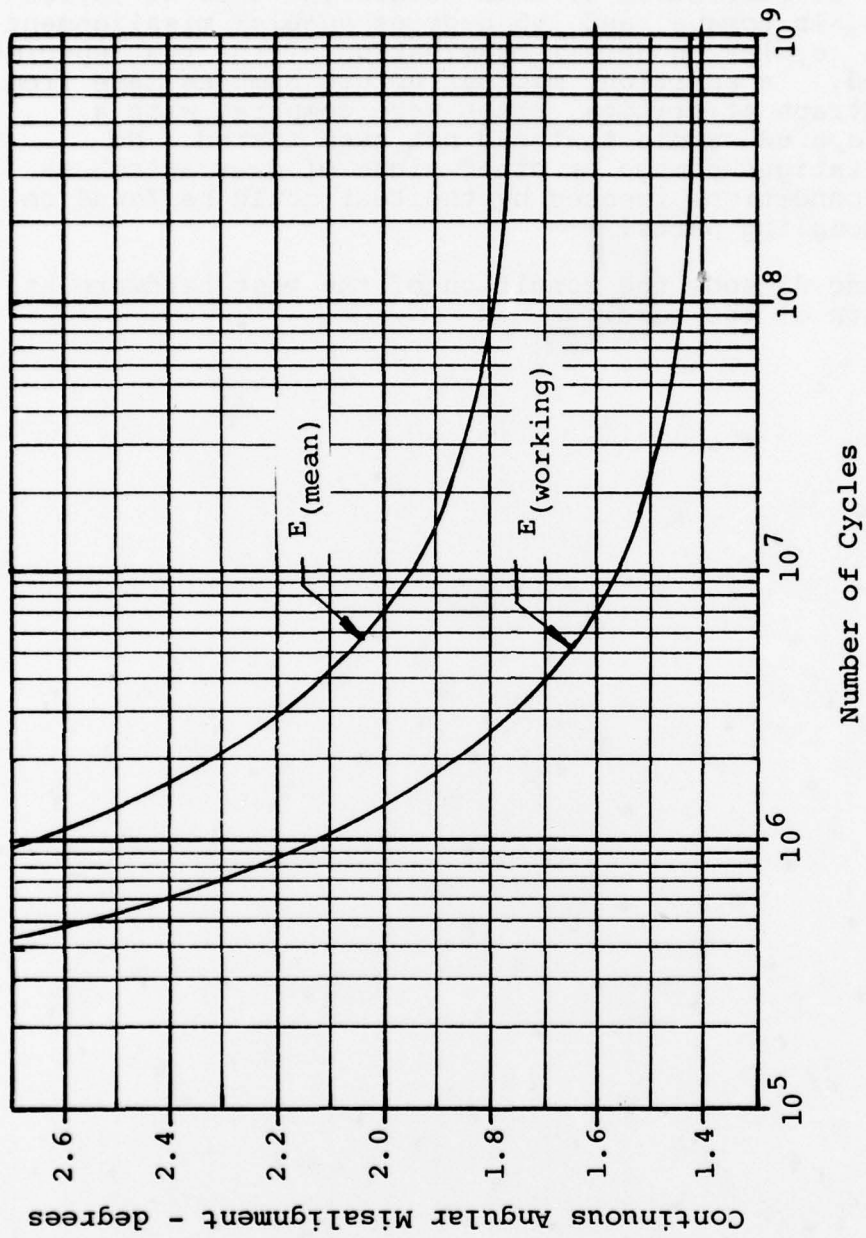


Figure 81. Working Endurance Limit, Steel Tension Strap Coupling.

Upon successful completion of this assessment test at 15,400 rpm, 4727 in₆-lb torque, and 1.5 degrees angular misalignment for 9.2×10^6 cycles, a detail examination of the test specimen was conducted. In addition, microstructure samples made from the tested straps at critical areas were compared with a similarly prepared sample that had not been tested. No evidence of fatigue damage or other signs of wear attributable to the conditions imposed by the test could be found on any of the coupling parts.

Figures 82 and 83 show the condition of the test hardware at the completion of the test.

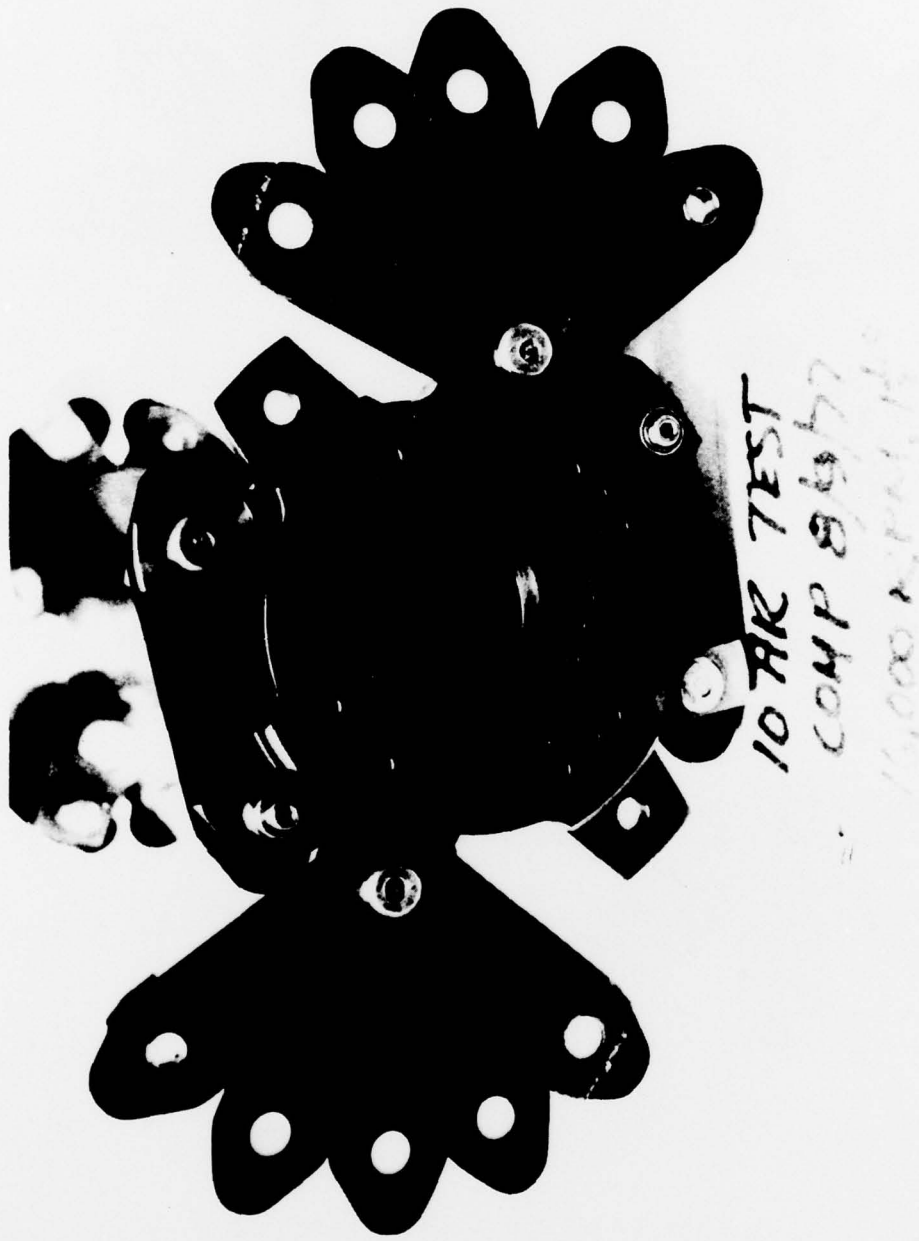


Figure 82. Dynamic Test Specimen Inspection - Coupling Assembly, Composite Strap Coupling.

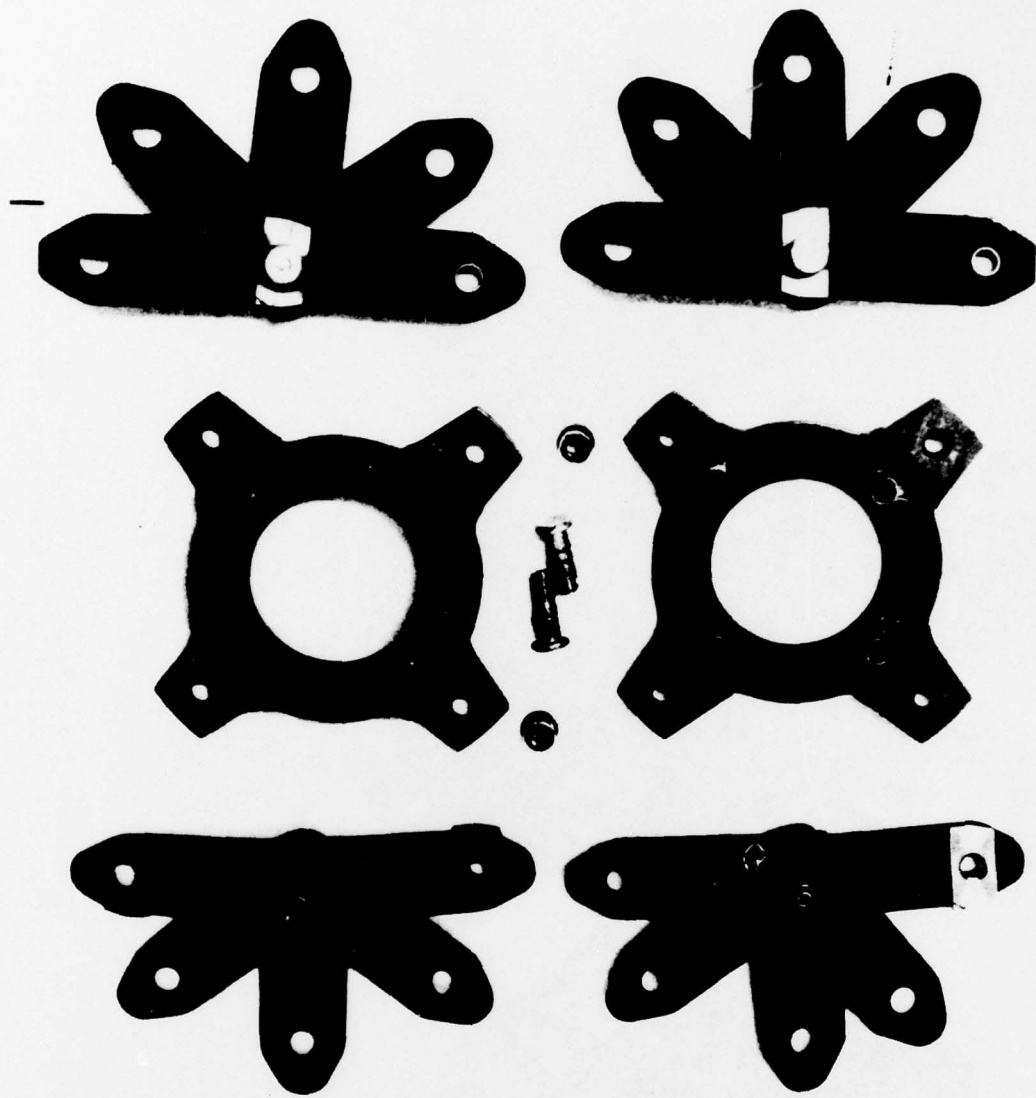


Figure 83. Dynamic Test Specimen Inspection -
Coupling Parts, Composite Strap Coupling.

CONCLUSIONS AND RECOMMENDATIONS

CONCLUSIONS

1. The testing conducted herein has demonstrated that a composite tension strap coupling has been developed to operate continuously at 1.5 degrees misalignment at 4727 in-lb torque and 15,400 rpm.
2. Present and future Army helicopters are not expected to require angular misalignment capacities greater than 1 degree for transmission drive shaft couplings; however, current rotor isolation systems under consideration may increase the coupling requirement to as high as 3° angular misalignment (steady state) and 5° misalignment (transient).
3. Flexure element couplings which do not require lubrication or service, are simple, lightweight, and can operate for an extended period of time after initial failure will probably continue to be used in most applications.
4. Composite materials should be used for future lightweight flexure element couplings, and the techniques that have currently been developed both to analyze and fabricate composite structures should be applied to the designs to obtain increased performance over state-of-the-art couplings.
5. For a given weight, composite flexure element couplings can be made that will offer improved ballistic tolerance over that exhibited by homogeneous metals.
6. Composite structures permit further simplification or reduction in the number of components of the coupling assembly. This increases its compatibility with balance considerations, increases reliability, and increases MTBR.
7. The use of composite materials for couplings developed in this program eliminated fretting which was the initiating cause of failure in the stainless steel coupling tested. Crack propagation rates in composites can also be controlled by ply matrix mix of the layup. Thus, the use of composites can attenuate both the origin and rate of failure.
8. The composite flexure element coupling offers maintenance-free life, improved survivability and reliability, and increased angular misalignment capacity without sacrificing simplicity, size, or weight.

9. Static tests indicate that composite flexure members can be made stiffer in torsion. Tailoring both torsional and bending stiffness which affects shaft dynamics is another option open to the coupling designer afforded by the use of composites.

RECOMMENDATIONS

1. It is recommended that the design of a composite coupling be pursued, with the ultimate goal being a one-piece shaft with integral couplings on either end. This shaft assembly would have desirable tamper-proof balance attributes for high-speed applications and would provide the optimum ballistic tolerance without adverse weight penalty. The materials, fabrication, and analytical techniques have recently been developed to take advantage of the high strength, low bending modulus, and excellent fatigue properties of these materials to develop such an advanced technology coupling.
2. It is recommended that the advanced technology coupling developed in this program be subjected to the Phase II Life Establishment Tests as originally planned, the Misalignment-versus-Life Test to establish angular misalignment capacity and potential, the Endurance Test to establish the fatigue properties of the graphite/epoxy ply mix, and the Environmental Tests to determine operational capability in an adverse environment.
3. It is recommended that testing be conducted using existing production flexure element couplings as a baseline to establish the increased performance capability of the composite design.
4. It is recommended that the initial testing for future coupling programs be conducted on static test equipment that simulates the basic loading. In this manner basic data can be established for static loads so that the future dynamic testing can establish the specific influence of the dynamic environment. This procedure would be less expensive and provide more data.